Transformation processes of nitrogen, phosphorus and iron in sub-euphotic waters and surface sediments

Dissertation zur Erlangung des
Doktorgrades der Naturwissenschaften
-Dr. rer. nat.-

dem Fachbereich Geowissenschaften
der Universität Bremen
vorgelegt von

Sarah Sokoll

Bremen, Oktober 2013

1. Gutachter: Prof. Dr. Marcel M. M. Kuypers
2. Gutachter: PD Dr. Matthias Zabel

Datum des Promotionskolloquiums: 20.11.2014

Table of contents

Abstract

In the surface ocean, concentrations and the ratios of key nutrients nitrogen (N), phosphorus (P) and iron (Fe) determine growth and community structure of primary producers. In upwelling regions, nutrient-rich deep waters that reach the surface fuels this primary production. Knowledge of nutrient transformation processes in deep waters, however, is still scarce and how these transformations influence concentrations of N, P and Fe is in parts not well constrained. Oxygen minimum zones (OMZs) are often found in the sub-euphotic waters underlying productive upwelling regions. These are formed when primary productivity derived from high nutrient fluxes lead to enhanced O_2 consumption due to remineralization in the water column and sediments. Consequently, altered redox conditions drive microbially mediated transformation of N, as well as the sorption and desorption processes of P and Fe.

The aim of this dissertation was to investigate microbial transformation processes of N, P and Fe in the sub-euphotic water column and surface sediments, especially in upwelling regions. To investigate these processes, incubation experiments with stable isotopes (^{15}N) and radioactive tracers (^{33}P, ^{55}Fe) were combined with molecular and chemical analysis, extraction methods and nanoscale mass spectrometric imaging. N-removal via denitrification and anaerobic ammonium oxidation (anammox) was investigated in sediments off Pakistan and Mauritania, while P and Fe transformation processes in the water column were investigated off Namibia, Mauritania and in the Baltic Sea.

In the Arabian Sea, benthic N-loss via denitrification and anammox was determined using ^{15}N incubation experiments along a depth transect across the OMZ. Denitrification rates in the sediments decreased from 2.7 to 1.5 mmol N m^{-2} d^{-1} with water depth, while anammox rates increased from 0.2 to 0.9 mmol N m^{-2} d^{-1}. Hence, the contribution from anammox to total benthic N-loss increased to ~40% at ~1400 m water depth. Quantification of the biomarker *nirS* genes, encoding for the *cd*$_1$-containing nitrite reductase in denitrifiers and anammox bacteria supported the rate determinations. Interestingly, phylogenetic analysis showed a distinct clustering pattern of denitrifiers *nirS* with water depth, while clustering of the anammox *nirS* was not restricted to water depth. Overall the results suggested that up to 50% of the N-loss in the Arabian Sea was due to benthic N-removal emphasizing the high potential of sediments to contribute to the N-deficit in the water column.

Similarly, a comprehensive sampling campaign and ^{15}N incubations of Mauritanian sediments showed that anammox contribution to the N-loss was more prominent at greater water depths and accounted for up to 80% at ~3000 m depth. Denitrification, in contrast, was the dominant N-loss pathway in shallow sediments. Unlike sediments investigated in the

Arabian Sea, the shelf off Mauritania is characterized by sandy permeable sediments. It was found that denitrification rates in sandy sediments correlated well with sediment grain size rather than benthic organic carbon content, indicating a strong causal relationship between benthic denitrification rates and advective porewater transport in these permeable sediments. This correlation was used to estimate denitrification rates for the entire shelf off Mauritania and Senegal. The estimates were significantly higher compared to those of previous studies based on surface primary production, indicating that the presence of benthic advective porewater transport is a more effective multiplier for predictions of benthic denitrification, than estimates from surface ocean organic carbon content alone.

On the shelf off Mauritania and Namibia, P-uptake was investigated in sub-euphotic waters and in the benthic boundary layer (BBL), the latter representing the particle-rich transition zone between water column and sediment. The transformation of dissolved phosphate (P_i) into particulate P was investigated with the radioactive tracer ^{33}P. This uptake of ^{33}P was largely biologically driven, as shown by a sequential extraction of ^{33}P and nanoscale analysis, and increased towards the seafloor off Mauritania, likely due to higher microbial activity close to the sediments. Rapid exchange of ^{33}P and ^{31}P on particles in the anoxic water column off Namibia masked microbial P-uptake and indicated that a second exchangeable pool of adsorbed P is available in these anoxic waters. In present models of marine P-cycling, uptake of P in sub-euphotic water column and BBL is not considered. This study highlighted cycling of P through the organic fraction in deep waters and the potential of ^{33}P experiments for nanoscale analysis to gain insight into specific P transformation processes that otherwise would remain unnoticed in bulk P concentration measurements.

Furthermore, P and Fe exchange between sediment and water column was investigated using sediment cores from the Baltic Sea. Applying the radiotracers ^{33}P and ^{55}Fe, the temporal change of dissolved and particulate pools of P and Fe could be investigated under variable redox conditions. A delayed transformation from the dissolved to the particulate pool under oxic conditions suggested that abiotic Fe oxidation and P sorption was significantly hindered, most likely by complexation with dissolved organics.

In conclusion, transformation processes determine concentration and bioavailability of N, P and Fe in the sub-euphotic water column and the sediments and may eventually have an impact on the primary production and the N:P ratio in the surface ocean. Biological activity plays an important role for the transformation processes of nutrients in sub-euphotic waters and surface sediments, especially in the investigated highly productive upwelling regions.

Kurzfassung

Das Wachstum und die Organismenzusammensetzung der Primärproduktion im Meer wird durch Konzentrationen und Verhältnisse der Hauptnährstoffe Stickstoff (N), Phosphor (P) und Eisen (Fe) gesteuert. In Auftriebsgebieten erreicht nährstoffreiches Tiefenwasser die Oberfläche und versorgt die Primärproduzenten. Das Wissen über Umwandlungsprozesse der Nährstoffe im Tiefenwasser ist immer noch gering und ihr Einfluss auf die Konzentrationen von N, P und Fe ist nicht vollständig bekannt. Unterhalb von produktiven Auftriebsgebieten bilden sich oft Sauerstoffminimumzonen (OMZs). Aufgrund des nährstoffreichen Wassers und der hohen Primärproduktion kommt es zu erhöhter Sauerstoffzehrung in der Wassersäule und im Sediment. Die dadurch schwankenden Redoxbedingungen beeinflussen die mikrobielle Umwandlung von N, genauso wie die Adsorption und Desorption von P und Fe.

Die Zielstellung dieser Dissertation war die Untersuchung von mikrobiellen Umwandlungsprozessen von N, P und Fe unterhalb der lichtdurchfluteten (sub-euphotischen) Zone und in Oberflächensedimenten. Um diese Prozesse zu untersuchen, wurden Inkubationsexperimente mit stabilen (^{15}N) und radioaktiven Isotopen (^{33}P, ^{55}Fe) durchgeführt und mit molekularbiologischen und chemischen Untersuchungen, Extraktionen und der Massenspektrometrie im Nanomaßstab kombiniert. N-Verlust durch Denitrifikation und anaerobe Ammonium-Oxidation (anammox) wurde in Sedimenten vor Pakistan und Mauretanien untersucht, während P und Fe Umwandlungsprozesse in der Wassersäule vor Namibia, Mauretanien und in der Ostsee untersucht wurden.

Im Arabiaschen Meer wurde der benthische N-Verlust durch Denitrifkation und Anammox mit ^{15}N Inkubationsexperimenten entlang eines Tiefenprofils in der OMZ untersucht. Denitrifikationsraten in den Sedimenten nahmen mit der Wassertiefe von 2.7 auf 1.5 mmol N m^{-2} d^{-1} ab, während Anammoxraten von 0.2 auf 0.9 mmol N m^{-2} d^{-1} zunahmen, so dass der Beitrag von Anammox zum benthischen N-Verlust auf ~40% in ~1400 m Wassertiefe stieg. Die Quantifizierung des Biomarker Gens *nirS,* welches für die cd_1-Nitrit-Oxidase kodiert, unterstützte diese Beobachtung. Interessanterweise zeigten Phylogenetische Analysen, dass die Gruppenbildung der *nirS* Gene der denitrifizierenden Bakterien von der Wassertiefe der Sedimente abhing, während die *nirS* Gene der Anammox-Bakterien keine wassertiefenspezifische Gruppenbildung erkennen ließen. Insgesamt könnte 50% des Stickstoffverlusts im Arabischen Meer den Sedimenten zuzuschreiben sein und zum N-Mangel in der Wassersäule beitragen.

Eine umfassende Studie von ^{15}N Inkubationsexperimenten mit Sedimenten vor der mauretanischen Küste zeigte, dass auch hier der Beitrag von Anammox mit der Wassertiefe

zunahm, auf 80% in 3000 m. Im Gegensatz dazu war Denitrifikation der vorherrschende Prozess in Sedimenten aus flachem Wasser. Anders als die Sedimente aus dem Arabischen Meer, sind die Sedimente vor Mauretanien sandig und permeabel. Die Denitrifikationsraten korrelierten mit der Korngröße der Sedimente anstatt mit dem organischen Kohlenstoffgehalt, was auf einen starken Zusammenhang zwischen Denitrifikationsraten und dem advektiven Transport in den permeablen Sedimenten hindeutet. Die Korrelation konnte benutzt werden, um die Denitifikationsraten über den gesamten Schelf vor Mauretanien zu modellieren. Der Stickstoffverlust für diese Region war deutlich höher verglichen mit vorherigen Berechnungen, die auf Primärproduktion basierten, und zeigt, dass advektiver Porenwassertransport die Voraussagen für benthische Denitrifikation gegenüber den auf Biomasse basierten Berechnungen erhöht.

Auf dem Schelf vor Mauretanien und Namibia wurde die P-Aufnahme in der sub-euphotischen Zone und der benthischen Grenzschicht (BBL), welche die partikelreiche Zone oberhalb dem Sediment darstellt, untersucht. Umwandlungsprozesse von gelösten Phosphat (P_i) in partikulären P wurden mit dem radioaktiven ^{33}P untersucht. Diese Aufnahme von ^{33}P wurde vor allem von biologischen Prozessen bestimmt, wie eine sequentielle Extraktion von ^{33}P und Untersuchungen im Nanomaßstab zeigten, und nahm zum Meeresboden in der BBL zu, wahrscheinlich aufgrund der erhöhten mikrobiellen Aktivität. In der OMZ vor Namibia überdeckte ein schneller Austausch von ^{33}P und ^{31}P an Partikeln die hohe P-Aufnahme durch Organismen und deutete auf einen zweiten Pool von adsorbierten P_i in dem anoxischen Gewässer hin. In den gegenwärtigen Modellen von P-Kreislauf wird P-Aufnahme in der sub-euphotischen Zonen bisher nicht berücksichtigt. Diese Studie zeigte jedoch, dass P_i einen organischen Pool im Tiefenwasser durchläuft. Des weiteren wurde das Potential von ^{33}P Experimenten im Nanomeßbereich für die Erforschung von P Umwandlungsprozesse aufgezeigt, die in Gesamtanalysen von P nicht erkennbar wären.

Darüber hinaus wurde der Austausch von P und Fe zwischen Sediment und Wassersäule mit Hilfe von Sedimentkernen aus der Ostsee untersucht. Unter Verwendung der radioaktiven Elemente ^{33}P und ^{55}Fe konnte der Wechsel von gelösten in partikuläre Phasen unter variablen Redoxbedingungen untersucht werden. Eine verzögerte Umwandlung von der gelösten zur partikulären Phase lässt darauf schließen, dass abiotische Fe-Oxidation und P-Adsorption gehemmt wurden, wahrscheinlich durch Komplexierung mit gelösten organischen Substanzen.

Abschließend betrachtet, bestimmen die Umwandlungsprozesse von N, P und Fe die Konzentration und Verfügbarkeit dieser Elemente in der sub-euphotischen Wassersäule und

den Sedimenten und haben am Ende einen Einfluss auf die Primärproduktion und das N:P Verhältnis in der Meeresoberfläche. Für die Umwandlungsprozesse der Nährstoffe in der sub-euphorischen Wassersäule, der benthischen Grenzschicht und den Oberflächensedimenten in den untersuchten hochproduktiven Auftriebsgebieten der Kontinentalabhänge spielt die biologische Aktivität eine entscheidende Rolle.

Introduction

This dissertation concerns transformation processes of nutrient (biolimiting) elements nitrogen (N), phosphorus (P) and iron (Fe) in the water column below the sunlight influenced (sub-euphotic) zone and in surface sediments. Concentrations and cycling of these elements in the subsurface waters can eventually affect primary production at the surface, because deep waters may reach the surface ocean by upwelling. Moreover, ratios of nutrients reaching the surface have an influence on the community structure of the primary producers. The ratios of the nutrients are influenced e. g. by removal of nitrogen and uptake of phosphorus, which were investigated during this study.

Coupling between water column and sediments

Nitrogen and phosphorus are both major nutrients, essential for all organisms on earth. Found in nucleic acids, amino acids, proteins and membrane lipids they are important for, storage of genetic information, energy gain, as well as membrane structural requirements. As essential nutrients, one or the other often becomes a limiting factor for the growth of primary producers in the ocean (Falkowski 1997; Tyrrell 1999). Primary production in the surface ocean is driven by sunlight as an energy source, hence photosynthesis is restricted to a zone with enough sunlight to support autotrophic growth (euphotic zone). Photosynthesis in the surface is fueled by different nutrient sources (Figure 1). In the coastal marine system, riverine input of nutrients or transport of nutrient rich deep waters by diffusion, wind-driven mixing or upwelling supply necessary nutrients to the surface (Wollast 1998). In contrast, in the open ocean upward diffusion and wind-driven mixing of nutrient rich deep waters are the main sources of nutrients (Wollast 1998).

Primary production fixes inorganic carbon dioxide (CO_2) from the atmosphere into organic carbon (org-C) and is therefore an important factor for the global CO_2 budget (Raven and Falkowski 1999). In the surface, heterotrophic organisms benefit from primary production and feed on the remains of autotrophic organisms. Nutrients are remineralized in the surface by the heterotrophic community and this “microbial loop” is channeling nutrients back to the primary producers (Azam et al. 1983). Dead cells, byproducts of grazers (such as fecal pellets), and other organic detritus often form particles or aggregates which sink as “marine snow” towards the seafloor (Suess 1980). With these aggregates, CO_2 from the atmosphere is exported to the deeper waters and eventually the sediments in form of organic carbon (Raven and Falkowski 1999). This, mechanism, which is also called the “biological carbon pump”, plays an important role for the atmospheric CO_2 concentration and

sequestration in the marine system. Sinking aggregates are often densely populated with heterotrophic microorganisms, especially bacteria that lead to degradation of organic matter during the transport through the water column (Wollast 1998). Due to the respiration activities in the water column, oxygen is consumed, which can lead to oxygen minimum zones (OMZ) underlying particularly productive regions in the oceans.

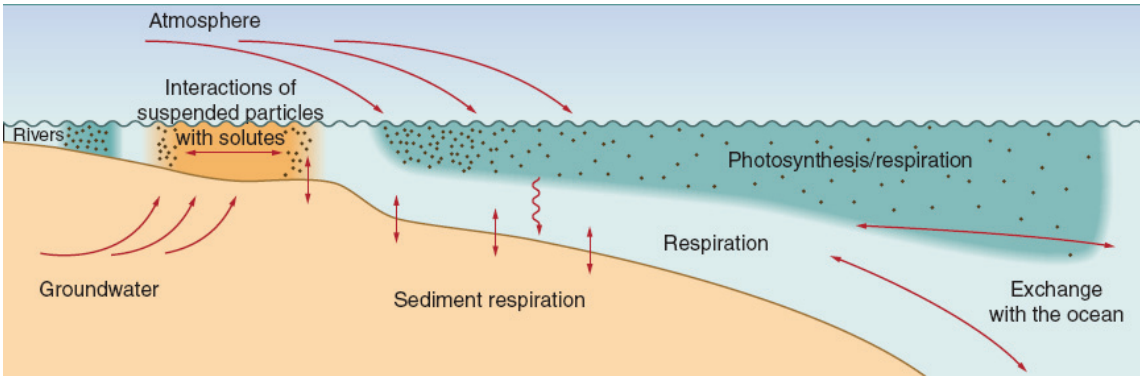

Figure 1: Coupling of water column and sediment in coastal areas. In shallow waters, processes in the surface water column and the sediment are directly coupled. Riverine input, mixing and particle resuspension affecting the nutrient concentrations in the water column (Slomp 2011, after Jickells 1998).

The benthic boundary layer (BBL), the first few meters above the seafloor acts as a transition zone between water column and sediment. Resuspension of sediment particles and sinking organic particles from the surface, leads to a high turbidity in the BBL, especially in productive areas (Thomsen et al. 2002). Various abiotic and biotic interactions of particles and organism influence the bioavailability of nutrients in the BBL (Ritzrau et al. 1997). At the seafloor and in the sediments, organic matter is degraded further and most of the remineralized nutrients are released to the water column and the porewater. Due to respiration activity, oxygen is depleted usually within the surface mm or cm in sediments, depending on sediment type and amount of organic carbon supplied from the water column (Glud 2008) . The regenerated nutrients in turn can further fuel primary production if they reach the surface by upwelling or mixing processes, a form of "benthic-pelagic coupling" (Graf 1992). In shallow coastal waters, much more organic matter reaches the seafloor, resulting in a rich benthic community which lives on the organic carbon import from the surface (Wollast 1998). The coupling of the water column and the sediments is much tighter in coastal environments than in the open ocean, where much less organic material reaches the seafloor and the deep water column separates the nutrient rich deep waters form the nutrient poor surface waters (Suess 1980).

Processes in nitrogen cycling

Most N exists as dinitrogen gas (N_2) in the atmosphere (79%). Only a small fraction of nitrogen (N) is available in a fixed, reactive form, e. g. ammonium (NH_4^+) or nitrate (NO_3^-). In the marine system fixed nitrogen has different sources: atmospheric deposition, riverine input and fixation of N into organic nitrogen mediated by specialized microorganisms (Codispoti et al. 2001). Similarly, microorganisms are also responsible for the conversion of different nitrogen compounds into N_2, therefore sources and sinks of N are controlled by microorganisms. Only few groups of prokaryotes, so-called diazotrophs, have the capability to convert, or "fix" the inert gas N_2 into organic nitrogen ($N_2 \rightarrow NH_4^+ \rightarrow$organic N, Figure 2). Amongst the N-fixing organisms both types occur, heterotrophs as well as autotrophs and the best known are probably the cyanobacteria. Since this process consumes a lot of energy diazotrophs often benefit from a phototrophic lifestyle and are predominately found in the photic surface of the water column or shallow sediments (Herbert 1999). The process of N-fixation, often realised by the oxygen sensitive enzyme nitrogenase, is energy consuming and avoided if bioavailable forms of N, such as NO_3^- and NH_4^+, are present. In water column and sediments, different N compounds are recycled by organisms not capable of fixing N_2.

Nitrogen has different functions in the ecosystem, firstly as a nutrient and secondly as a redox-active compound used to gain energy. Therefore, cycling of this element in the ocean is very complex. The oxidation states in which N occurs in the environment range between -3 and +5 (Figure 2). Nitrogen inorganic matter is made available by ammonification, a catabolic process which includes the enzymatic break down of the organic molecules and deamination, by which ammonium is produced (organic $N \rightarrow NH_4^+$). The capability of ammonification is wide spread amongst microorganisms and high ammonification activity was found in coastal marine sediments (Herbert 1999). Ammonium can be used to build up new biomass via assimilation or converted to other N compounds by oxidation processes. Chemoautotrophic nitrification is such an oxidation process, which converts ammonium via a two step reaction pathway into nitrite and nitrate ($NH_4^+ \rightarrow NO_2^- \rightarrow NO_3^-$) and is conducted by bacteria, and in some cases by *Crenarcheota*. Even though nitrification has been shown to occur in anoxic waters (Fuessel et al. 2012), the process is predominantly performed at oxic conditions, which has the effect of restricting nitrification to oxic sediment layers. Other organisms benefit from the conversion of ammonium into nitrate and nitrite, since it allows the subsequent use of the N compounds as electron acceptor by dissimilatory nitrate reduction to ammonium (DNRA), denitrification and anaerobic ammonium oxidation (anammox). DNRA is a heterotrophic reaction that converts the nitrate to ammonium through fermentative or a sulphur oxidation.

This process has for a long time been known to occur in anoxic and sulfidic sediments, but was also shown to occur in sandy sediments (Rao et al. 2007; Gao et al. 2012) and in the water column OMZ off Peru and the Omani shelf (Lam et al. 2009; Jensen et al. 2011; Lam et al. 2011).

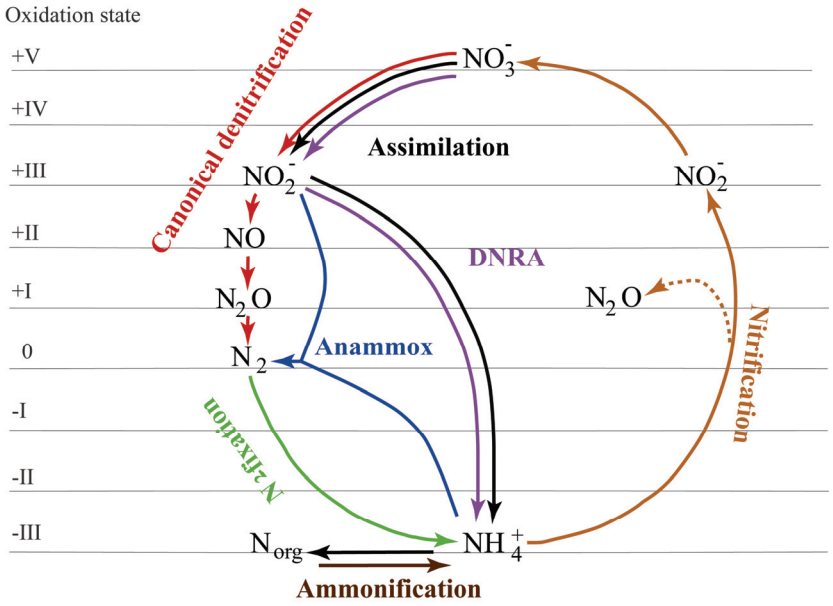

Figure 2: Nitrogen cycle, oxidation states and transformation processes. DNRA: dissimilatory nitrate reduction to ammonium. Anammox: anaerobe ammonium oxidation. modified from Codispoti et al. (2001).

Fixed nitrogen can be removed from marine ecosystems by production of N_2 gas. N-loss processes play an important role in the marine N-cycling because the activities of the respective microorganisms decrease the amount of bioavailable N in the marine environment. Several microbial processes are known to remove N_2 from the marine environment: canonical denitrification, nitrite-driven anaerobic methane oxidation and anaerobic oxidation of ammonium (anammox). The nitrate driven anaerobic methane oxidation by oxygenic bacteria has only recently been discovered (Ettwig et al. 2010) and to date the importance of this process is uncertain, also due to the limitation to areas with methane supply. Canonical denitrification is very widespread in marine sediments and a multi-step terminal electron acceptor process that includes an initial nitrate reduction ($NO_3^- \rightarrow NO_2^-$) the subsequent dissimilatory reduction of nitrite via nitric oxide and nitrous oxide (an important greenhouse gas in parts also released during the process), and finally to dinitrogen ($NO_2^- \rightarrow NO \rightarrow N_2O \rightarrow N_2$). The predominantly heterotrophic process of denitrification is usually

linked to the oxidation of the organic matter in oxygen depleted environments. However, denitrification may also be linked to chemoautotrophic processes such as sulphide oxidation (Fossing et al. 1995; Jørgensen and Gallardo 1999; Otte et al. 1999; Schulz et al. 1999), methane oxidation (Raghoebarsing et al. 2006), as well as iron or hydrogen oxidation (Straub et al. 1996; Weber et al. 2006). As a predominantly heterotrophic process, denitrification rates are heavily dependent on the availability of organic carbon supply. Thus, shallow sediments with high organic carbon content are usually considered to harbour higher denitrification activity than the abyssal sediments (Christensen et al. 1987; Devol et al. 1997).

Anammox is, in contrast to denitrification, a chemoautotrophic process that forms N_2 by the combination of nitrite and ammonium ($NH_4^+ + NO_2^- \rightarrow N_2$). Anammox was detected for the first time in waste water treatment plants (Mulder et al. 1995; van de Graaf et al. 1997). The process involved the reaction of nitric oxide with ammonium to form hydrazine ($NO + NH_4^+ \rightarrow N_2H_4$). Hydrazine is oxidized to N_2 ($N_2H_4 \rightarrow N_2$), which drives the proton pump for ATP production to gain energy for autotrophic growth via the Acetyl-CoA pathway (Schalk et al. 1998; Schalk et al. 2000; Strous et al. 2006). In the environment, anammox activities were first detected in estuarine and marine sediments in 2002 (Dalsgaard and Thamdrup 2002; Thamdrup and Dalsgaard 2002). In the water column, N-loss due to anammox was first detected in the Black Sea (Kuypers et al. 2003) and the Golfo Dulce, Costa Rica (Dalsgaard et al. 2003). N-loss in oxygen minimum zones (OMZ) underlying productive upwelling areas off Peru, Chile, Namibia and Oman were found to be mainly attributed to anammox (Kuypers et al. 2005; Thamdrup et al. 2006; Hamersley et al. 2007; Lam et al. 2009; Jensen et al. 2011; Kalvelage et al. 2013). These OMZs are estimated to account for 30-50% of total oceanic nitrogen loss, which was previously attributed to denitrification (Gruber and Sarmiento 1997; Codispoti et al. 2001), but subsequently revised and attributed to anammox (Devol 2003).

Even afterdecades of research the marine N budget is still a matter of debate. While some studies have balanced marine N sources and sinks (Gruber and Sarmiento 1997; Gruber 2004), other N budget calculations fail to establish the steady state in the ocean (Codispoti et al. 2001). Recent discoveries have led to the assumption that the N-fixation has been underestimated and the recent estimates of N_2-fixation might balance the marine N budget (Grosskopf et al. 2012).

Benthic nitrogen loss

Since sediments are believed to contribute 35 to 70% to the global marine N-loss they play a key role in the N-budget (Middelburg et al. 1996; Gruber and Sarmiento 1997; Codispoti et al. 2001). Anammox has been shown to contribute up to 80% to N-loss in sediments (Dalsgaard et al. 2005) and is therefore an important process also in the marine N-cycling. Recent studies lead to the conclusion that benthic anammox might be more important in deeper sediments, possibly due to the limitation of denitrifiers by organic matter (Dalsgaard et al. 2005; Trimmer and Nicholls 2009).

In cohesive sediments, substrates for the various redox processes are usually provided by diffusion. Substrate limitation in the sediments results in a zonation of the occurrence of the various N species and the different N-cycling processes in distinct layers. In surface sediments, nitrate may be present due to NO_3^- fluxes from the water column into the sediment as well as remineralisation and nitrification activities. Nitrate and nitrite decrease with sediment depth, where they are consumed by denitrification, anammox and DNRA in the suboxic and anoxic zones of the sediment. Ammonium usually increases with sediment depth due to remineralisation processes and accumulates due the limitation of nitrification by low oxygen concentration. In contrast to cohesive, muddy sediments, sandy permeable sediments were generally believed to be rather insignificant for the N-loss, due to their high oxygen concentrations and low carbon contents (Vance-Harris and Ingall 2005). In muddy sediment, diffusion is the mode of transportation of porewater while in sandy sediments, advective porewater transport dominates and rates of denitrification vary greatly (Table 1). Underestimation of the N-loss potential in permeable sediments may have resulted from improper application of diffusion-based methods, e.g. whole core incubations. Advection - based methods, such as flow through cores, have been used to investigate N-loss in permeable sediments and have led to upwardly revised estimates of N-cycling rates (Rao et al. 2007; Rao et al. 2008; Gao et al. 2010; Evrard et al. 2012; Gao et al. 2012; Santos et al. 2012). These recent studies indicate high potential of N-loss in sediments influenced by advection. On the continental shelf, sandy sediments are believed to cover up to 70% of the seafloor (Emery 1968). Furthermore, coastal sediments are often subject to anthropogenic N input by rivers. High levels of N-loss activity in these sediments return the N back to the atmosphere and act as a natural filter preventing eutrophication of greater areas of the ocean (Andersen and Helder 1987; Huettel and Rusch 2000; Huettel et al. 2003).

Table 1: Selected denitrification rates in marine sediments. Denitrification rates vary within one study due to spatial or temporal distance. In general, different methods are used to determine denitrification rates, however, selected rates were determined with ^{15}N stable isotope experiments.

Region	Water depth [m]	Sediment	Rate [mmol N m^{-2} d^{-1}]	Reference
NE Atlantic	50-1000	impermeable	0.01-0.16	Trimmer and Nicholls (2009)
Gulf of Mexico	<2	permeable	0.12-0.87	Gihring et al. (2010)
Sagami Bay, Japan	1450	impermeable	1.1	Glud et al. (2009)
Victoria, Australia	intertidal	permeable	1.6	Kessler et al. (2012)
Concepción Bay , Chile	85	impermeable	0.6-2.9	Farias et al. (2004)
Helsingør, Denmark	1 m	permeable	0.05-3.8	Cook et al. (2006)
Wadden Sea, Germany	intertidal	permeable	4.1-25	Gao et al. (2012)

Coupled phosphorus and iron cycling

The essential macronutrient element phosphorus (P) plays a key role with nitrogen in marine nutrient cycling. Unlike N which undergoes plenty of changes in the oxidation states due to various redox reactions, P mainly occurs in the oxidations state + V (e.g. as is phosphate HPO_4^{2-}). Phosphorus is the limiting nutrient for primary production on longer time scales (Tyrrell 1999). Most of the P in the ocean occurs as dissolved inorganic P (DIP). Some dissolved organic P (DOP) exists, but this DOP is usually only significant in P depleted surface waters (Canfield et al. 2005). Unlike N_2 in the atmosphere, which can be converted and fixed into organic N by specialized organisms, P solely enters the ocean as product of weathering, volcanic activity or anthropogenic industrial production. P is mainly introduced to the marine environment via riverine (dissolved) or dust (particulate) input (Figure 3) and is taken up by primary producers in the surface ocean (Delaney 1998; Benitez-Nelson 2000). Moreover, algae were also shown to adsorb P to a great amount in surface waters (Sanudo-Wilhelmy et al. 2004). In general, two different phosphate (P_i) transport systems used by microorganisms, a high affinity transporter (Pst) and a low affinity uptake system (Pit). The high affinity pst system is more abundant in surface waters with depleted phosphate concentrations and requires energy in form of ATP for the selective transport. In contrast, the pit system is a constitutive symport of P_i with cations such as Mg^{2+}, Ca^{2+}, Mn^{2+} and used if P_i concentrations are high enough to support growth (Rosenberg et al. 1977; van Veen et al. 1993).

In the surface P_i is already remineralized by e.g. heterotrophic bacteria and taken up again by primary producers and microbial heterotrophs, while export of organic matter and of organic P into the deeper water column takes place due to particle formation and subsequent

sinking to the seafloor. While sinking through the water column, organic P is mineralized and leads to an increase of P_i concentrations and accumulation in the deep water. As a consequence P_i concentrations are higher in the Pacific Ocean than in the Atlantic Ocean due to the greater age of Pacific water. Upwelling of deep water can fuel primary production in the surface ocean by the input of P_i. In open ocean environments, only small amounts of P are exported from the surface while the export of organic P in coastal environments is much higher. Therefore major sinks for P in the ocean are continental slopes, because parts of the organic matter are buried in shallow sediments underlying productive areas and especially anoxic zones (Berner 1973; Froelich et al. 1982; Wheat et al. 1996; Slomp and van Cappellen 2007). In contrast, in deep sea sediments the major burial form of P is the mineral apatite [$Ca_5(PO_4)_3(F,Cl,OH)$] (Palastanga et al. 2011). Poly-P_i which typically serves as energy storage in bacteria can contribute up to 45% of the sinking material from the water column and can act as nucleate for apatite formation in sediments (Diaz et al. 2008; Diaz et al. 2012). In sediments, organic P is further remineralized and partially released to pore fluids.

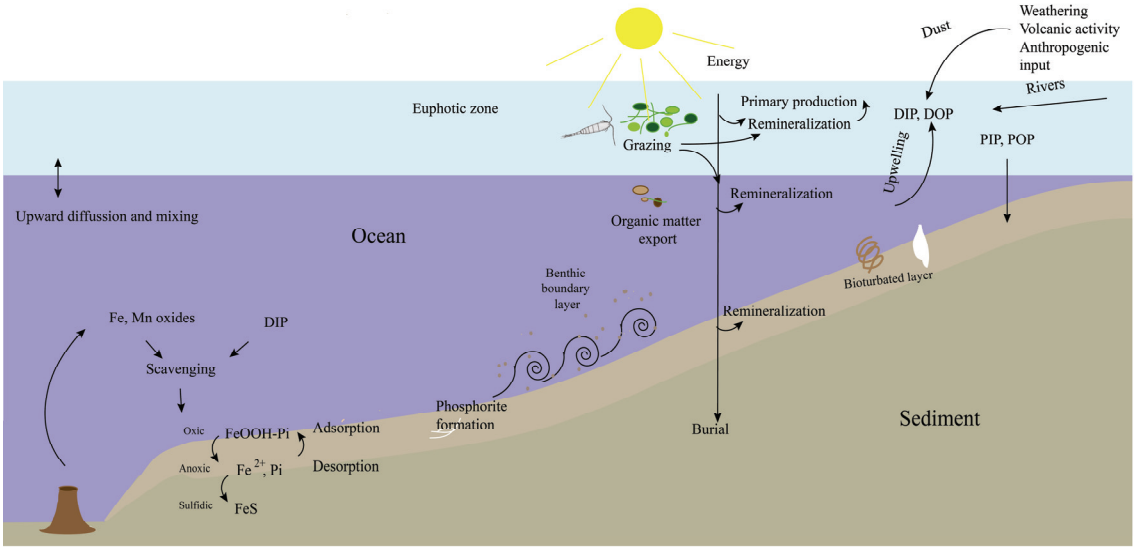

Figure 3: Marine phosphorus cycling. Modified after Compton et al. (2000) and Paytan and McLaughlin (2007). DIP: dissolved inorganic phosphorus, DOP: dissolved organic phosphorus, PIP: particulate inorganic phosphorus, POP: particulate organic phosphorus.

The cycling of P_i is greatly influenced by the interaction with manganese (Mn) and iron (Fe) particles, and is thus dependent on redox reactions of these metals. Iron itself is an important micronutrient and can limit primary production in certain areas of the ocean. Amongst these regions are the high nutrient low chlorophyll area (HNLC), which are subject to several studies of Fe-fertilisation to enhance primary production and the biological carbon pump

(Boyd et al. 2007; Trick et al. 2010; Smetacek et al. 2012). The tight coupling of Fe and P_i cycling especially affects environments that undergo changes in oxygen concentrations, such as sediments or OMZs. In oxic environments Fe mainly exist in form of insoluble Fe(III)-oxyhydoxides (FeOOH.) while at reducing conditions Fe occurs in its more soluble form Fe(II). The affinity of P_i to adsorb to FeOOH is very high and formation of Fe-P_i particles occurs very quickly (Ruttenberg and Sulak 2011). Furthermore, of P onto iron particles can account for 9% of the removal of P_i from the marine environment (Bjerrum and Canfield 2002; Canfield et al. 2005).

In sediments rich in reactive Fe, P_i is scavenged in the redox layer on the surface and the P_i flux to the water column is prevented by this "iron-cap" (Canfield et al. 2005). Changing oxygen concentrations in the water column occur in the Baltic Sea and the chemocline of the Black Sea. For these regions, P_i shuttle mechanisms with Fe and Mn at the oxic/anoxic interface are described to explain anomalies in the P_i profile (Shaffer 1986; Turnewitsch and Pohl 2010; Jilbert and Slomp 2013). These shuttle and pump mechanisms exist due to the formation and dissolution of FeS at sulfidic interfaces as well as of Fe-HOOH at oxic/anoxic interfaces and desorption/adsorption of P_i onto Fe-HOOH particles. In sediments underlying anoxic water columns, Fe-HOOH dissolves releasing adsorbed P_i from the particles into the overlying water column. Within redox active zones in sediments, formation of authigentic carbonate fluorapatite (CFA) may be enhanced. Fe-P_i particles may represent an important intermediate in the formation of CFA (Slomp et al. 1996). In addition to CFAs, a fraction of P_i are also associated and buried as Fe-oxyhydroxides, manganese-calcium-carbonates and Fe(II)-P such as vivianite (Suess 1979; Ruttenberg and Berner 1993). Under sulfidic conditions, Fe-oxyhdroxides react with sulfide to form pyrite (FeS_2) , thus resulting in P_i-desorption from the particles. Escape of P_i into the water column is usually enhanced in anoxic marine waters (Sundby et al. 1986; Ingall and Jahnke 1994; van Cappellen and Ingall 1994) and is thought to enhance algal blooms in marine systems (Rozan et al. 2002).

Microorganisms are not only responsible for the incorporation of organic P into particles (POP) by uptake and adsorption processes, but can also influence inorganic phosphate reactions. Poly-P_i storing sulfur bacteria have been shown to influence the formation of phosphorites and enhance the burial of P at the edges of the Namibian OMZ by affecting P_i concentrations in the sediments (Schulz and Schulz 2005; Goldhammer et al. 2010). Hence, microorganisms can have a great impact on the bioavailability of P in the marine system.

N:P ratios in the ocean

The two elements N and P are essential for all organisms on earth and can limit primary production in the ocean (Falkowski 1997; Tyrrell 1999). It has been known for a long time, that the ratio of C:N:P is more or less constant at 106:16:1 (Redfield et al. 1963) in the world ocean. This so-called Redfield ratio is attributed to photosynthesis and the uptake of the elements in a constant ratio

$$106CO_2 + 16HNO_3 + H_3PO_4 + 122H_2O \xrightarrow{light} C_{106}H_{263}O_{110}N_{16}P + 138O_2$$

that leads to similar composition of phytoplankton and ultimately the regeneration of the nutrients by remineralisation of the organic matter in the same ratio (Takahashi et al. 1985; Anderson and Sarmiento 1994). In reality, different organisms have different nutrient preferences and compatibilities, e. g. N-fixing Cyanobacteria are more competitive at high P and low N concentrations (Karl et al. 2002). The Redfield ratio averages the wide range of N:P ratios in phytoplankton in different environments and is also a result of the ocean circulation (Klausmeier et al. 2004; Wallenstein et al. 2006; Weber and Deutsch 2010). The concentrations of N and P therefore limit primary production, but it is the ratio of these nutrients which can greatly influence community structure of phytoplankton communities (Geider and La Roche 2002; Quigg et al. 2003) .

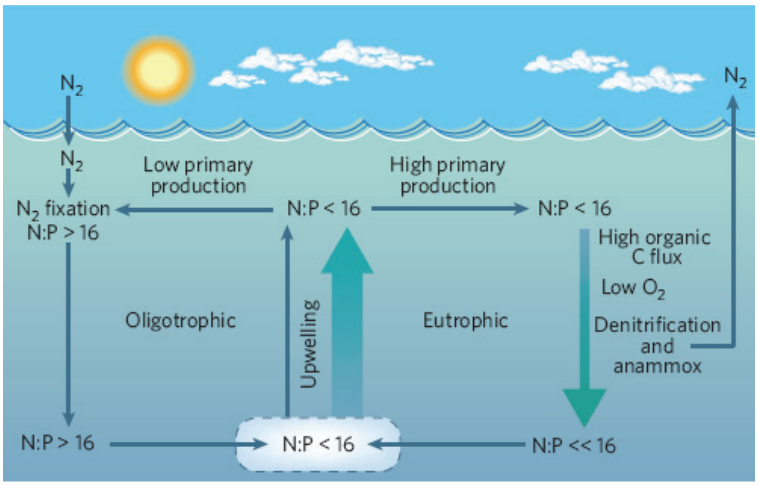

Figure 4: The N:P ratios in oligotrophic and eutrophic waters with low oxygen concentrations. In the water column of eutrophied upwelling regions, N:P ratios decreas due to N-loss in the water column. In oligotrophic areas, N_2 fixation leads to an increase of N:P compared to the Redfield ratio of 16 (Arrigo 2005).

In some areas of the ocean, especially OMZs, higher P concentrations and a lower N:P ratio have been used to define anomalies of the Redfield ratio (Figure 4). The so-called N-deficit is often used to estimate the N-loss in the water column of OMZs (Codispoti et al. 2001;

Deutsch et al. 2001). The N-deficit is based on the assumption that P concentrations are conservative relative to N, the latter of which is subject to N-loss. However, in OMZs, concentrations of P may be very dynamic due to release of P from sediments into the water column under anoxic conditions, formation of iron-oxyhydroxides at higher oxygen concentration and subsequent adsorption of P mentioned in the previous section. Recent expansion of the OMZs underlying major upwelling regions has been detected , and will probably influence all marine life (Oschlies et al. 2008; Stramma et al. 2008). Some long-term models of nutrient cycling suggest that negative feedbacks will lead to a stabilization of the oceans instead of a continuous decrease of oxygen in the marine system (van Cappellen and Ingall 1996), but this point is contentious. Human induced increase of CO_2 in the atmosphere is thought to have severe effects on the ocean circulation, the melting of the global ice and in terms the distribution of primary production (Schmittner et al. 2009). Therefore, knowledge in the marine nutrient cycles is essential for the understanding of the anthropogenic impact on the ocean and the response of the marine environment to the global climate change (Howarth et al. 1996; Vitousek et al. 1997; Boyer et al. 2006).

Approaches to study nutrient transformation processes

Transformation processes of chemical compounds in the marine environment are often investigated based on the chemical concentrations. Based on concentrations of various N-compounds, N-transformation processes can be modelled for the water column (Deutsch et al. 2001; Deutsch et al. 2007; DeVries et al. 2012). Benthic lander chambers and the change in chemical concentrations may also be used to determine fluxes and chemical transformation processes of e. g. N-compounds and P across the sediment-water interface of OMZs (Bohlen et al. 2011; Noffke et al. 2012). However, neither of these approaches lead to a mechanistic understanding of controls and regulation of nutrient cycles. Direct experimental approaches, in contrast, provide the opportunity to elucidate the various transformation processes of the nutrients in the ocean. In this study, radioactive and stable isotope tracers were used to track and quantify transformation processes of nitrogen, phosphorus and iron. Stable isotope techniques are based on the fact that some isotopes of an element are less abundant on earth than other stable isotopes. The quantity of different masses of the isotopes are measured with mass spectrometers. For nitrogen, the ^{15}N is used as a tracer, since the abundance on earth is only 0.366% compared to ^{14}N with 99.6%. Lately, the approach to use ^{15}N stable isotopes has been widely applied to investigate the various processes in the marine N-cycling in water column and sediments (Nielsen 1992; Thamdrup and Dalsgaard 2000; Kuypers et al. 2003).

Stable isotopes enable the tracking of labelled ^{15}N compound in different N compounds such as N_2, NO_3^-, NO_2^-, NH_4^+. These methods use the direct measurements of the N_2 gas (Holtappels et al. 2011) produced by denitrification and anammox or the measurement of N_2 gas after conversion of NO_3^-, NO_2^- or NH_4^+ to N_2 with sulphanilamide, cadmium or hydroxylamine to quantify the ^{15}N conversion in nitrification and DNRA (Lipschultz et al. 1990; Warembourg 1993; Fuessel et al. 2012). With this approach, the activity of the respective mechanisms can be identified and quantified.

The advantage of the radiotracer technique of ^{33}P for the investigation of P-cycling is the low concentration needed to detect the radioactivity. The decay of the radioactive isotopes is measured and hence gives information about the concentration of the tracer in a sample. For uptake experiments of surface samples in P depleted marine systems, ^{33}P has been used (Thingstad et al. 1993; Zubkov et al. 2007). Recently, uptake of P by sulphur bacteria has been shown with a combination of ^{33}P-radiotracer incubation and the a sequential extraction of P (SEDEX) to verify the importance of sulphurbacteria for the phosphorite formation in the Benguela upwelling system (Goldhammer et al. 2010). SEDEX has been developed for the sediments (Ruttenberg 1992) and only rarely been used for water column samples so far (Diaz et al. 2012). Another advantage of the ^{33}P is the rapid decay of ^{33}P to ^{33}S, the latter of which has a natural abundance of 0.75%, and hence can be quantified by mass spectrometry. Iron and its transformation processes can be analyzed with radiotracers (^{55}Fe) or the stable isotopes ^{56}Fe, ^{57}Fe, ^{58}Fe. Amongst the stable isotopes, the ^{56}Fe is most abundant in the earth system (91.7%) and the use of ^{57}Fe as a tracer most convenient, since its abundance is only 0.28%.

These tracer methods can be combined with molecular ecological tools to provide insight into nutrient cycles. Most of environmental microorganisms are not cultivable or difficult to culture (Amann *et al.* 1995) and molecular techniques enable culture independent quantification of organisms. Molecular techniques provide a high sensitivity such that low numbers of organisms and even small amounts of nucleic acids can be detected and quantified or used for characterization of microbial communities or functional groups (Zehr *et al.* 2009). Based on known gene sequences from different organisms, primer and probes can be designed to amplify specific genes of particular groups of microbes of interest in the environment. For prokaryotes, the 16S rRNA approach is often used, as the 16S rRNA gene is known to have highly conservative regions and enables phylogenetic analyses and detection of organisms belonging to specific groups of bacteria (Olsen et al. 1986). Unfortunately, organisms capable of performing denitrification are phylogenetically very diverse, such that a 16S rRNA approach is not particularly useful. Instead, functional genes encoding for specific enzymes

are more useful to investigate denitrifiers. The reduction of nitrite to nitric oxide ($NO_2^- \rightarrow NO$) is mediated by a periplasmic nitrite reductases (NIR, Figure 5), which contains either copper (NirK) or cytochrome cd_1 (NirS) (Zumft 1997). The *nirS* genes encode for the latter are often used as a functional gene biomarker for denitrifiers and often used as indicator for denitrification (Jayakumar et al. 2004; Castro-Gonzalez et al. 2005; Tiquia et al. 2006; Dang et al. 2009; Dong et al. 2009). A cd_1-nitrite:nitric oxide oxidoreductase (NirS) is also used by anammox bacteria and the *nirS* genes similarly to the denitrifier *nirS* genes used as a biomarker (Strous et al. 2006; van de Vossenberg et al. 2008; Lam et al. 2009; Jensen et al. 2011; Lam et al. 2011). Moreover, anammox bacteria have a special membrane structure, made of the unique ladderane lipids ("anammoxosome") (Damste et al. 2002; van Niftrik et al. 2004), which have been used as biomarker for these organisms as well (Kuypers et al. 2003; Jaeschke et al. 2007; Jaeschke et al. 2010).

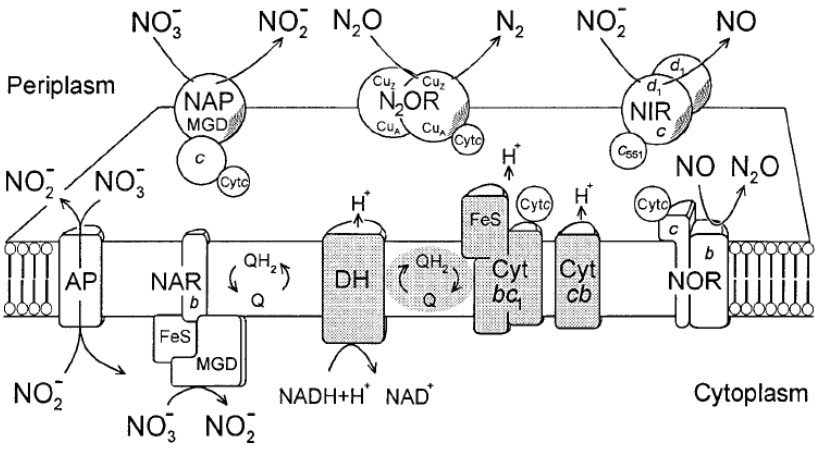

Figure 5: Organization and sideness of the anaerobic electorn transfer chain of Pseudomonas stutzeri. The shaded areas represent the components of the constitutive aerobic respoiratory chain consisting of an NADH dehydrogenase complex (DH), quinone cycle (Q, QH_2), cyctochrome bc_1 complex (Cyt bc_1), and the cytochrome *cb* terminal oxidase complex (Cyt *cb*). The denitrification system comprises respiratory nitrate reductase (NAR), nitrite reductase (NIR), NO reductase (NOR), and N_2O reductase (N2OR). FeS: iron-sulfur centers; *b, c* and d_1: heme B, heme C, heme D_1; cyt *c*: unsepcified c-type cytochromes accepting electorns form the bc_1 complex and acting on N_2OR and NOR; cyt c_{551}: cyctochrome c_{551}; AP: postulated nitrate/nitrite antiporter. (Zumft 1997)

The quantitative real-time PCR (qPCR) approach has been used for detection and quantification of prokaryotic groups, since it is culture-and microscopy-independent (Gruntzig et al. 2001; Wallenstein and Vilgalys 2005; Schippers and Neretin 2006). The qPCR approach uses the exponential increase of DNA during amplification with the enzyme polymerase, which enables a back calculation of the quantity of DNA templates in the sample

at the beginning. Absolute quantification of template DNA in a sample can be calculated, if standards are run together with the sample. Functional genes can also be used to describe phylogenetic relationships and to identify previously unknown organisms, which improve the knowledge about differences in the prokaryotic community in various environments (Liu et al. 2003; Castro-Gonzalez et al. 2005; Tiquia et al. 2006; Dang et al. 2009).

Objectives

In this dissertation, nutrient transformation processes were examined using the aforementioned methods in four areas exhibiting high rates of primary production (Figure 6): the Eastern boundary upwelling areas off Namibia and Mauritania, the monsoon driven upwelling area in the Arabian Sea and finally the Baltic Sea. In all of these environments, oxygen in the water column is reduced due to high primary production and subsequently high rates of respiration of organic matter in the water column.

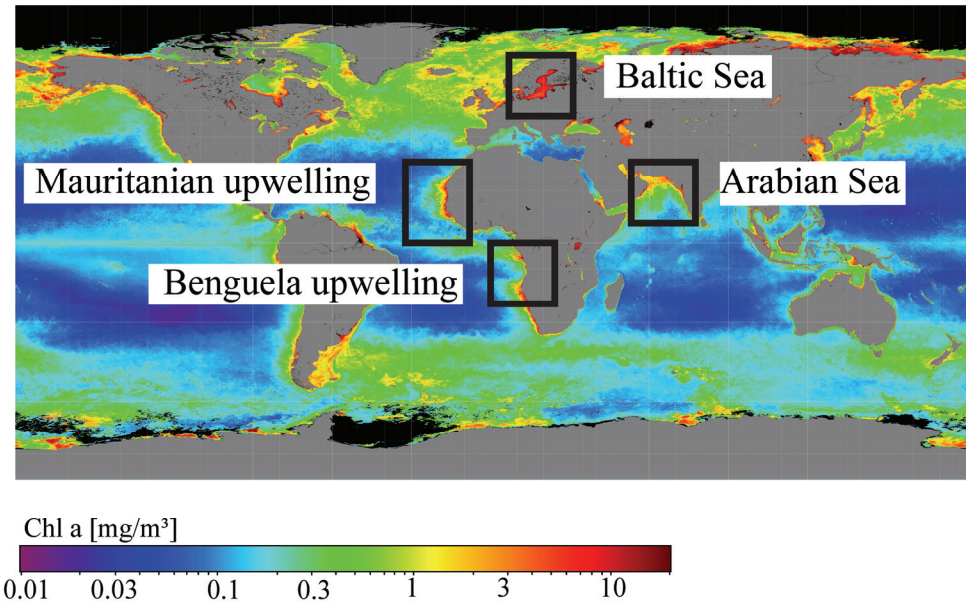

Figure 6: Annual chlorophyll concentration (2010) in surface waters of the regions investigated in this dissertation The high chlorophyll concentrations off Mauritania and Namibia, as well as in the Arabian Sea indicate that the investigated upwelling regions are amongst of the most productive areas in the ocean due to natural nutrient input. The high primary production is anthropogenically influenced. (downloaded from http://oceancolor.gsfc.nasa.gov).

In the Arabian Sea, pelagic denitrification activities are responsible for a N-deficit in the water column (Naqvi et al. 1991; Naqvi 1994; Naqvi et al. 2006; Ward et al. 2009). Therefore, the water column has been thought to play a major role in global N-loss, but

estimated rates vary greatly (Devol et al. 2006). More recent studies show that N-loss in the central Arabian Sea is not as high as previously thought (Jensen et al. 2011; Lam et al. 2011) and therefore it is not known, how much the sediments contributes to the N-deficit in the water column. Benthic N_2 production has been measured in the Arabian Sea (Schwartz et al. 2009), but no distinction was made between denitrification and anammox. Moreover, only few studies investigate the N-loss in sediments underlying oxygen minimum zones (Farías et al. 2004; Schwartz et al. 2009; Bohlen et al. 2011), such that the contribution of sediments in OMZs to the N-deficits in the water column is still unclear. To investigate whether benthic N-loss contributes to the N-deficit in the water column, and if anammox plays an important role for the benthic N-loss in the Arabian Sea, a combination of rate measurements with ^{15}N stable isotopes, quantification and phylogenetic analysis of the biomarker functional genes *nirS* for denitrifiers and anammox bacteria were used (chapter II).

While in the Arabian Sea N-loss activities in sediments are limited by substrate diffusion from the water column, most parts of the seafloor on the continental shelf off Western and NW-Africa are covered by sandy sediment (Holz et al. 2004). In these sediments advective processes as well as bioturbation and irrigation may occur, which provide substrates to deeper sediment layers. From other parts of the worlds ocean, these permeable sediments are known to potentially harbour high N-loss rates via denitrification (Cook et al. 2006; Rao et al. 2007; Rao et al. 2008; Gao et al. 2012; Santos et al. 2012). However, the areas where high N-loss rates were detected in permable sediments are anthopogenically eutophied. The N-loss in permeable subtidal sediments has rarely been investigated and no N-loss measurements have been previously performed on the Western African shelf, although it is a very productive upwelling region and therefore naturally eutrophied. Molecular evidence for the occurrence of anammox bacteria has been found in the sediments (Jaeschke et al. 2010) and benthic N-loss was estimated by a modeling approach based on primary production for the shelf sediments of 0-200 m water depth (Seitzinger and Giblin 1996). To shed light on the question how permeable sediments influence the N-cycling on the NW-African shelf, N-loss has been investigated over an area between 12° and 21° N off Mauritania and Senegal in a range of water depths from 50-3000 m with ^{15}N stable isotope incubations techniques (chapter III).

In the suboxic water column of the Benguela upwelling, high P concentrations in the BBL and high N-loss under anoxic conditions lead to a very low N:P ratio of 1.9 in the bottom water off Namibia (Kuypers et al. 2005). Release of P_i from the sediments might be responsible for these high P concentrations in the BBL. However, it is not known if P is also trapped in the water column by uptake onto particles and organisms. In general, P-uptake in

the sub-euphotic water column is not well constrained and not considered in P-cycling (Delaney 1998; Benitez-Nelson 2000; Paytan and McLaughlin 2007). To investigate P-uptake in the sub-euphotic water column and BBL and how P-uptake in the BBL influences the N:P ratio in the sub-euphotic water column $^{33}PO_4^{3-}$ -uptake experiments were performed (chapter IV). ^{33}P uptake was combined with sequential P extraction (SEDEX) and nanoSIMS analysis to characterize P-uptake mechanisms in the sub-euphotic water columns off Namibia and Mauritania.

In the final chapter (chapter V), the release of P and Fe from sediments undergoing changing oxygen concentrations in the water column was examined with longterm ^{33}P and ^{55}Fe incubations of cores from the Baltic Sea. The Baltic Sea is an enclosed sea lying within the watershed of a heavily populated area (Elmgren 2001). The Baltic Sea exhibits one of the largest so-called "dead-zones" in the world (Diaz and Rosenberg 2008). Seasonal high rates of primary productivity and stratification lead to anoxic and sulfidic conditions in the deep basins and in the shelf areas in summer. Therefore, the Baltic Sea provides an ideal site for expanding repertoire of combined iron and phosphate tracer methods to investigate the interactions of iron and phosphorus cycling in the near-sediment environments.

References

Amann, R. I., W. Ludwig and K. H. Schleifer (1995). "Phylogenetic identification and in-situ detection of individual microbial-cells without cultivation." Microbiological Reviews 59(1): 143-169.

Andersen, F. O. and W. Helder (1987). "Comparison of oxygen microgradients, oxygen flux rates and electron-transport system activity in coastal marine-sediments." Marine Ecology Progress Series 37(2-3): 259-264.

Anderson, L. A. and J. L. Sarmiento (1994). "Redfield ratios of remineralization determined by nutrient data-analysis." Global Biogeochemical Cycles 8(1): 65-80.

Arrigo, K. R. (2005). "Marine microorganisms and global nutrient cycles." Nature 437(7057): 349-355.

Azam, F., T. Fenchel, J. G. Field, J. S. Gray, L. A. Meyerreil and F. Thingstad (1983). "The ecological role of water-column microbes in the sea." Marine Ecology Progress Series 10(3): 257-263.

Benitez-Nelson, C. R. (2000). "The biogeochemical cycling of phosphorus in marine systems." Earth-Science Reviews 51(1-4): 109-135.

Berner, R. A. (1973). "Phosphate removal from sea-water by adsorption on volcanogenic ferric oxides." Earth and Planetary Science Letters 18(1): 77-86.

Bjerrum, C. J. and D. E. Canfield (2002). "Ocean productivity before about 1.9[thinsp]Gyr ago limited by phosphorus adsorption onto iron oxides." Nature 417(6885): 159-162.

Bohlen, L., A. W. Dale, S. Sommer, T. Mosch, C. Hensen, A. Noffke, F. Scholz and K. Wallmann (2011). "Benthic nitrogen cycling traversing the Peruvian oxygen minimum zone." Geochimica Et Cosmochimica Acta 75(20): 6094-6111.

Boyd, P. W., T. Jickells, C. S. Law, S. Blain, E. A. Boyle, K. O. Buesseler, K. H. Coale, J. J. Cullen, H. J. W. de Baar, M. Follows, M. Harvey, C. Lancelot, M. Levasseur, N. P. J. Owens, R. Pollard, R. B. Rivkin, J. Sarmiento, V. Schoemann, V. Smetacek, S. Takeda, A. Tsuda, S. Turner and A. J. Watson (2007). "Mesoscale iron enrichment experiments 1993-2005: Synthesis and future directions." Science 315(5812): 612-617.

Boyer, E. W., R. W. Howarth, J. N. Galloway, F. J. Dentener, P. A. Green and C. J. Vorosmarty (2006). "Riverine nitrogen export from the continents to the coasts." Global Biogeochemical Cycles 20(1): 9.

Canfield, D. E., E. Kristensen and B. Thamdrup (2005). Aquatic geomicrobiology. San Diego, Elsevier Academic Press.

Castro-Gonzalez, M., G. Braker, L. Farias and O. Ulloa (2005). "Communities of nirS-type denitrifiers in the water column of the oxygen minimum zone in the eastern South Pacific." Environmental Microbiology 7(9): 1298-1306.

Christensen, J. P., J. W. Murray, A. H. Devol and L. A. Codispoti (1987). "Denitrification in continental shelf sediments has major impact on the oceanic nitrogen budget." Global Biogeochemical Cycles 1: 97-116.

Codispoti, L. A., J. A. Brandes, J. P. Christensen, A. H. Devol, S. W. A. Naqvi, H. W. Paerl and T. Yoshinari (2001). "The oceanic fixed nitrogen and nitrous oxide budgets: Moving targets as we enter the anthropocene?" Scientia Marina 65: 85-105.

Compton, J., D. Mallinson, C. R. Glenn, G. Filippelli, K. FÃ–Llmi, G. Shields and Y. Zanin (2000). Variations in the global phosphorus cycle. Marine Authigenesis: From Global to Microbial, SEPM (Society for Sedimentary Geology). 66: 21-33.

Cook, P. L. M., F. Wenzhoefer, S. Rysgaard, O. S. Galaktionov, F. J. R. Meysman, B. D. Eyre, J. Cornwell, M. Huettel and R. N. Glud (2006). "Quantification of denitrification in permeable sediments: Insights from a two-dimensional simulation analysis and experimental data." Limnology and Oceanography-Methods 4: 294-307.

Dalsgaard, T., D. E. Canfield, J. Petersen, B. Thamdrup and J. Acuna-Gonzalez (2003). "Anammox is a significant pathway of N_2 production in the anoxic water column of Golfo Dulce, Costa Rica." Nature 422: 606-608.

Dalsgaard, T. and B. Thamdrup (2002). "Factors controlling anaerobic ammonium oxidation with nitrite in marine sediments." Applied Environmental Microbiology 68(8): 3802-3808.

Dalsgaard, T., B. Thamdrup and D. E. Canfield (2005). "Anaerobic ammonium oxidation (anammox) in the marine environment." Research in Microbiology 156(4): 457-464.

Damste, J. S. S., M. Strous, W. I. C. Rijpstra, E. C. Hopmans, J. A. J. Geenevasen, A. C. T. van Duin, L. A. van Niftrik and M. S. M. Jetten (2002). "Linearly concatenated cyclobutane lipids form a dense bacterial membrane." Nature 419(6908): 708-712.

Dang, H., C. Wang, J. Li, T. Li, F. Tian, W. Jin, Y. Ding and Z. Zhang (2009). "Diversity and distribution of sediment NirS-encoding bacterial assemblages in response to environmental gradients in the eutrophied Jiaozhou Bay, China." Microbial Ecology 58(1): 161-169.

Delaney, M. L. (1998). "Phosphorus accumulation in marine sediments and the oceanic phosphorus cycle." Global Biogeochemical Cycles 12(4): 563-572.

Deutsch, C., N. Gruber, R. Key, J. L. Sarmiento and A. Ganachaud (2001). "Denitrification and N_2 fixation in the Pacific Ocean." Global Biogeochemical Cycles 15(2): 483-506.

Deutsch, C., J. L. Sarmiento, D. M. Sigman, N. Gruber and J. P. Dunne (2007). "Spatial coupling of nitrogen inputs and losses in the ocean." Nature 445(7124): 163-167.

Devol, A. H. (2003). "Solution to a marine mystery." Nature 422: 575-576.

Devol, A. H., L. A. Codispoti and J. P. Christensen (1997). "Summer and winter denitrification rates in western Arctic shelf sediments." Continental Shelf Research 17(9): 1029-1033.

Devol, A. H., S. W. A. Naqvi and L. A. Codispoti (2006). Nitrogen cycling in the suboxic waters of the Arabian Sea. NATO Science Series IV Earth and Environmental Sciences : 64, Past and Present Water Column Anoxia. L. Neretin. Amsterdam, IOS Press and Kluwer Academic Publishers in conjunction with the NATO Scientific Affairs Division: 283-310.

DeVries, T., C. Deutsch, F. Primeau, B. Chang and A. Devol (2012). "Global rates of water-column denitrification derived from nitrogen gas measurements." Nature Geosci 5(8): 547-550.

Diaz, J., E. Ingall, C. Benitez-Nelson, D. Paterson, M. D. de Jonge, I. McNulty and J. A. Brandes (2008). "Marine polyphosphate: A key player in geologic phosphorus sequestration." Science 320(5876): 652-655.

Diaz, J. M., E. D. Ingall, S. D. Snow, C. R. Benitez-Nelson, M. Taillefert and J. A. Brandes (2012). "Potential role of inorganic polyphosphate in the cycling of phosphorus within the hypoxic water column of Effingham Inlet, British Columbia." Global Biogeochemical Cycles 26: 13.

Diaz, R. J. and R. Rosenberg (2008). "Spreading dead zones and consequences for marine ecosystems." Science 321(5891): 926-929.

Dong, L. F., C. J. Smith, S. Papaspyrou, A. Stott, A. M. Osborn and D. B. Nedwell (2009). "Changes in benthic denitrification, nitrate ammonification, and anammox process rates and nitrate and nitrite reductase gene abundances along an estuarine nutrient gradient (the Colne Estuary, United Kingdom)." Applied and Environmental Microbiology 75(10): 3171-3179.

Elmgren, R. (2001). "Understanding human impact on the Baltic ecosystem: Changing views in recent decades." Ambio 30(4-5): 222-231.

Emery, K. O. (1968). "Relict sediments on continental shelves of world." AAPG Bulletin 52(3): 445-464.

Ettwig, K. F., M. K. Butler, D. Le Paslier, E. Pelletier, S. Mangenot, M. M. M. Kuypers, F. Schreiber, B. E. Dutilh, J. Zedelius, D. de Beer, J. Gloerich, H. Wessels, T. van Alen, F. Luesken, M. L. Wu, K. T. van de Pas-Schoonen, H. den Camp, E. M. Janssen-Megens, K. J. Francoijs, H. Stunnenberg, J. Weissenbach, M. S. M. Jetten and M. Strous (2010). "Nitrite-driven anaerobic methane oxidation by oxygenic bacteria." Nature 464(7288): 543-548.

Evrard, V., R. Glud and P. M. Cook (2012). "The kinetics of denitrification in permeable sediments." Biogeochemistry: 1-10.

Falkowski, P. G. (1997). "Evolution of the nitrogen cycle and its influence on the biological sequestration of CO2 in the ocean." Nature 387: 272-275.

Farías, L., M. Graco and O. Ulloa (2004). "Temporal variability of nitrogen cycling in continental-shelf sediments of the upwelling ecosystem off central Chile." Deep-Sea Research Part II-Topical Studies in Oceanography 51(20-21): 2491-2505.

Fossing, H., V. A. Gallardo, B. B. Jorgensen, M. Huttel, L. P. Nielsen, H. Schulz, D. E. Canfield, S. Forster, R. N. Glud, J. K. Gundersen, J. Kuver, N. B. Ramsing, A. Teske, B. Thamdrup and O. Ulloa (1995). "Concentration and Transport of Nitrate by the Mat-Forming Sulfur Bacterium Thioploca." Nature 374(6524): 713-715.

Froelich, P. N., M. L. Bender, N. A. Luedtke, G. R. Heath and T. Devries (1982). "The marine phosphorus cycle." American Journal of Science 282(4): 474-511.

Fuessel, J., P. Lam, G. Lavik, M. M. Jensen, M. Holtappels, M. Günter and M. M. M. Kuypers (2012). "Nitrite oxidation in the Namibian oxygen minimum zone." ISME Journal 6(6): 1200-1209.

Gao, H., M. Matyka, B. Liu, A. Khalili, J. E. Kostka, G. Collins, S. Jansen, M. Holtappels, M. M. Jensen, T. H. Badewien, M. Beck, M. Grunwald, D. de Beer, G. Lavik and M. M. M. Kuypers (2012). "Intensive and extensive nitrogen loss from intertidal permeable sediments of the Wadden Sea." Limnology and Oceanography 57(1): 185-198.

Gao, H., F. Schreiber, G. Collins, M. M. Jensen, J. E. Kostka, G. Lavik, D. de Beer, H.-y. Zhou and M. M. M. Kuypers (2010). "Aerobic denitrification in permeable Wadden Sea sediments." Isme Jounal 4(3): 417-426.

Geider, R. and J. La Roche (2002). "Redfield revisited: variability of C:N:P in marine microalgae and its biochemical basis." European Journal of Phycology 37(1): 1-17.

Gihring, T. M., A. Canion, A. Riggs, M. Huettel and J. E. Kostka (2010). "Denitrification in shallow, sublittoral Gulf of Mexico permeable sediments." Limnology and Oceanography 55(1): 43-54.

Glud, R. N. (2008). "Oxygen dynamics of marine sediments." Marine Biology Research 4(4): 243-289.

Glud, R. N., B. Thamdrup, H. Stahl, F. Wenzhoefer, A. Glud, H. Nomaki, K. Oguri, N. P. Revsbech and H. Kitazato (2009). "Nitrogen cycling in a deep ocean margin sediment (Sagami Bay, Japan)." Limnology and Oceanography 54(3): 723–734.

Goldhammer, T., V. Brüchert, T. G. Ferdelman and M. Zabel (2010). "Microbial sequestration of phosphorus in anoxic upwelling sediments." Nature Geoscience 3(8): 557-561.

Graf, G. (1992). "Benthic-pelagic coupling: a benthic view." Oceanography and Marine Biology: An Annual Review 30.

Grosskopf, T., W. Mohr, T. Baustian, H. Schunck, D. Gill, M. M. M. Kuypers, G. Lavik, R. A. Schmitz, D. W. R. Wallace and J. LaRoche (2012). "Doubling of marine dinitrogen-fixation rates based on direct measurements." Nature 488(7411): 361-364.

Gruber, N. (2004). The dynamics of the marine nitrogen cycle and its influence on atmospheric CO_2 variations NATO Science Series IV Earth and Environmental Sciences : 40, The Ocean Carbon Cycle and Climate. M. Follows and T. Oguz. Dordrecht, Kluwer Academic Publishers: 97-148.

Gruber, N. and J. L. Sarmiento (1997). "Global patterns of marine nitrogen fixation and denitrification." Global Biogeochemical Cycles 11(2): 235-266.

Gruntzig, V., S. C. Nold, J. Z. Zhou and J. M. Tiedje (2001). "Pseudomonas stutzeri nitrite reductase gene abundance in environmental samples measured by real-time PCR." Applied and Environmental Microbiology 67(2): 760-768.

Hamersley, M. R., G. Lavik, D. Woebken, J. E. Rattray, P. Lam, E. C. Hopmans, J. S. S. Damste, S. Kruger, M. Graco, D. Gutierrez and M. M. M. Kuypers (2007). "Anaerobic ammonium oxidation in the Peruvian oxygen minimum zone." Limnology and Oceanography 52(3): 923-933.

Herbert, R. A. (1999). "Nitrogen cycling in coastal marine ecosystems." FEMS Microbiology Reviews 23(5): 563-590.

Holtappels, M., G. Lavik, M. M. Jensen and M. M. M. Kuypers (2011). ^{15}N-labeling experiments to dissect the contributions of heterotrophic denitrification and anammox to nitrogen removal in the OMZ waters of the ocean. Methods in Enzymology: Research on Nitrification and Related Processes, Vol 486, Part A. M. Klotz. San Diego, Elsevier Academic Press Inc. 486: 223-251.

Holz, C., J. B. W. Stuut and R. Henrich (2004). "Terrigenous sedimentation processes along the continental margin off NW Africa: implications from grain-size analysis of seabed sediments." Sedimentology 51(5): 1145-1154.

Howarth, R. W., G. Billen, D. Swaney, A. Townsend, N. Jaworski, K. Lajtha, J. A. Downing, R. Elmgren, N. Caraco, T. Jordan, F. Berendse, J. Freney, V. Kudeyarov, P. Murdoch and Z. L. Zhu (1996). "Regional nitrogen budgets and riverine N & P fluxes for the drainages to the North Atlantic Ocean: Natural and human influences." Biogeochemistry 35: 75-139.

Huettel, M., H. Roy, E. Precht and S. Ehrenhauss (2003). "Hydrodynamical impact on biogeochemical processes in aquatic sediments." Hydrobiologia 494(1-3): 231-236.

Huettel, M. and A. Rusch (2000). "Transport and degradation of phytoplankton in permeable sediment." Limnology and Oceanography 45(3): 534-549.

Ingall, E. and R. Jahnke (1994). "Evidence for enhanced phosphorus regeneration from marine-sediments overlain by oxygen depleted waters." Geochimica Et Cosmochimica Acta 58(11): 2571-2575.

Jaeschke, A., B. Abbas, M. Zabel, E. C. Hopmans, S. Schouten and J. S. S. Damste (2010). "Molecular evidence for anaerobic ammonium-oxidizing (anammox) bacteria in continental shelf and slope sediments off northwest Africa." Limnology and Oceanography 55(1): 365-376.

Jaeschke, A., E. C. Hopmans, S. G. Wakeham, S. Schouten and J. S. S. Damste (2007). "The presence of ladderane lipids in the oxygen minimum zone of the Arabian Sea indicates nitrogen loss through anammox." Limnology and Oceanography 52(2): 780-786.

Jayakumar, D. A., C. A. Francis, S. W. A. Naqvi and B. B. Ward (2004). "Diversity of nitrite reductase genes (nirS) in the denitrifying water column of the coastal Arabian Sea." Aquatic Microbial Ecology 34(1): 69-78.

Jensen, M. M., P. Lam, N. P. Revsbech, B. Nagel, B. Gaye, M. S. M. Jetten and M. M. M. Kuypers (2011). "Intensive nitrogen loss over the Omani Shelf due to anammox coupled with dissimilatory nitrite reduction to ammonium." Isme Journal 5(10): 1660-1670.

Jickells, T. D. (1998). "Nutrient Biogeochemistry of the Coastal Zone." Science 281(5374): 217-222.

Jilbert, T. and C. P. Slomp (2013). "Iron and manganese shuttles control the formation of authigenic phosphorus minerals in the euxinic basins of the Baltic Sea." Geochimica et Cosmochimica Acta 107(0): 155-169.

Jørgensen, B. B. and V. A. Gallardo (1999). "Thioploca spp: filamentous sulfur bacteria with nitrate vacuoles." Fems Microbiology Ecology 28(4): 301-313.

Kalvelage, T., G. Lavik, P. Lam, S. Contreras, L. Arteaga, C. R. Loscher, A. Oschlies, A. Paulmier, L. Stramma and M. M. M. Kuypers (2013). "Nitrogen cycling driven by organic matter export in the South Pacific oxygen minimum zone." Nature Geosci 6(3): 228-234.

Karl, D., A. Michaels, B. Bergman, D. Capone, E. Carpenter, R. Letelier, F. Lipschultz, H. Paerl, D. Sigman and L. Stal (2002). "Dinitrogen fixation in the world's oceans." Biogeochemistry 57(1): 47-98.

Kessler, A. J., R. N. Glud, M. B. Cardenas, M. Larsen, M. F. Bourke and P. L. M. Cook (2012). "Quantifying denitrification in rippled permeable sands through combined flume experiments and modeling." Limnology and Oceanography 57(4): 1217-1232.

Klausmeier, C. A., E. Litchman, T. Daufresne and S. A. Levin (2004). "Optimal nitrogen-to-phosphorus stoichiometry of phytoplankton." Nature 429(6988): 171-174.

Kuypers, M. M. M., G. Lavik, D. Woebken, M. Schmid, B. M. Fuchs, R. Amann, B. B. Jørgensen and M. S. M. Jetten (2005). "Massive nitrogen loss from the Benguela upwelling system through anaerobic ammonium oxidation." Proceedings of the National Academy of Sciences of the United States of America 102(18): 6478-6483.

Kuypers, M. M. M., A. O. Sliekers, G. Lavik, M. Schmid, B. B. Jorgensen, J. G. Kuenen, J. S. S. Damste, M. Strous and M. S. M. Jetten (2003). "Anaerobic ammonium oxidation by anammox bacteria in the Black Sea." Nature 422(6932): 608-611.

Lam, P., M. M. Jensen, A. Kock, K. A. Lettmann, Y. Plancherel, G. Lavik, H. W. Bange and M. M. M. Kuypers (2011). "Origin and fate of the secondary nitrite maximum in the Arabian Sea." Biogeosciences 8(6): 1565-1577.

Lam, P., G. Lavik, M. M. Jensen, J. van de Vossenberg, M. Schmid, D. Woebken, G. Dimitri, R. Amann, M. S. M. Jetten and M. M. M. Kuypers (2009). "Revising the nitrogen cycle in the Peruvian oxygen minimum zone." Proceedings of the National Academy of Sciences of the United States of America 106(12): 4752-4757.

Lipschultz, F., S. C. Wofsy, B. B. Ward, L. A. Codispoti, G. Friedrich and J. W. Elkins (1990). "Bacterial transformations of inorganic nitrogen in the oxygen-deficient waters of the Eastern Tropical South Pacific Ocean." Deep Sea Research Part A. Oceanographic Research Papers 37(10): 1513-1541.

Liu, X. D., S. M. Tiquia, G. Holguin, L. Y. Wu, S. C. Nold, A. H. Devol, K. Luo, A. V. Palumbo, J. M. Tiedje and J. Z. Zhou (2003). "Molecular diversity of denitrifying genes in continental margin sediments within the oxygen-deficient zone off the Pacific coast of Mexico." Applied and Environmental Microbiology 69(6): 3549-3560.

Middelburg, J. J., K. Soetaert, P. M. J. Herman and C. H. R. Heip (1996). "Denitrification in Marine Sediments: A Model Study." Global Biogeochemical Cycles 10(4).

Mulder, A., A. A. Vandegraaf, L. A. Robertson and J. G. Kuenen (1995). "Anaerobic Ammonium Oxidation Discovered in a Denitrifying Fluidized-Bed Reactor." Fems Microbiology Ecology 16(3): 177-183.

Naqvi, S. W. A. (1994). "Denitrification Processes in the Arabian Sea." Proceedings of the Indian Academy of Sciences-Earth and Planetary Sciences 103(2): 279-300.

Naqvi, S. W. A., H. Naik, A. Pratihary, W. D'Souza, P. V. Narvekar, D. A. Jayakumar, A. H. Devol, T. Yoshinari and T. Saino (2006). "Coastal versus open-ocean denitrification in the Arabian Sea." Biogeosciences 3(4): 621-633.

Naqvi, S. W. A., R. J. Noronha, M. S. Shailaja, K. Somasundar and R. S. Gupta (1991). Some aspects of the nitrogen cycling in the Arabian Sea. International Symp on the Oceanography of the Indian Ocean (Isoio), Goa, India, A a Balkema.

Nielsen, L. P. (1992). "Denitrification in sediment determined from nitrogen isotope pairing." Fems Microbiology Ecology 86(4): 357-362.

Noffke, A., C. Hensen, S. Sommer, F. Scholz, L. Bohlen, T. Mosch, M. Graco and K. Wallmann (2012). "Benthic iron and phosphorus fluxes across the Peruvian oxygen minimum zone." Limnology and Oceanography 57(3): 851-867.

Olsen, G. J., D. J. Lane, S. J. Giovannoni, N. R. Pace and D. A. Stahl (1986). "Microbial ecology and evolution - a ribosomal-RNA approach." Annual Review of Microbiology 40: 337-365.

Oschlies, A., K. G. Schulz, U. Riebesell and A. Schmittner (2008). "Simulated 21st century's increase in oceanic suboxia by CO2-enhanced biotic carbon export." Global Biogeochemical Cycles 22(4): n/a-n/a.

Otte, S., J. G. Kuenen, L. P. Nielsen, H. W. Paerl, J. Zopfi, H. N. Schulz, A. Teske, B. Strotmann, V. A. Gallardo and B. B. Jorgensen (1999). "Nitrogen, carbon, and sulfur metabolism in natural Thioploca samples." Applied and Environmental Microbiology 65(7): 3148-3157.

Palastanga, V., C. P. Slomp and C. Heinze (2011). "Long-term controls on ocean phosphorus and oxygen in a global biogeochemical model." Global Biogeochemical Cycles 25.

Paytan, A. and K. McLaughlin (2007). "The oceanic phosphorus cycle." Chemical Reviews 107(2): 563-576.

Quigg, A., Z. V. Finkel, A. J. Irwin, Y. Rosenthal, T.-Y. Ho, J. R. Reinfelder, O. Schofield, F. M. M. Morel and P. G. Falkowski (2003). "The evolutionary inheritance of elemental stoichiometry in marine phytoplankton." Nature 425(6955): 291-294.

Raghoebarsing, A. A., A. Pol, K. T. van de Pas-Schoonen, A. J. P. Smolders, K. F. Ettwig, W. I. C. Rijpstra, S. Schouten, J. S. S. Damste, H. J. M. Op den Camp, M. S. M. Jetten and M. Strous (2006). "A microbial consortium couples anaerobic methane oxidation to denitrification." Nature 440(7086): 918-921.

Rao, A. M. F., M. J. McCarthy, W. S. Gardner and R. A. Jahnke (2007). "Respiration and denitrification in permeable continental shelf deposits on the South Atlantic Bight: Rates of carbon and nitrogen cycling from sediment column experiments." Continental Shelf Research 27(13): 1801-1819.

Rao, A. M. F., M. J. McCarthy, W. S. Gardner and R. A. Jahnke (2008). "Respiration and denitrification in permeable continental shelf deposits on the South Atlantic Bight: N_2 : Ar and isotope pairing measurements in sediment column experiments." Continental Shelf Research 28(4-5): 602-613.

Raven, J. A. and P. G. Falkowski (1999). "Oceanic sinks for atmospheric CO2." Plant, Cell & Environment 22(6): 741-755.

Redfield, A. C., B. H. Ketchum and F. A. Richards (1963). "The influence of organisms on the composition of sea-water." Hill, M.N. (Ed.) (1963). The composition of seawater. Comparative and descriptive oceanography. The sea: ideas and observations on progress in the study of the seas 2: 26-77.

Ritzrau, W., L. Thomsen, R. J. Lara and G. Graf (1997). "Enhanced microbial utilisation of dissolved amino acids indicates rapid modification of organic matter in the benthic boundary layer." Marine Ecology-Progress Series 156: 43-50.

Rosenberg, H., R. G. Gerdes and K. Chegwidden (1977). "Two systems for the uptake of phosphate in Escherichia coli." Journal of Bacteriology 131(2): 505-511.

Rozan, T. F., M. Taillefert, R. E. Trouwborst, B. T. Glazer, S. F. Ma, J. Herszage, L. M. Valdes, K. S. Price and G. W. Luther (2002). "Iron-sulfur-phosphorus cycling in the sediments of a shallow coastal bay: Implications for sediment nutrient release and benthic macroalgal blooms." Limnology and Oceanography 47(5): 1346-1354.

Ruttenberg, K. C. (1992). "Development of a Sequential Extraction Method for Different Forms of Phosphorus in Marine-Sediments." Limnology and Oceanography 37(7): 1460-1482.

Ruttenberg, K. C. and R. A. Berner (1993). "Authigenic apatite formation and burial in sediments from non-upwelling, continental margin environments." Geochimica et Cosmochimica Acta 57(5): 991-1007.

Ruttenberg, K. C. and D. J. Sulak (2011). "Sorption and desorption of dissolved organic phosphorus onto iron (oxyhydr)oxides in seawater." Geochimica Et Cosmochimica Acta 75(15): 4095-4112.

Santos, I. R., B. D. Eyre and R. N. Glud (2012). "Influence of porewater advection on denitrification in carbonate sands: Evidence from repacked sediment column experiments." Geochimica Et Cosmochimica Acta 96: 247-258.

Sanudo-Wilhelmy, S. A., A. Tovar-Sanchez, F. X. Fu, D. G. Capone, E. J. Carpenter and D. A. Hutchins (2004). "The impact of surface-adsorbed phosphorus on phytoplankton Redfield stoichiometry." Nature 432(7019): 897-901.

Schalk, J., S. de Vries, J. G. Kuenen and M. S. M. Jetten (2000). "Involvement of a novel hydroxylamine oxidoreductase in anaerobic ammonium oxidation." Biochemistry 39(18): 5405-5412.

Schalk, J., H. Oustad, J. G. Kuenen and M. S. M. Jetten (1998). "The anaerobic oxidation of hydrazine: a novel reaction in microbial nitrogen metabolism." Fems Microbiology Letters 158(1): 61-67.

Schippers, A. and L. N. Neretin (2006). "Quantification of microbial communities in near-surface and deeply buried marine sediments on the Peru continental margin using real-time PCR." Environmental Microbiology 8(7): 1251-1260.

Schmittner, A., A. Oschlies, H. D. Matthews and E. D. Galbraith (2009). "Future changes in climate, ocean circulation, ecosystems, and biogeochemical cycling simulated for a business-as-usual CO2 emission scenario until year 4000 AD (vol 23, art no GB3005, 2009)." Global Biogeochemical Cycles 23.

Schulz, H. N., T. Brinkhoff, T. G. Ferdelman, M. H. Marine, A. Teske and B. B. Jorgensen (1999). "Dense populations of a giant sulfur bacterium in Namibian shelf sediments." Science 284(5413): 493-495.

Schulz, H. N. and H. D. Schulz (2005). "Large sulfur bacteria and the formation of phosphorite." Science 307(5708): 416-418.

Schwartz, M. C., C. Woulds and G. L. Cowie (2009). "Sedimentary denitrification rates across the Arabian Sea oxygen minimum zone." Deep Sea Research Part II: Topical Studies in Oceanography 56(6-7): 324-332.

Seitzinger, S. and A. Giblin (1996). "Estimating denitrification in North Atlantic continental shelf sediments." Biogeochemistry 35(1): 235-260.

Shaffer, G. (1986). "Phosphate pumps and shuttles in the Black-Sea." Nature 321(6069): 515-517.

Slomp, C. P. (2011). Phosphorus Cycling in the Estuarine and Coastal Zones: Sources, Sinks, and Transformations. Treatise on Estuarine and Coastal Science. W. E. a. M. DS, Waltham: Academic Press. 5: 201-229.

Slomp, C. P., E. H. G. Epping, W. Helder and W. van Raaphorst (1996). "A key role for iron-bound phosphorus in authigenic apatite formation in North Atlantic continental platform sediments." Journal of Marine Research 54(6): 1179-1205.

Slomp, C. P. and P. van Cappellen (2007). "The global marine phosphorus cycle: sensitivity to oceanic circulation." Biogeosciences 4(2): 155-171.

Smetacek, V., C. Klaas, V. H. Strass, P. Assmy, M. Montresor, B. Cisewski, N. Savoye, A. Webb, F. d'Ovidio, J. M. Arrieta, U. Bathmann, R. Bellerby, G. M. Berg, P. Croot, S. Gonzalez, J. Henjes, G. J. Herndl, L. J. Hoffmann, H. Leach, M. Losch, M. M. Mills, C. Neill, I. Peeken, R. Röttgers, O. Sachs, E. Sauter, M. M. Schmidt, J. Schwarz, A. Terbruggen and D. Wolf-Gladrow (2012). "Deep carbon export from a Southern Ocean iron-fertilized diatom bloom." Nature 487(7407): 313-319.

Stramma, L., G. C. Johnson, J. Sprintall and V. Mohrholz (2008). "Expanding oxygen-minimum zones in the tropical oceans." Science 320(5876): 655-658.

Straub, K. L., M. Benz, B. Schink and F. Widdel (1996). "Anaerobic, nitrate-dependent microbial oxidation of ferrous iron." Applied and Environmental Microbiology 62(4): 1458-1460.

Strous, M., E. Pelletier, S. Mangenot, T. Rattei, A. Lehner, M. W. Taylor, M. Horn, H. Daims, D. Bartol-Mavel, P. Wincker, V. Barbe, N. Fonknechten, D. Vallenet, B. Segurens, C. Schenowitz-Truong, C. Medigue, A. Collingro, B. Snel, B. E. Dutilh, H. J. M. Op den Camp, C. van der Drift, I. Cirpus, K. T. van de Pas-Schoonen, H. R. Harhangi, L. van Niftrik, M. Schmid, J. Keltjens, J. van de Vossenberg, B. Kartal, H. Meier, D. Frishman, M. A. Huynen, H. W. Mewes, J. Weissenbach, M. S. M. Jetten, M. Wagner and D. Le Paslier (2006). "Deciphering the evolution and metabolism of an anammox bacterium from a community genome." Nature 440(7085): 790-794.

Suess, E. (1979). "Mineral phases formed in anoxic sediments by microbial decomposition of organic matter." Geochimica et Cosmochimica Acta 43(3): 339-352.

Suess, E. (1980). "Particulate organic-carbon flux in the oceans - surface productivity and oxygen utilization." Nature 288(5788): 260-263.

Sundby, B., L. G. Anderson, P. O. J. Hall, A. Iverfeldt, M. M. R. Vanderloeff and S. F. G. Westerlund (1986). "The effect of oxygen on release and uptake of cobalt, manganese, iron and phosphate at the sediment-water interface." Geochimica Et Cosmochimica Acta 50(6): 1281-1288.

Takahashi, T., W. S. Broecker and S. Langer (1985). "Redfield ratio based on chemical data from isopycnal surfaces." Journal of Geophysical Research: Oceans 90(C4): 6907-6924.

Thamdrup, B. and T. Dalsgaard (2000). "The fate of ammonium in anoxic manganese oxide-rich marine sediment." Geochimica et Cosmochimica Acta 64(24): 4157-4164.

Thamdrup, B. and T. Dalsgaard (2002). "Production of N_2 through anaerobic ammonium oxidation coupled to nitrate reduction in marine sediment." Applied and Environmental Microbiology 68(3): 1312-1318.

Thamdrup, B., T. Dalsgaard, M. M. Jensen, O. Ulloa, L. Farias and R. Escribano (2006). "Anaerobic ammonium oxidation in the oxygen-deficient waters off northern Chile." Limnology and Oceanography 51(5): 2145-2156.

Thingstad, T. F., E. F. Skjoldal and R. A. Bohne (1993). "Phosphorus cycling and algal-bacterial competition in Sandsfjord, Western Norway." Marine Ecology-Progress Series 99(3): 239-259.

Thomsen, L., T. vanWeering and G. Gust (2002). "Processes in the benthic boundary layer at the Iberian continental margin and their implication for carbon mineralization." Progress in Oceanography 52(2-4): 315-329.

Tiquia, S. M., S. A. Masson and A. Devol (2006). "Vertical distribution of nitrite reductase genes (nirS) in continental margin sediments of the Gulf of Mexico." Fems Microbiology Ecology 58(3): 464-475.

Trick, C. G., B. D. Bill, W. P. Cochlan, M. L. Wells, V. L. Trainer and L. D. Pickell (2010). "Iron enrichment stimulates toxic diatom production in high-nitrate, low-chlorophyll areas." PNAS 107(13): 5887-5892.

Trimmer, M. and J. C. Nicholls (2009). "Production of nitrogen gas via anammox and denitrification in intact sediment cores along a continental shelf to slope transect in the North Atlantic." Limnology and Oceanography 54(2): 577-589.

Turnewitsch, R. and C. Pohl (2010). "An estimate of the efficiency of the iron- and manganese-driven dissolved inorganic phosphorus trap at an oxic/euxinic water column redoxcline." Global Biogeochemical Cycles 24.

Tyrrell, T. (1999). "The relative influences of nitrogen and phosphorus on oceanic primary production." Nature 400(6744): 525-531.

van Cappellen, P. and E. D. Ingall (1994). "Benthic phosphorus regeneration, net primary production, and ocean anoxia - a model of the coupled marine biogeochemical cycles of carbon and phosphorus." Paleoceanography 9(5): 677-692.

van Cappellen, P. and E. D. Ingall (1996). "Redox stabilization of the atmosphere and oceans by phosphorus-limited marine productivity." Science 271(5248): 493-496.

van de Graaf, A. A., P. de Bruijn, L. A. Robertson, M. S. M. Jetten and J. G. Kuenen (1997). "Metabolic pathway of anaerobic ammonium oxidation on the basis of N_{15} studies in a fluidized bed reactor." Microbiology-Uk 143: 2415-2421.

van de Vossenberg, J., J. E. Rattray, W. Geerts, B. Kartal, L. van Niftrik, E. G. van Donselaar, J. S. S. Damste, M. Strous and M. S. M. Jetten (2008). "Enrichment and characterization of marine anammox bacteria associated with global nitrogen gas production." Environmental Microbiology 10(11): 3120-3129.

van Niftrik, L. A., J. A. Fuerst, J. S. S. Damste, J. G. Kuenen, M. S. M. Jetten and M. Strous (2004). "The anammoxosome: an intracytoplasmic compartment in anammox bacteria." Fems Microbiology Letters 233(1): 7-13.

van Veen, H. W., T. Abee, G. J. J. Kortstee, W. N. Konings and A. J. B. Zehnder (1993). "Mechanism and energetics of the secondary phosphate-transport system of Acinetobacter-Johnsonii-210a." Journal of Biological Chemistry 268(26): 19377-19383.

Vance-Harris, C. and E. Ingall (2005). "Denitrification pathways and rates in the sandy sediments of the Georgia continental shelf, USA." Geochemical Transactions 6(1): 12-18.

Vitousek, P. M., J. D. Aber, R. W. Howarth, G. E. Likens, P. A. Matson, D. W. Schindler, W. H. Schlesinger and G. D. Tilman (1997). "Human alteration of the global nitrogen cycle: Sources and consequences." Ecological Applications 7(3): 737-750.

Wallenstein, M. D., D. D. Myrold, M. Firestone and M. Voytek (2006). "Environmental controls on denitrifying communities and denitrification rates: insights from molecular methods." Ecological Applications 16(6): 2143-2152.

Wallenstein, M. D. and R. J. Vilgalys (2005). "Quantitative analyses of nitrogen cycling genes in soils." Pedobiologia 49(6): 665-672.

Ward, B. B., A. H. Devol, J. J. Rich, B. X. Chang, S. E. Bulow, H. Naik, A. Pratihary and A. Jayakumar (2009). "Denitrification as the dominant nitrogen loss process in the Arabian Sea." Nature 461(7260): 78-81.

Warembourg, F. R. (1993). Nitrogen fixation in soil and plant systems. Nitrogen isotopes techniques. K. Knowles and T. H. Blackburn. San Diego, USA, Academic Press: 157–180.

Weber, K. A., L. A. Achenbach and J. D. Coates (2006). "Microorganisms pumping iron: anaerobic microbial iron oxidation and reduction." Nature Reviews Microbiology 4(10): 752-764.

Weber, T. S. and C. Deutsch (2010). "Ocean nutrient ratios governed by plankton biogeography." Nature 467(7315): 550-554.

Wheat, C. G., R. A. Feely and M. J. Mottl (1996). "Phosphate removal by oceanic hydrothermal processes: An update of the phosphorus budget in the oceans." Geochimica Et Cosmochimica Acta 60(19): 3593-3608.

Wollast, R. (1998). "Evaluation and comparison of the global carbon cycle in the coastal zone and in the open ocean." The sea 10: 213-252.

Zehr, J. P., I. Hewson and P. Moisander (2009). "Molecular biology techniques and applications for ocean sensing." Ocean Science. 5(2): 101-113.

Zubkov, M. V., I. Mary, E. M. S. Woodward, P. E. Warwick, B. M. Fuchs, D. J. Scanlan and P. H. Burkill (2007). "Microbial control of phosphate in the nutrient-depleted North Atlantic subtropical gyre." Environmental Microbiology 9(8): 2079-2089.

Zumft, W. G. (1997). "Cell biology and molecular basis of denitrification." Microbiology and Molecular Biology Reviews 61(4): 533-616.

Overview of manuscripts

Chapter II:

Benthic nitrogen loss in the Arabian Sea off Pakistan

Sarah Sokoll, Moritz Holtappels, Phyllis Lam, Gavin Collins, Michael Schlüter, Gaute Lavik and Marcel M. M. Kuypers.

Sampling campaign and experimental design was initiated by M. M. M. Kuypers, G. Lavik and G. Collins. M. Holtappels and G. Collins performed the on-board experiments and sampling. S. Sokoll measured $^{15}N_2$ and performed the molecular analysis with advice of P. Lam. M. Schlüter measured the pore water. Data analysis was done by S. Sokoll, M. Holtappels, P. Lam and G. Lavik. The manuscript was written by S. Sokoll with input of P. Lam, M. Holtappels, G. Lavik and M. M. M. Kuypers.

Published in Frontiers in Microbiology. 3:395. 2012

Chapter III:

Extensive nitrogen loss from permeable sediments off North West Africa

Sarah Sokoll, Moritz Holtappels, Gaute Lavik, Stefan Sommer, Tobias Goldhammer, and Marcel M. M. Kuypers

The study was initiated by S. Sokoll, M. Holtappels, G. Lavik and M. M. M. Kuypers. The on-board incubation experiments were performed by S. Sokoll and G. Lavik. Pore water analysis on P398 was performed by T. Goldhammer and on MSM 17/4 by S. Sommer. $^{15}N_2$ and water nutrients were measured by S. Sokoll. The data was analyzed by S. Sokoll and M. Holtappels. The denitrification model was designed by M. Holtappels. The manuscript was written by S. Sokoll with input of the co-authors.

Manuscript in preparation.

Chapter IV:

Intense biological phosphate uptake in the sub-euphotic zone of upwelling areas

Sarah Sokoll, Timothy G. Ferdelman, Moritz Holtappels, Tobias Goldhammer, Sten Littmann, Morten H. Iversen and Marcel M. M. Kuypers

S. Sokoll designed the study with input of T. Ferdelman, T. Goldhammer, M. Holtappels, M. M. M. Kuypers. The ^{33}P experiments and the extraction were performed by S. Sokoll. T. Goldhammer analyzed the extracts at the ICP. M. H. Iversen measured the particulate organic carbon for MSM19/1. S. Littmann performed the nanoSIMS analysis. Data was analysed by S. Sokoll and T. Ferdelman. S. Sokoll wrote the manuscript with input of the co-authors.

Manuscript in preparation for Nature Geoscience

Chapter V:

Iron and phosphorus dynamics in bottom waters under variable redox conditions

Sarah Sokoll, Timothy G. Ferdelman and Moritz Holtappels

S. Sokoll designed the study with input of T. Ferdelman and M. Holtappels. Sediment samples were collected by M. Holtappels. S. Sokoll and M. Holtappels designed the incubation set-up. Sampling and sample analysis was performed by S. Sokoll. Data was analyzed by S. Sokoll. The report was written by S. Sokoll with the input of the co-authors.

Research report

Chapter II

Benthic nitrogen loss in the Arabian Sea off Pakistan

Sarah Sokoll[1], Moritz Holtappels[1], Phyllis Lam[1], Gavin Collins[2], Michael Schlüter[3], Gaute Lavik[1] and Marcel M. M. Kuypers[1]

[1] Max Planck Institute for Marine Microbiology, Bremen, Germany
[2]School of Natural Sciences, National University of Ireland, Galway, Ireland
[3]Alfred Wegener Institute, Bremerhaven, Germany

Abstract

A pronounced deficit of nitrogen (N) in the oxygen minimum zone (OMZ) of the Arabian Sea suggests the occurrence of heavy N-loss that is commonly attributed to pelagic processes. However, the OMZ water is in direct contact with sediments on three sides of the basin. Contribution from benthic N-loss to the total N-loss in the Arabian Sea remains largely unassessed. In October 2007, we sampled the water column and surface sediments along a transect cross-cutting the Arabian Sea OMZ at the Pakistan continental margin, covering a range of station depths from 360 to 1430 m. Benthic denitrification and anammox rates were determined by using ^{15}N-stable isotope pairing experiments. Intact core incubations showed declining rates of total benthic N-loss with water depth from 0.55 to 0.18 mmol N m^{-2} d^{-1}. While denitrification rates measured in slurry incubations decreased from 2.73 to 1.46 mmol N m^{-2} d^{-1} with water depth, anammox rates increased from 0.21 to 0.89 mmol N m^{-2} d^{-1}. Hence, the contribution from anammox to total benthic N-loss increased from 7% at 360 m to 40% at 1430 m. This trend is further supported by the quantification of *nirS*, the biomarker functional gene encoding for cytochrome cd_1-nitrite reductases of microorganisms involved in both N-loss processes. Anammox-like *nirS* genes within the sediments increased in proportion to total *nirS* gene copies with water depth. Moreover, phylogenetic analyses of *nirS* revealed different communities of both denitrifying and anammox bacteria between shallow and deep stations. Together, rate measurement and *nirS* analyses showed that anammox, determined for the first time in the Arabian Sea sediments, is an important benthic N-loss process at the continental margin off Pakistan, especially in the sediments at deeper water depths. Extrapolation from the measured benthic N-loss to all shelf sediments within the basin suggests that benthic N-loss may be responsible for about half of the overall N-loss in the Arabian Sea.

Introduction

The Arabian Sea is the semi-enclosed, north-western part of the Indian Ocean. Connected with the Red Sea and the Persian Gulf, it also receives discharge from some of the largest rivers in the world and is fringed by amongst the densest human populations. Although covering only 1% of the ocean surface, the Arabian Sea accounts for approximately 5% of the global phytoplankton production, which has characteristic seasonal variability driven by two monsoons each year (Marra and Barber, 2005;Wiggert et al., 2005). Owing to the high seasonal surface production, high respiration in subsurface waters along with slow ventilation produces a pronounced oxygen minimum zone (OMZ) at depths between ~100 and 1000 m. This OMZ is associated with a high nitrogen deficit (Codispoti et al., 2001;Deutsch et al., 2001) and a strong secondary nitrite maximum found at similar depths, which have been attributed to high pelagic N-loss activities therein (Naqvi, 1994;Naqvi et al., 2006;Ward et al., 2009). Due to its size, the Arabian Sea OMZ is assumed to be one of the biggest pelagic N-sinks, with annual estimated rates varying between ~30 and 60 Tg N yr^{-1} (Bange et al., 2000;Codispoti et al., 2001;Devol et al., 2006).

On the other hand, N-loss processes also occur in marine sediments. In fact, benthic N-loss is believed to contribute ~50-70% of global oceanic N-loss (Codispoti et al., 2001;Galloway et al., 2004;Gruber, 2004). Because of the geographical configuration of the Arabian Sea, OMZ waters therein impinge on the sediments along the continental margins off the coasts of India, Pakistan as well as Oman. Consequently, any *in situ* N-transformations within the OMZ waters would undoubtedly affect the N-budget of the sediments, and vice versa. Nevertheless, despite the obvious importance of benthic N-loss in the Arabian Sea, benthic N-loss activities have hardly been assessed, and thus estimates of the benthic contribution to the N-deficit and overall N-loss in the Arabian Sea remain poorly constrained. Based on depth-integrated primary production rates (Seitzinger and Giblin, 1996), Bange et al. (2000) estimated that shelf and margin sediments may account for 17% of the N-loss in the Arabian Sea; or up to 26% estimated by Schwartz et al. (2009) from the changes in N_2:Ar and nitrate consumption rates in Arabian Sea sediments. No direct measurements have been made, however, to distinguish the benthic N-loss pathways, nor have the potential interactions with overlying OMZ waters been much considered.

In general, two processes are known to remove nitrogen from marine systems: the N_2O and N_2 production via canonical denitrification ($NO_3^- \rightarrow NO_2^- \rightarrow NO \rightarrow N_2O \rightarrow N_2$) and the N_2 production by anaerobic ammonium oxidation (anammox, $NH_4^+ + NO_2^- \rightarrow N_2$). In marine

environments, anammox activities were first detected in sediments (Dalsgaard and Thamdrup, 2002;Thamdrup and Dalsgaard, 2002), and later in the suboxic water columns of the Black Sea (Kuypers et al., 2003) and Golfo Dulce, Costa Rica (Dalsgaard et al., 2003). Since then anammox bacteria have been found in marine habitats ranging from the Arctic sea ice (Rysgaard et al., 2004) to deep-sea hydrothermal vents (Byrne et al., 2009). In sediments, anammox has been shown to contribute up to 80% to the N_2 production (Dalsgaard et al., 2005), but anammox rates measured by ^{15}N stable isotope pairing experiments in sediments underlying a major OMZ to our knowledge have never been made before.

The reduction of nitrite to nitric oxide is an essential step in both anammox and denitrification, and is mediated by specific nitrite reductases (Nir) (Schalk et al., 2000;Strous et al., 2006;Kartal et al., 2011). In general, two different types of nitrite reductases are known to occur, the copper- (NirK) and the cd_1-containing nitrite reductase (NirS), but organisms harbour either of the reductases. The *nirK* genes are not only present in denitrifiers, but also known to occur in nitrifiers and therefore not suitable for the quantification of denitrifiers. Hence, genes encoding for the (*nirS*) are more commonly used as biomarkers for denitrifiers (Jayakumar et al., 2004;Castro-Gonzalez et al., 2005;Tiquia et al., 2006;Dang et al., 2009) and found to be more abundant in general and in an estuary system (Abell et al., 2010). Meanwhile, anammox bacteria also use a NirS, which is phylogenetically distinct from denitrifier NirS. Hence, *nirS* can be a useful biomarker to distinguish between denitrifiers and anammox bacteria, as evidenced by studies in the Peruvian and Arabian Sea pelagic OMZs (Lam et al., 2009).

In this study, we determined N-loss rates of denitrification and anammox in surface sediments at the continental margin off Pakistan, via ^{15}N-stable isotope experiments in intact core incubations and slurry incubations. The relative abundances of denitrifying and anammox bacteria in the sediment were quantified based on their respective *nirS* genes and their phylogenies were further evaluated to characterize the benthic microbial communities at various station depths. In order to explore the potential interaction between benthic and OMZ N-loss rates, stations with water depths between 360 and 1430 m were sampled. Accordingly, sediments at one station lay below the OMZ, while the others were within OMZ waters.

Material and Methods

Sampling procedures and chemical analyses

Sampling was conducted during the *R/V Meteor* cruise M74/2, on 7th to 28th October 2007, in the Arabian Sea over the Pakistan shelf (Makran region, Figure 1). Four stations ranging from

360 m to 1430 m were selected for detailed sampling and sediment incubations. (Please note, that original station names have been shortened for simplicity, from e.g. GeoB12204 to station 04). Dissolved oxygen and temperature of the water column were measured with a conductivity-temperature-depth (CTD) probe, equipped with an oxygen sensor (Sea Bird Electronics). The oxygen concentration was calibrated against Winkler titration. Water samples were taken with a CTD-rosette. On ship board, concentrations of ammonium and nitrite were measured fluorometrically (Holmes et al., 1999) and photometrically (Grasshoff and Johannsen, 1972), respectively. Additional sub-samples were stored at -20°C for later analyses for ammonium, nitrate, nitrite and phosphate in a shore-based laboratory using an autoanalyzer (TRAACS 800, Bran & Luebbe)

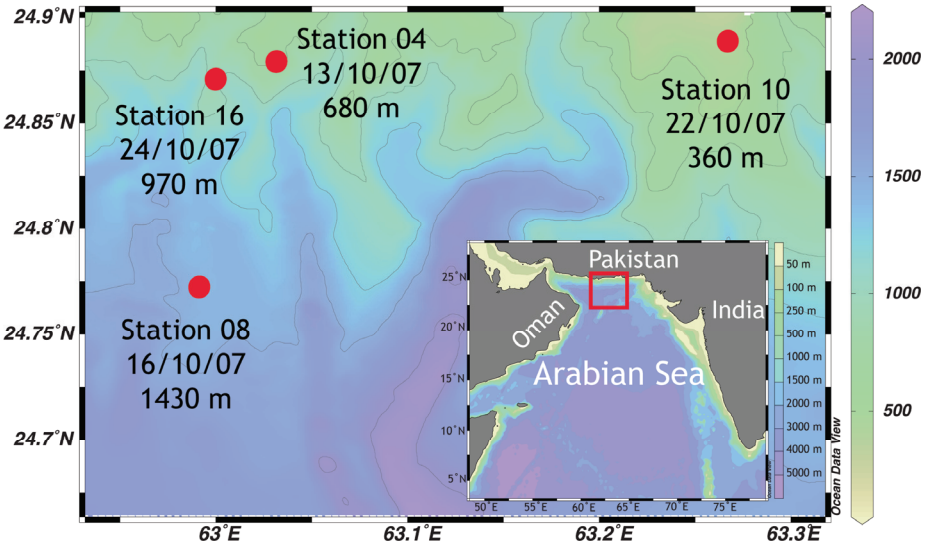

Figure 1: Sampling area of the *R/V Meteor* cruise M74/2 in October 2007, in the Makran region at the Pakistan continental margin. Colour scale on the right denotes water depth.

Sediment cores were taken with a multicorer (MUC) equipped with 8 acrylic liners (10 cm diameter). Sub-samples for molecular analyses were taken directly from MUC cores at 2 cm intervals from the surface down to 8 cm. DNA samples were stored at -80°C, shipped on dry ice and kept at -80°C until DNA extraction. Pore water extraction was conducted on board, sediment cores were sliced in a resolution of 0.5 cm (sediment depth 0-1 cm), 1 cm (sediment depth 2-5 cm) and 4 cm (sediment depth 5-30 cm), and porewater was squeezed out of the sediment slices with a porewater press (Schlüter, 1990). Porewater samples for nitrate and nitrite were kept frozen until measurement with a chemoluminescence NO_x analyzer (Thermo Environmental Instruments Inc; (Braman and Hendrix, 2002)) in a shore based laboratory. For

analyses of dissolved iron and sulphide, sediment cores were sampled on board with rhizones at 1 cm (sediment depth 0-5 cm) and 2 cm intervals (sediment depth 5-30 cm). Subsequently the obtained porewater was analyzed for Fe^{2+} and HS^- on board according to Grasshoff *et al.* (1999) and Cline *et al.* (1969). Concentrations of organic carbon and nitrogen were determined by combustion/gas chromatography (Carlo Erba NA-1500 CNS analyzer) of dried sediment samples after acidification with 3 mol l^{-1} phosphoric acid in a shore based laboratory.

Incubation experiments

Benthic denitrification and anammox rates were determined from N_2 production of ^{15}N-labeled slurry and intact core incubations. Rates from slurry incubations were used to calculate the contribution of anammox and denitrification to the total N-loss. Furthermore, volumetric rates from slurry incubations were integrated over the nitrate penetration depth to derive areal N-loss rates. Areal rates were also estimated from intact core incubations according to the revised isotope pairing technique (rIPT) detailed in Risgaard-Petersen *et al*. (2003).

Intact core incubations. Sediment cores (10 cm diameter) were subsampled with 3.6 cm-diameter liners and the overlying water was adjusted to a height of 12.5 cm above sediment surface. $^{15}NO_3^-$ (Campro Scientific GmbH) was added to a final concentration of 50 µmol l^{-1} in the overlying water, which was constantly mixed with magnetic stirrers. After pre-incubation for 8 to 12 hours, the cores were sealed with rubber stoppers and incubated without gas phase in the dark at *in situ* temperature (6-16°C). Five time points were taken at approximately 0, 2, 6, 10 and 15 hours after the cores have been sealed. At each time point, three cores were randomly selected and sacrificed by first removing the rubber stopper and injecting 1 ml of 50% (w/v) zinc chloride to the overlying water to precipitate any free sulfide. Then the first 6 cm of the sediment were mixed with the overlying water. A subsample of the slurry was transferred into 12 ml gas tight sterile glass vials (Exetainer®, Labco), poisoned with 100 µl of saturated $HgCl_2$ solution to stop biological activity and kept at room temperature in the dark until further processing.

Slurry incubations. Vertical distributions of denitrification and anammox rates within the sediment were estimated from slurry incubation experiments in gas-tight bags made of plastic-laminated aluminum-foil (Gao et al., 2009). Briefly, multicorer sediment cores were sliced in 2 cm intervals between 0 and 8 cm depth. Each slice (volume of ~160 cm^3) was transferred into a gas tight bag that was subsequently heat-sealed from all sides. To prepare

the slurry, 200 ml of degassed bottom water, taken from the overlying water in the MUC cores, was injected through a gas tight port into the bag. The residual air was removed from the bag and the slurry was thoroughly mixed. After pre-incubating the bags for 2 hours, to remove potential air-contamination introduced by the sub-sampling, ^{15}N-labelled substrates were injected into the bags and the slurries were again thoroughly mixed. Incubations were performed in the dark at *in situ* temperatures. In experiment 1, $^{15}NH_4^+$ and $^{14}NO_2^-$ were added to the slurries to final concentrations of 200 µmol l^{-1} and 100 µmol l^{-1} respectively. Furthermore, allylthiourea (ATU) was added to a final concentration of 86 µmol l^{-1} (Ginestet et al., 1998) to inhibit possible bacterial ammonia oxidation. In experiment 2, $^{15}NO_3^-$ was added to the slurries to a final concentration of 200 µmol l^{-1}. For both experiments, a subsample of 6 ml was drawn from the bags immediately after tracer addition, transferred into sterile gas-tight glass vials (Exetainer®, Labco) and fixed with 100 µl of saturated $HgCl_2$ solution. Between 5 and 7 subsamples were drawn from the bags during the subsequent 26-28 hours. The exetainers containing the subsamples were kept and shipped upside down in the dark at room temperature.

In the laboratory, a 2 ml helium headspace was introduced into the 12 ml exetainer of the whole core incubations while a headspace of 1 ml was used for the 6 ml exetainer of the slurries. The exetainers were shaken vigorously to allow N_2 to equilibrate between the headspace and the liquid phase. The N_2 isotope ratio ($^{28}N_2$, $^{29}N_2$, and $^{30}N_2$) of the headspace was determined by gas chromatography-isotopic ratio mass spectrometry (VG Optima, Micromass) by direct injections from the headspace according to Kuypers *et al.* (2005). Concentrations of $^{30}N_2$ and $^{29}N_2$ were normalized to $^{28}N_2$ and calculated as excess relative to air according to Holtappels et al. (2011). N_2 production rates were calculated from the $^{29}N_2$ and $^{30}N_2$ increase over time. Only production with a significant linear slope ($p<0.05$) over time without delay was used for further calculations.

Calculation of N-loss in the sediment slurries. In experiment 1, the anammox pathway ($NH_4^+ + NO_2^- \rightarrow N_2$) combines either $^{14}NH_4^+$ or $^{15}NH_4^+$ with $^{14}NO_2^-$ to form $^{28}N_2$ and $^{29}N_2$. Anammox activity was indicated when the production of $^{29}N_2$ ($p^{29}N_2$) was measured without any production of $^{30}N_2$ ($p^{30}N_2$). The production of $^{30}N_2$ was not detected in our samples, only a small amount of $^{30}N_2$ production was measured at station 16, depth 2-4 cm. The total N_2 production via anammox in experiment 1 ($A_{(Ex1)}$) was calculated from:

$$A_{(Ex1)} = \frac{p^{29}N_2}{F_{NH_4^+}} \quad (1)$$

where F_{NH4+} is the labeling percentage of the ^{15}N-substrate:

$$(F_{NH_4^+} = {}^{15}NH_4^+ / ({}^{14}NH_4^+ + {}^{15}NH_4^+)$$

For experiment 1, F_{NH4+} was calculated from the measured $^{14}NH_4^+$- concentrations in bottom waters and porewaters and the known addition of $^{15}NH_4^+$.

In experiment 2, the addition of $^{15}NO_3^-$ to background concentrations of $^{14}NO_3^-$ and $^{14}NH_4^+$ would produce $^{28}N_2$ and $^{29}N_2$ via anammox and $^{28}N_2$, $^{29}N_2$ and $^{30}N_2$ via denitrification. Thus, the production of $^{30}N_2$ ($p^{30}N_2$) indicates active denitrification. The total N_2 production by denitrification in experiment 2 ($D_{(Ex2)}$) was calculated according to Thamdrup and Dalsgaard (2002) from $p^{30}N_2$:

$$D_{(Ex2)} = \frac{p^{30}N_2}{\left(F_{NO_3^-}\right)^2} \tag{2}$$

where F_{NO3-} is the labeling percentage of nitrate: $F_{NO_3^-} = {}^{15}NO_3^- / ({}^{14}NO_3^- + {}^{15}NO_3^-)$

In experiment 2, both, anammox and denitrification produce $^{29}N_2$. To calculate anammox from experiment 2, equation 1 is modified to: $A_{(Ex2)} = \left(p^{29}N_2 - p^{29}N_{2(Den)}\right) / F_{NO_3^-}$, where $p^{29}N_{2(Den)}$ is the $^{29}N_2$ production via denitrification.

With $p^{29}N_{2(Den)} = 2\ p^{30}N_2\ (1 - F_{NO_3^-}) / F_{NO_3^-}$ (Thamdrup and Dalsgaard, 2002), we derive:

$$A_{(Ex2)} = \left(p^{29}N_2 - 2\frac{(1 - F_{NO_3^-})}{F_{NO_3^-}} p^{30}N_2 \right) \cdot \frac{1}{F_{NO_3^-}} \tag{3}$$

Results from slurry incubations indicated the presence of NO_3^--storing organisms releasing intracellular $^{14}NO_3^-$ in the course of the experiment (for further details, see discussion). An estimate of F_{NO3-} on the basis of measured $^{14}NO_3^-$ bottom water and porewater concentrations was therefore not possible. Instead, we calculated F_{NO3-} from equation 3 by inserting the measured $p^{29}N_2$ and $p^{30}N_2$ and by assuming $A_{(Ex1)} = A_{(Ex2)}$. The derived F_{NO3-} value, in the following referred to as $^*F_{NO3-}$, was then used to estimate denitrification according to equation 2. For sediments without the release of stored nitrate we expected F_{NO3-} equals $^*F_{NO3-}$, whereas $^*F_{NO3-} < F_{NO3-}$ indicated an additional source of $^{14}NO_3^-$, which was not dissolved initially in the porewater. We denoted the additional nitrate as excess $^{14}NO_3^-$ that was calculated from $^*F_{NO3-}$, F_{NO3-} and the known concentration of $^{15}NO_3^-$ in the slurry:

$$\text{Excess}{}^{14}NO_3^- = {}^{15}NO_3^- \left(\frac{1}{{}^*F_{NO_3^-}} - \frac{1}{F_{NO_3}} \right) \tag{4}$$

Calculation of N-loss in intact sediment cores. From the slurry incubation, the contribution of anammox to the total N-loss was estimated as $ra = A_{(Ex1)} / (A_{(Ex1)} + D_{(Ex2)})$. The total N-loss due to denitrification and anammox was calculated according to Risgaard-Petersen et al. (2003) from ra and the production of $^{30}N_2$ and $^{29}N_2$ in the core incubations:

$$N - loss = 2 \cdot \frac{(1 - ra)\, R^{29} - ra}{2 - ra} \cdot \left[p^{29}N_2 + p^{30}N_2 \left(1 - \frac{(1 - ra)\, R^{29} - ra}{2 - ra} \right) \right] \quad (5)$$

where R^{29} is the ratio between the $^{29}N_2$ and $^{30}N_2$ production.

Detection and phylogenetic analyses of denitrifier and anammox *nirS* genes

The biomarker functional gene *nirS*, encoding the *cd1*-containing nitrite reductase, for both denitrifiers and marine anammox bacteria were targeted using qualitative and quantitative analyses. Nucleic acids were extracted from the sediment layers corresponding to those used for rate measurements (0-2, 2-4, 4-6 and 6-8 cm respectively), by applying the UltraClean™ Soil DNA Isolation Kit (MO BIO Labratories Inc.) according to the manufacturer's instructions. Triplicate DNA extractions were made for each sample to reduce bias through the extraction procedure and pooled together through purification with the Wizard® Genomic DNA Purification Kit (Promega GmbH). DNA was stored in 10 mMTris-HCl at -80°C until further analyses. The concentrations of the DNA in the samples were measured spectrophotometrically with a NanoDrop instrument (Thermo Fisher Scientific Inc.).

Denitrifier *nirS* gene fragments were PCR amplified with the primers cd3aF/R3cd (5′-GTSAACGTSAAGGARACSGG-3′ (Michotey et al., 2000)/5′- GASTTCGGRTGSGTCTTGA-3′ (Throback et al., 2004)). The primers Scnir372F/Scnir845R (5′-TGTAGCCAGCATTGTAGCGT-3′/5′- TCAAGCCAGACCCATTTGCT-3′) (Lam et al., 2009) were used to target the specific *nirS* for marine anammox bacteria, so far believed to all fall into the *Candidatus* Scalindua clade. PCR reactions were performed with the Master *Taq* Kit (5 Prime) on a thermal cycler (Eppendorf AG) and were examined with gel electrophoresis on 1% LE agarose gels (Biozym Scientific GmbH).

Subsequently, clone libraries were constructed from PCR amplicons of correct sizes. The PCR products were purified with the QIAquick PCR Purification Kit (QIAGEN) and the cloning reactions were performed with the TOPO TA Cloning® Kit for sequencing (pCR4 vector) with One Shot® TOP10 chemically competent *E. coli* cells (Invitrogen GmbH). Clones were screened for correct inserts by performing PCR with the primers M13F/M13R (5′-GTAAAACGACGGCCAG-3′/5′- CAGGAAACAGCTATGAC-3′) and the number of non *nirS*

sequences was ≤2 per library. PCR products of the correct size were sequenced using the dye terminator sequencing method (Sanger et al., 1977) with the BigDye® Terminator v3.1 Cycle Sequencing Kit (Applied Biosystems Inc.) and the T7 primer (5´-TAATACGACTCACTATAGGG-3´). Sequencing was performed on an ABI3730 capillary sequencer system (ABI) according to the manufacturer's protocol. For the primers cd3aF/R3cd, sequence length used for phylogenetic analyses was above 400 base pairs (bp), while for primers Scnir372F/Scnir845R sequences had a minimum length of 440 bp.

Sequences were initially processed using BioEdit (Hall, 1999), aligned with ClustalW (Thompson et al., 1994) and screened for NirS encoding genes in the GenBank using the BLAST searches (Altschul et al., 1997). Mothur (Schloss et al., 2009) was used to calculate a similarity cut-off for operational taxonomic units (OTUs) based on nucleic acids of ≥95% and rarefaction curves. The screened sequences were imported into the ARB software package for phylogenetic analyses (Ludwig et al., 2004). Phylogenetic analyses were performed according to the amino acid sequences translated from the obtained sequences, together with some related sequences retrieved from GenBank. Phylogenetic trees were calculated based on the algorithms of maximum likelihood and maximum parsimony. Bootstrapped analyses of 100 resamplings were conducted. The sequences were deposited in GenBank under the accession numbers KC111208 to KC111421.

Quantitative PCR

Both denitrifier- and *Scalindua*- specific *nirS* genes were further quantified with real-time PCR, using the primers cd3aF/R3cd (Michotey et al., 2000) and Scnir372F/Scnir845R (Lam et al., 2009), which result in amplicons of 425 and 473 bp, respectively. The reactions were performed on an iQ5 cycler (Bio-Rad Laboratories GmbH) with the *Power*SYBR®Green Master Mix (Applied Biosystems Inc.), as previously described (Lam et al., 2009;Jensen et al., 2011). All samples and non template controls were analyzed as triplicate and the standards were analyzed with every qPCR run. The specificities of PCR amplicons were checked with subsequent melt curve analyses, as well as with 2% agarose gel electrophoresis.

Results

Hydro- and geochemistry

The compiled oxygen concentration profiles of the four investigated stations revealed an oxygen minimum zone with a vertical expanse of ~900 m (Figure 2). Within the oxycline

(50-100 m), oxygen concentrations decreased from ~200 µmol O_2 l^{-1} to ~5 µmol O_2 l^{-1}. From 200 m to 300 m, an intrusion of Persian Gulf Water identified by higher salinity (Shetye et al., 1994) led to increased oxygen concentrations of up to 16 µmol O_2 l^{-1}. At 300 m, oxygen concentrations dropped below the detection limit (~1 µmol O_2 l^{-1}) and increased again below ~900 m water depth. Bottom water oxygen concentrations of 23 µmol O_2 l^{-1} were measured at the deepest station (1430 m), whereas no oxygen was detectable in the bottom water of the three shallower stations.

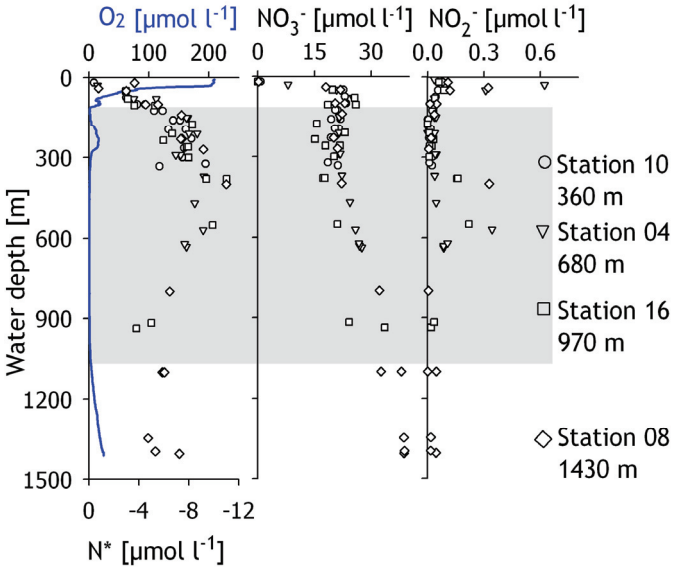

Figure 2: Concentrations of dissolved oxygen, N*, nitrate and nitrite, in the water column of the Pakistan continental margin in the Arabian Sea, with data compiled from all four sampling stations. N* was calculated according to Gruber and Sarmiento (1997). The shaded region depicts the extent of the oxygen minimum zone, while the different symbols denote the data points from different sampled stations.

Concentrations of ammonium were low throughout the water column (< 0.1 µmol NH_4^+ l^{-1}, data not shown). Nitrite concentrations were close to the detection limit of 0.01 µmol NO_2^- l^{-1} but peaked at distinct depths to maximum concentrations of 0.7 µmol NO_2^- l^{-1} at 30 m depth and 0.33 µmol l^{-1} between 400 to 600 m (Figure 2). Nitrate was depleted in the surface waters but increased below the oxycline (Figure 2) so that bottom water concentrations increased from 22 µmol NO_3^- l^{-1} at the shallowest station to 39 µmol NO_3^- l^{-1} at the deepest station. The nitrogen deficit, calculated according to Gruber and Sarmiento (1997) as N* = $[NH_4^+]+[NO_2^-]+[NO_3^-]-16*[PO_4^{3-}]+2.9$, was zero in surface waters (Figure 2), then decreased to -11 µmol N l^{-1} between 300 and 600 m depth and rose slightly to -7 µmol N l^{-1} below 800 m depth.

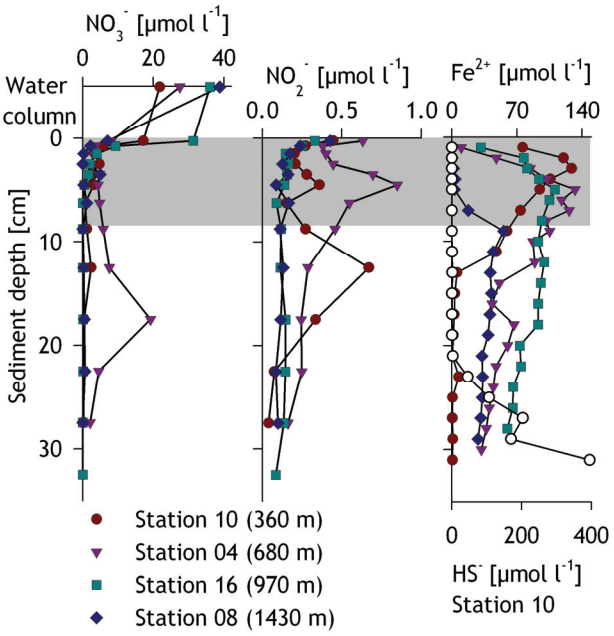

Figure 3: Pore water profiles for nitrate, nitrite, iron and sulphide for the investigated stations. The grey zone indicates the layers sampled for slurry incubations and DNA extraction, while the zone immediately above in the first panel represents the water column or bottom water. Samples for nitrate concentrations in the bottom water were retrieved from the bottom-most CTD sample. Sulphide was only measurable at and thus shown for station 10.

Within the sediments, the pore water was analyzed for the upper ~30 cm (Figure 3). Nitrate concentrations in the first 0.5 cm of the sediment ranged from 7 to 31 µmol NO_3^- l^{-1} and dropped sharply to <3 µmol NO_3^- l^{-1} below. Similar to nitrate, nitrite generally declined within the upper centimetres from ~0.5 µmol NO_2^- l^{-1} at the surface to 0.2 µmol NO_2^- l^{-1} below 2 cm. Significant subsurface maxima of nitrate (19 µmol NO_3^- l^{-1} at 17.5 cm, station 04) and nitrite (up to 0.9 µmol NO_2^- l^{-1}, stations 10 and 04) were sometimes found at the shallower stations. Concentrations of dissolved Fe^{2+} increased from 0.2 µmol l^{-1} at the surface to maximum concentrations ranging from 55 to 133 µmol l^{-1} at 5-9 cm depth and decreased within the layers below (Figure 3 c). Sulphide was detected only at the shallowest station 10 below 23 cm sediment depth where it increased with depth to a maximum of ~400 µmol HS^- l^{-1} at the lowermost sampled layer (31 cm, Figure 3 c).

Organic carbon and nitrogen contents were measured in the sediment layers corresponding to the slurry incubations (Table 1). Within the OMZ, the organic carbon content (% of dry weight) in the surface sediment layer increased from 1.6% at 360 m to 2.4% at 970 m, but decreased again to 1.7% below the OMZ at 1430 m. Although organic carbon and nitrogen contents decreased within sediment depth at all stations, there was no clear trend for C:N ratios with sediment depth. However, the C:N ratios were slightly enhanced with

station depth within the OMZ (C:N = 8-9 at 680 m and 970 m), compared to the shallowest and deepest stations (C:N = 7-8).

Table 1: Organic carbon and nitrogen, C:N ratios, N-loss rates and gene copy numbers of the investigated sediment layers. Abbreviations: n. s.: not significant, n.d.: not detectable, sed: sediment.

Station	Sediment depth	Organic carbon	Organic nitrogen	C:N	Excess nitrate	DNA
	[cm]	[% dry wt]	[% dry wt]	[mol:mol]	[nmol (cm sed)$^{-3}$]	[ng DNA (mg dry sed)$^{-1}$]
10	0-2	1.6	0.26	7.2	95.8	4.92±0.03
	2-4	1.5	0.23	7.8	22.2	3.69±0.23
	4-6	1.5	0.21	8.2	12.3	3.47±0.23
	6-8	1.2	0.21	7.1	n.d.	3.05±0.24
04	0-2	2.2	0.31	8.4	110.6	9.18±0.65
	2-4	2.0	0.28	8.1	23.6	5.04±0.59
	4-6	1.9	0.25	8.8	3.1	6.42±0.84
	6-8	1.8	0.26	8.1	n.d.	3.96±0.33
16	0-2	2.4	0.31	9.0	222.0	5.08±0.14
	2-4	2.1	0.28	8.6	n.d.	5.61±0.49
	4-6	2.0	0.27	8.7	n.d.	4.43±0.43
	6-8	1.3	0.19	8.0	n.d.	3.12±0.41
08	0-2	1.7	0.24	8.3	111.6	6.48±0.41
	2-4	1.6	0.23	7.8	n.d.	5.13±0.21
	4-6	1.4	0.21	7.9	n.d.	5.62±0.40
	6-8	1.2	0.19	7.4	n.d.	2.70±0.08

Benthic N-loss rates

Benthic N-loss activity was detected in both sediment slurries and intact sediment cores. In the intact core incubations, total benthic N-loss rates increased within the OMZ waters from 0.39 mmol N m^{-2} d^{-1} at 360 m to a maximum of 0.52 mmol N m^{-2} d^{-1} at 680 m (Figure 5 a). At the lower boundary of the OMZ, rates decreased to 0.22 mmol N m^{-2} d^{-1} (970 m) and were the lowest at 1430 m (0.18 mmol N m^{-2} d^{-1}). The relative contribution of denitrification and anammox to the total N-loss was estimated from slurry incubations. Denitrification rates in intact sediment cores ranged between 0.11 and 0.46 mmol N m^{-2} d^{-1}, while anammox rates increased from 0.03 mmol N m^{-2} d^{-1} at the shallowest station to 0.07 mmol N m^{-2} d^{-1} at the deepest station (Figure 5 a).

There were strong indications of the release of intracellular $^{14}NO_3^-$ during the slurry incubations. The release of stored $^{14}NO_3^-$ was most apparent in the NO_3^- measurements in the $HgCl_2$-fixed subsamples from the initial time-point (T_0). NO_3^- concentrations at T_0 were significantly above the total sum of NO_3^- in the bottom water, porewater and ^{15}N-amendment combined, thus indicating an excess of $^{14}NO_3^-$ in the slurry. Unfortunately, the true labeling

percentage (F_{NO3-}) during the slurry incubation could not be determined from these subsamples, since any residual intracellular nitrate would have been released after poisoning with $HgCl_2$. For this reason, $^{*}F_{NO3-}$ was calculated from equation 3 (see Methods) and subsequently the excess concentrations of $^{14}NO_3^-$ were calculated according to equation 4. Excess nitrate was calculated for all depths with denitrification rates (Table 1) and generally decreased with sediment depth. Excess nitrate ranged between 222 nmol N (cm^3 sediment)$^{-1}$ in the surface at station 16 and 3.1 nmol N (cm^3 sediment)$^{-1}$ in 4-6 cm at station 04.

In slurry incubations, both denitrification and anammox rates generally decreased with increasing sediment depth (Figure 4 a, b). Due to insignificant $^{29}N_2$ and $^{30}N_2$ production, denitrification rates could not be obtained for 6-8 cm at all stations and 4-6 cm at stations 16 and 08. Denitrification rates at the sediment surface (0-2 cm layer) decreased with increasing water depth, from 136 nmol N cm^{-3} d^{-1} at 360 m to 73 nmol N cm^{-3} d^{-1} at 1430 m (Figure 4 a). Anammox rates in surface sediments were lower than denitrification rates. However, in contrast to denitrification rates, anammox rates increased with water depth from 10 nmol N cm^{-3} d^{-1} at 360 m to 45 nmol N cm^{-3} d^{-1} at 1430 m (Figure 4 b).

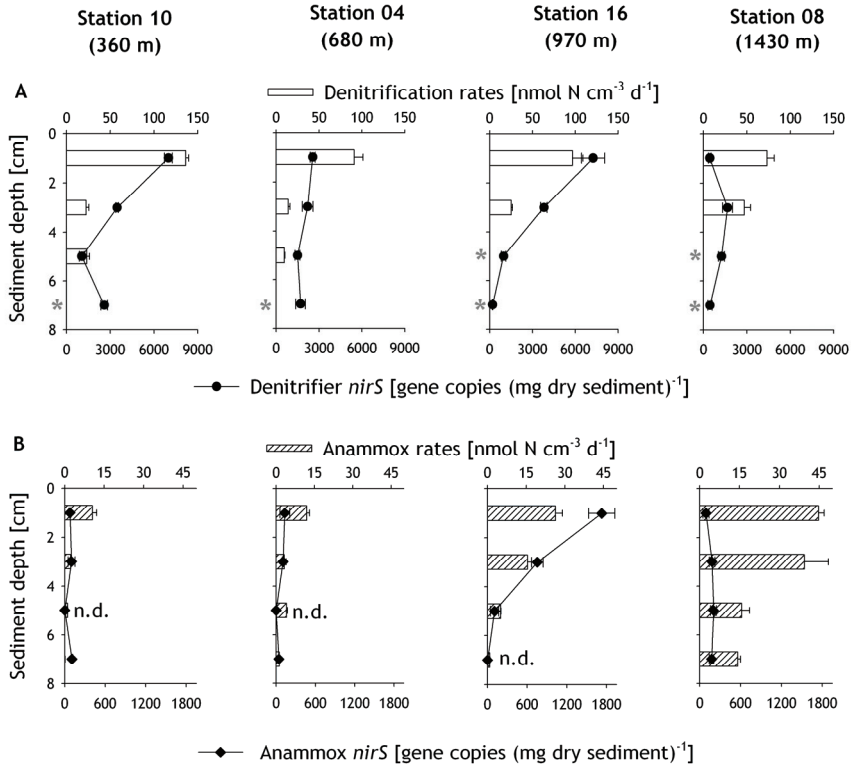

Figure 4: Denitrification (a) and anammox (b) rates determined from slurry incubation experiments, along with the corresponding gene copy numbers of denitrifier *nirS* (a) and anammox *nirS* (b) quantified by real-time qPCR in the sediments. The asterisks mark the incubations that showed insignificant ^{15}N-N_2 production. Abbreviations: 'n. d.' refers to non-detectable anammox *nirS* gene copy numbers

Anammox and denitrification rates from slurry incubations were integrated down to the nitrate penetration depth of 2 cm (Figure 5 b), which represents a rather conservative estimate, given that nitrate was found deeper in the sediment at some stations. Integrated denitrification rates decreased from 2.7 (±0.07) mmol m^{-2} d^{-1} at 360 m to 1.5 (±0.17) mmol m^{-2} d^{-1} at 1430 m. Anammox rates on the other hand increased with water depth from 0.21 (±0.03) mmol m^{-2} d^{-1} at 360 m to 0.89 (±0.04) mmol m^{-2} d^{-1} at the deepest station. As a result, the relative contribution of anammox to total N-loss increased with water depth from 7% at the shallowest station to 38% at the deepest station (Figure 5 c).

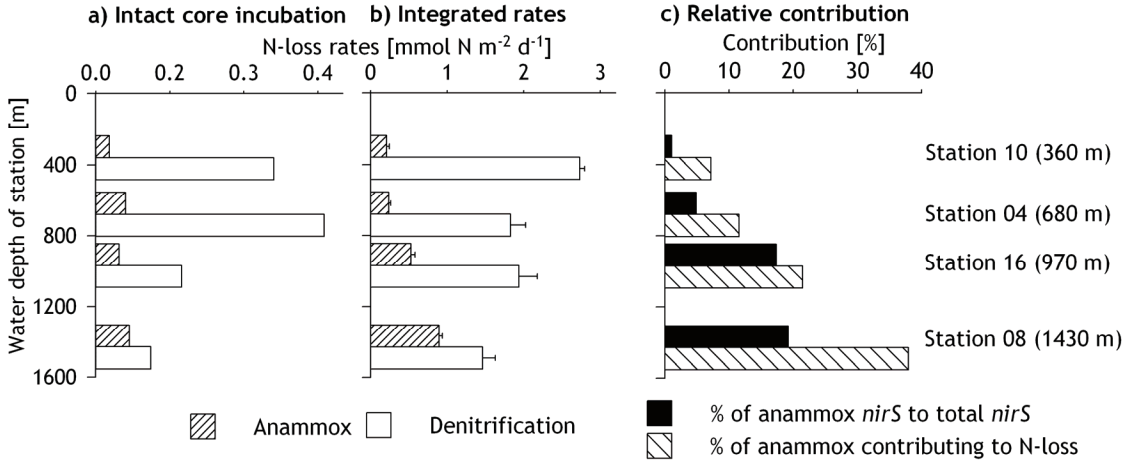

Figure 5: a) Anammox and denitrification rates measured in intact core incubation experiments, using the rIPT method described by Risgaard-Petersen *et al.* (2003). b) Areal depth-integrated rates of anammox and denitrification measured in slurry incubations for the uppermost 2 cm of the sediment. c) Contribution of anammox to the total benthic N-loss of the slurry incubations and the ratio of anammox *nirS* gene copy numbers to total *nirS* gene copy numbers in the surface layer (0-2cm) of the sediment.

Detection of *nirS* genes from denitrifiers and anammox bacteria

The presence of microorganisms mediating the denitrification and anammox processes was verified by the detection of their respective biomarker functional genes *nirS*. Altogether, 225 denitrifier *nirS* sequences were obtained, and they formed 114 OTUs that could be grouped into seven clusters (Figure 6, supplementary Table 1). The *nirS* sequences from the Pakistan continental margin are diverse, and show clustering pattern that seems to be depth-related: Certain clusters are dominated by sequences from the two shallow stations (10 and 04), while others are dominated by sequences from the two deeper stations (16 and 08).

Figure 6: Continued

Figure 6: Phylogenetic reconstruction of the denitrifier NirS based on amino acids sequences translated from gene sequences. Sequences were retrieved from clone libraries constructed for sediments of all stations based on maximum likelihood and maximum parsimony algorithms. Bootstrapped values of >50% are shown for maximum likelihood/maximum parsimony. Indicated in black are the related reference sequences obtained from GenBank. Labelling of sequences: station=04, 08, 10 or 16, 'nir'=amplicons from primers cd3aF/R3cd, or 'sc'=amplicons from primers Scnir372F/Scnir845R, followed by unique sequence number. Numbers in parentheses are the numbers of sequences represented by the same OTU with ≥95% nucleic acids sequence similarity. OTUs from the shallow stations are in orange red, while OTUs from deep stations are in purple. D1-D7 indicate the different clusters identified in this study, while the ratio below gives the ratio of sequences from shallow stations (10 and 04) to the deeper stations (08 and 16).

The majority of the sequences derived from stations 10 and 04 are found in clusters D2 (33 sequences) and D3 (49 sequences), to which the contributions from the deep stations (08 and 16) are considerably lower (only 13 sequences for D2 and 6 for D3). Meanwhile, clusters D1, D4, D5 and D6 seemed to be dominated by sequences from the deeper stations (08 and 16), with 41, 29, 6 and 9 sequences, respectively. Although the cd3aF-R3cd primer pair amplified predominantly denitrifier *nirS* genes, 2 sequences (OTU 04nir375) obtained from station 04 (680 m) were found to be more closely affiliated with the freshwater anammox bacterium *Candidatus "*Kuenenia stuttgartiensis*"* in cluster D7*,* with a similarity of 73% based on amino acid sequence. It should be noted that cluster D7 also includes cultured species like *Halomonas campisalis* and *Methylomirabilis oxyfera*, which share up to 59% and 69% amino acid sequence similarity, respectively, to the Arabian Sea D7 sequences obtained in this study.

A total of 109 OTUs from 241 anammox *nirS* sequences were retrieved from the Pakistani margin sediments (Figure 7), and they formed 3 clusters that might also carry some water-depth-related pattern, though not as obvious as for the denitrifier *nirS* sequences. Cluster S1 and S3, closely related to OTUs from the Arabian Sea water column, were dominated by sequences from deep stations (16 and 08) with 33 sequences compared to 17 and 22 sequences from the shallow stations (10 and 04). In contrast, cluster S2 affiliated with OTUs from the Peruvian water column seemed to have similar contributions from both shallow and deep stations.

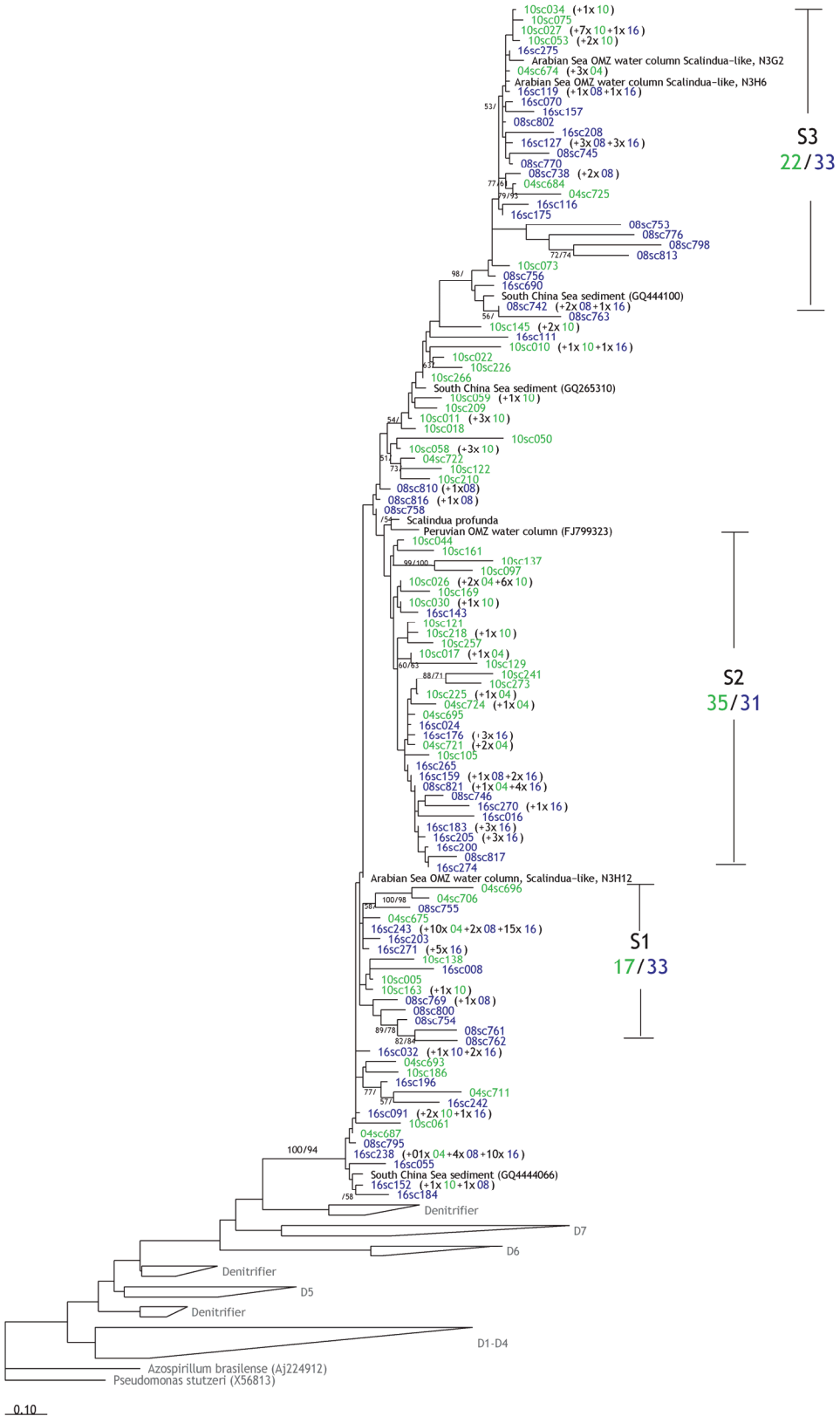

Figure 7: Phylogenetic reconstruction of the anammox (Scalindua) NirS based on amino acids sequences. In blue are the OTUs from the deep stations (08 and 16), while the green sequences were obtained from the shallow stations (10 and 04). Please refer to Figure 6 for additional information regarding the sequence labels in tree.

Quantification of denitrifier- and anammox- *nirS* genes

Consistent with benthic N-loss rate measurements, the anammox *nirS* genes were generally less abundant than denitrifier *nirS* genes (Figure 4 a, b). Both *nirS* gene copy numbers showed a decreasing trend with sediment depth. Amongst all stations, the highest denitrifier *nirS* gene abundance of 7245 ± 813 gene copies (mg dry sediment)$^{-1}$ was detected in the surface sediment layer at station 16 (970 m), whereas the lowest denitrifier *nirS* abundance of 439 (±90) gene copies (mg dry sediment)$^{-1}$ was detected in the uppermost 2 cm at the deepest station 08.

The abundance of anammox *nirS* genes was usually an order of magnitude lower than that of the denitrifier *nirS* (Figure 4 b), and was often found to be close to the detection limit. Similar to the denitrifier *nirS* genes, the highest numbers of anammox *nirS* genes were also detected at station 16, ranging from 1728±198 gene copies (mg dry sediment)$^{-1}$ in the surface to undetectable at 6-8 cm. Although the highest rates of anammox were measured in the slurry incubation experiment at station 08, only low gene copy numbers of anammox *nirS* ,in the range of 93±44 to 203±44 gene copies (mg dry sediment)$^{-1}$, were detected.

The relative contribution of the anammox *nirS* to the total *nirS* gene copy numbers in the uppermost 2 cm increased with water depth from 1% at 360 m to 19% at station 16 (Figure 5 c). These results are consistent with depth-integrated rates, which show an increase of anammox contribution to total N-loss with increasing water depth.

Discussion

Benthic N-loss due to denitrification

Consistent with previous benthic N-loss studies from other continental slopes, e.g. the North Atlantic (Trimmer and Nicholls, 2009), denitrification along the Pakistan margin was shown to be the primary N_2 production process, as measured in slurry incubation experiments and further corroborated by the abundance of the biomarker functional gene *nirS*. Measurements of benthic N-loss rates in the Arabian Sea are rare and so far estimates from direct sediment incubations using ^{15}N labelled substrates have not been reported. Schwartz and co-workers (Schwartz et al., 2009) estimated benthic denitrification rates across the Pakistan continental margin to be 0.40 to 3.78 mmol N m^{-2} d^{-1}. However, these estimates were based on nitrate uptake measurements that would have included the nitrate uptake by nitrate-storing organisms (e. g. sulphur bacteria, foraminifera) as well as the dissimilatory nitrate reduction to ammonium (DNRA). In contrast, N_2 production rates (determined as the N_2/Ar ratio) from the

same study were lower (0.05 to 0.13 mmol N m^{-2} d^{-1}) than the total N-loss rates we measured with the intact core incubation experiments (0.18 to 0.52 mmol N m^{-2} d^{-1}).

Denitrification rates have been determined for the continental shelf sediments off central Chile, where seasonal hypoxia develops each year (Farías et al., 2004). The measured benthic denitrification rates of 0.6 to 2.9 mmol N m^{-2} d^{-1} are similar in magnitude to those estimated for the sediments underlying the Peruvian OMZ (0.2 to 2 mmol N m^{-2} d^{-1}) based on modelled porewater fluxes (Bohlen et al., 2011). In comparison, the denitrification rates measured in our intact core incubations for the Pakistan margin (0.11 to 0.46 mmol N m^{-2} d^{-1}) were at the lower end of those estimates for the Chilean and Peruvian sediments, while the integrated rates based on slurry incubations (1.46 to 2.73 mmol N m^{-2} d^{-1}) lay within the upper range. The actual *in situ* N-loss rates on the Pakistan margin are likely somewhere between these two sets of obtained rates – as the amended substrates in the slurry incubations could have stimulated additional N-loss activity, while intact cores might have underestimated N-loss activity due to insufficient diffusion of the ^{15}N-labeled substrates into deeper sediment layers. Moreover, intact core incubations could not account for any potential denitrification by nitrate-storing organisms (e.g. foraminifera) as would be discussed below. Therefore, rates derived from slurry incubations may be closer to reality than those from intact core incubations.

Several lines of observations collectively indicate the likely presence of nitrate-storing organisms in the sediments of the Pakistani margin. Firstly, high production of $^{29}N_2$ relative to $^{30}N_2$ was measured in the $^{15}NO_3^-$ incubations, which did not agree with the calculated labeling percentage and the measured anammox rates. Secondly, nitrate concentrations in the T_0 subsamples of the slurry incubations exceeded the sum of bottom water, porewater and ^{15}N-nitrate. Thirdly, subsurface maxima of porewater nitrate/nitrite, similar to those previously observed at the Pakistani margin (Woulds et al., 2009), were found during this study. These various findings combined suggest that intracellular NO_x^- had been released during the porewater squeezing and during the mixing of sediment slurries.

Nitrate-storing sulphur bacteria, such as *Thioploca* spp. and *Beggiotoa* spp., have been associated with high pore water nitrate concentrations (Fossing et al., 1995). However, despite the lack of detailed microscopic or molecular analyses to confirm their absence, these mat-forming sulphur bacteria were not visible to naked eyes in the collected samples. Besides, sulphide was only detectable at the shallowest station (Sta. 10) and only below 23 cm, while there were high concentrations of Fe^{2+} at all other stations that indicated the absence of free sulphide. Given such low availability (or lack) of electron donor for their energy production,

it was thus unlikely for these sulphur bacteria to thrive in the sediments examined. On the other hand, nitrate storage of up to 80% of the total benthic nitrate pool has been described for foraminifera in sediments (Risgaard-Petersen et al., 2006;Glud et al., 2009), including the Peruvian OMZ (Piña-Ochoa et al., 2010). Indeed, living foraminifera had been found particularly in the first cm of sediments underlying the OMZ at the Pakistan margin (Schumacher et al., 2007), which agrees well with the enhanced excess nitrate concentrations calculated for the uppermost sediment layer in our samples. The mean excess nitrate concentration in our study was ~135 nmol (cm^3 sediment)$^{-1}$, equivalent to twice as much as that reported in the anoxic zone of Gullmar Fjord, Sweden (~ 60 nmol (cm^3 sediment)$^{-1}$) (Risgaard-Petersen et al., 2006).

Denitrification from the stored NO_3^- by foraminifera would lead to false denitrification estimates if the intracellular labeling percentage (F_{NO3-}) was not known. However, the increased NO_3^- concentrations in the slurry subsamples at T_0 suggest that the stored $^{14}NO_3^-$ was released into the porewater when the slurry was mixed at the start of the experiment. Thus, a subsequent uptake of NO_3^- from the porewater would lead to an intracellular F_{NO3-} that is close to the porewater F_{NO3-}. Furthermore, the linear increase of $^{29}N_2$ and $^{30}N_2$ with time indicates that either intracellular F_{NO3-} did not change over time or that the N_2 production by foraminifera was minor, as was also observed in other regions (Glud et al., 2009). Nonetheless, nitrate-storing foraminifera would potentially lead to an underestimation of N-loss by intact core incubations, since the unlabeled intracellular nitrate was not accounted for. In order to fully explain the source of excess nitrate observed, additional sample collection and analyses, including some shipboard microscopic examination of live cells, would be necessary to especially target the nitrate-storing sulphur bacteria and foraminifera at the point of sampling. These were unfortunately unavailable in our current study and should be further investigated.

The dominance of denitrification in benthic N-loss in the Pakistan margin sediments is strongly supported by the high abundance of denitrifier *nirS* genes. Moreover, the gene copy numbers generally followed similar decreasing trends as the rates measured in slurry incubation within the sediments (Figure 4). Exceptions were noted particularly in the topmost layer(s) at the deepest station (Sta. 8), and these could potentially be due to nucleic acid extraction efficiency or biases, and/or the presence of PCR inhibitors. In addition, the primers used only target *nirS*, while any occurrence of the *nirK* genes would not have been accounted for. Although there are also primers designed for *nirK*, those currently available may also target those of nitrifiers. Consequently, quantification of *nirK* in addition to that of *nirS* would

likely overestimate denitrifier abundance instead. Future refinement of primer designs, or the assessment of multiple biomarker genes in parallel, may help shed light on the true quantitative distribution of denitrifiers in the environment. Compared to previous studies in various sediments, most of which also focussed on denitrifier *nirS* and found gene copy numbers ranging from ca. 0.6 x 10^3 copies (mg sediment)$^{-1}$ at the mouth of the Colne estuary (Smith et al., 2007) to 27.2 x 10^3 copies (mg sediment)$^{-1}$ at the mouth of the Rhône River (Michotey et al., 2000), denitrifier *nirS* abundance at the Pakistan margin (0.2-6.9 x 10^3 copies (mg sediment)$^{-1}$) lay within the same range.

In agreement with studies addressing *nirS* genes in the water column of the Arabian Sea (Jayakumar et al., 2004;Bulow et al., 2008), the denitrifier *nirS* community seems to be very diverse (Chao1 richness estimate=327). However, diversity seems to vary amongst the stations (Chao1 richness estimates of 48 to 239 were calculated), though the rarefaction analyses indicate that the sequences obtained from the two deeper stations may not be sufficient to represent the full denitrifier diversity therein (Supplementary figure 1 a, b). Phylogenetic analyses revealed some apparent differences in the shallow versus deep denitrifying communities, with certain clusters dominated by sequences from shallow stations, while others by sequences from the deeper stations (Figure 5). As suggested in other studies (Liu et al., 2003;Dang et al., 2009), such a clustering pattern could result from the adaptation of specific denitrifying communities to different environmental conditions that vary with water depth, such as oxygen, carbon and nitrate availabilities.

It is particularly interesting to find an OTU amplified with the primers targeting denitrifier *nirS* genes, to be related to the *Candidatus "*Kuenenia stuttgartiensis*"* (73% similarity, Figure 6). *Candidatus "*Kuenenia stuttgartiensis*"* is an anammox bacterium known to occur in freshwater (Jetten et al., 2003), though capable of adapting to higher salinity (Kartal et al., 2006), it has never been found in marine environments thus far. In the same cluster (D7), between the Scalindua cluster and a cluster (D6) affiliated with a sequence from the Arabian Sea water column (Jayakumar et al., 2004), sequences from the deep stations are most closely affiliated with the halophilic bacteria *Halomonas campisalis* (Mormile et al., 1999) and *Methylomirabilis oxyfera*, a freshwater methanotroph that denitrify via an alternative pathway (Ettwig et al., 2010). The interesting NirS phylogeny of the cluster D7 may indicate that these organisms were no ordinary denitrifiers, yet their exact metabolic pathways remain to be determined. Recent studies from a hydrothermal vent system (Byrne et al., 2009) and an estuary (Dang et al., 2010) report the presence of anammox bacteria, other than *Candidatus* "Scalindua". These results together with the finding of the OTU related to

*Candidatus "*Kuenenia stuttgartiensis*"* in this study may hint towards a different type of anammox bacteria, although the abundance seems to be very low. Further studies need to be conducted to verify the occurrence of anammox bacteria, other than *Candidatus* "Scalindua" in the marine environment.

Benthic N-loss via anammox

This study provides the first direct measurement of anammox activity in the sediments of the Arabian Sea, or any OMZs. The very recent study by Bohlen and co-workers in the Peruvian OMZ (2011) estimated benthic anammox rates based on modelled porewater fluxes of up to 0.43 mmol N m^{-1} d^{-1} for an anoxic station at 376 m, with lower rates at deeper as well as shallower stations. In general, anammox rates according to intact core incubations at the Pakistan continental margin are much lower (0.003 to 0.007 mmol N m^{-1} d^{-1}) than the estimates from the Peruvian OMZ. The integrated anammox rates based on slurry incubations, on the other hand, are comparable (0.21 mmol N m^{-1} d^{-1}) on the Pakistan margin at a similar water depth (360 m) and reached as high as 0.89 mmol N m^{-1} d^{-1} at the deepest sampled station (1430 m). In congruence with the rate measurements, anammox Scalindua-like *nirS* genes could be detected at all stations and are in lower abundance than the denitrifier *nirS* genes. The anammox *nirS* gene abundance (undetectable to 1.7 x 10^3 copies (mg sediment)$^{-1}$) detected at the Pakistan margin were an order of magnitude lower than those detected in deep sea sediments of South China Sea (up to 44.1(±3.3) × 10^3 copies (mg sediment)$^{-1}$) (Li et al., 2011) in which the same primers were used as in the current study.

Because the *nirS* gene is present as a single copy in anammox bacteria, according to the sequenced genomes of both the freshwater *Candidatus "*Kuenenia stuttgartiensis" (Strous et al., 2006) and marine *Candidatus "*Scalindua profunda" (van de Vossenberg et al., 2008), potential cell specific activity may be calculated from the anammox rates measured in slurry incubations and the anammox *nirS* gene copies quantified. Taking station 16 that lay within the OMZ as an example, cell specific anammox rates were calculated to be 10 to 24 fmol N $cell^{-1}d^{-1}$, which was highly similar to those estimated for the Arabian Sea OMZ waters (1.6-25 fmol N d^{-1} $cell^{-1}$) over the Omani Shelf (Jensen et al., 2011). However, likely lower DNA extraction efficiency in sediments has probably led to underestimated anammox *nirS* gene copy numbers particularly for the deepest station, which in turn would result in overestimated cell specific rates, and so are not presented here. In addition, a recent study reported the occurrence of *nirK* instead of *nirS* gene in a freshwater anammox bacterium from a bioreactor (Hira et al., 2012). Although *nirK*-containing anammox bacteria have not been

found in the marine environment to date, such possibility cannot be eliminated and the quantification of *nirS* genes alone might have underestimated the anammox bacterial abundance. In future studies, the recently discovered gene *hzsA,* encoding hydrazine synthase (Harhangi et al., 2012), might be a reasonable alternative or additional biomarker gene for the quantification of anammox bacteria, since it is also present as a single copy in the genomes analyzed until now.

According to the phylogenetic reconstruction of Scalindua NirS (Figure 6), three different clusters could be identified and the diversity of the community (Chao1 richness estimate=275), though lower than the diversity of the denitrifier NirS (Figure S1 a, c), seems to be higher compared to those found in the water column OMZ of the Arabian Sea (Chao1 richness estimate=8, (Jensen et al., 2011)) and Peru (Chao1 richness estimate=43, (Lam et al., 2009)). The higher diversity could have been caused by more distinct segregation of the organisms in the sediments compared to the water column. Similar to the denitrifier NirS tree, sequences from the deep stations appeared to predominate in two clusters, presumably due to their different adaptations to environmental conditions as mentioned earlier for the denitrifiers.

Anammox contribution increased with water depth

In agreement with other studies (Engström et al., 2009;Trimmer and Nicholls, 2009;Bohlen et al., 2011), we found an increasing contribution of anammox to the total benthic N-loss with increasing water depth. At a water depth of 1430 m, the contribution of anammox was the highest (38%) and similar to the mean anammox contribution of 37% measured by Glud and co-workers (2009) at comparable water depths (1450 m) in a basin with low oxygen concentrations (~60 µmol O_2 l^{-2}) off Japan (Sagami Bay). Even at the Washington margin with water depths >2700 m, the contribution of anammox to total N-loss was found to be 40% on average (Engström et al., 2009). These studies, all based on ^{15}N incubation experiments, suggest a consistent contribution of ~40% of anammox to the benthic N-loss at sites with water depths >1400 m in different regions across global oceans. Earlier studies, as summarized by Trimmer and Engström (2011), observed a decrease in both denitrification and anammox rates with increasing water depth, such that the overall increase in anammox contribution to total N-loss with water depth was attributed to less decrease in anammox activity relative to denitrification. In contrast, this study shows an increase of potential anammox activity in the slurry incubation experiments from 0.21 to 0.89 mmol N m^{-2} d^{-1} with station depth, while denitrification rates decreased from 2.7 to 1.5 mmol N m^{-2} d^{-1}. This trend

was further corroborated by the relative increase in anammox *nirS* gene copy abundance with the water depth (Figure 7).

Although anammox rates and cell abundance increase with water depth, it is unlikely that water depth or rather pressure itself is a direct regulating factor for the anammox contribution, since bacterial communities and denitrifiers in particular are able to cope with high pressure very well (Tamegai et al., 1997). More likely than pressure are factors that correlate with depth, such as temperature, organic carbon content and nitrate concentration. Trimmer and Nicholls (2009) attributed the increase of anammox contribution to total N-loss, amongst other factors, to the bottom water temperature. Experiments with different incubation temperatures suggested, that anammox might be more compatible with lower temperatures (Dalsgaard and Thamdrup, 2002). This could also be the case here as the measured bottom water temperature at the Pakistan margin decreased with the water depth from 15.7°C at the shallowest station to 6.1°C at the deep station. On the other hand, it is generally believed that temperature and metabolic rates correlate (Gillooly et al., 2001;Gillooly et al., 2002;Savage et al., 2004) such that temperature is unlikely the responsible factor for the increase in anammox rates with depth at the Pakistan margin.

Organic carbon concentrations usually decrease with water depth and therefore it is hypothesized in some studies (Nicholls and Trimmer, 2009) that a decrease in benthic carbon content favours the chemolithoautotrophic anammox process. In the meantime, denitrifiers seem to proliferate particularly in reactive sediments where the lability as well as content of organic matter are higher (Engström et al., 2005), due to their possibly stronger competition for nitrite as electron acceptor when the electron donors (i.e. organic matter) are abundant. However, at the Pakistan margin, benthic organic carbon content of surface sediments did not show a decreasing trend with water depth, but increased within the core OMZ. It has been suggested that downslope redistribution of shelf sediments and increased preservation of organic carbon under anoxic conditions have caused the high organic carbon content in the core OMZ (Schott et al., 1970). Indeed, the highest organic carbon content was found along with the highest C:N ratio at the bottom of the OMZ (station 16), which hints towards the assumption that the organic matter is more refractory. Unlike the dependence of heterotrophic denitrifiers on the availability of labile organic carbon, anammox bacteria can fix their own organic carbon and therefore likely have an advantage at the deeper stations, where the supply of organic carbon from the surface is lower due to probably reduced primary production with distance to the coast and/or greater extent remineralisation in the water column reaching those depths.

Anammox activity depends on sufficient supplies of NO_x^- (Dalsgaard and Thamdrup, 2002), which acts as the electron acceptor for the anammox reaction. The highest anammox rates were measured at the deepest station, where nitrate concentration was almost twice as high (~39 µmol l^{-1}) as at the shallow station in the upper OMZ (~22 µmol l^{-1}). Moreover, oxygen was present which could have stimulated nitrification and thus could enhance the availability of NO_x^- in the sediments. The high nitrate concentrations and to a lesser extent the more refractory organic carbon at the deeper stations could have led to incomplete denitrification (i.e. nitrate reduction to nitrite) and an overall increased availability of NO_x^- for anammox (Dalsgaard et al., 2005). This would be particularly important for deeper sediment layers, where NO_x^- availability is usually low. This postulation would be in good agreement with the high rates measured in deeper layers at station 08 (Figure 4b), the deepest station with the highest nitrate concentration and oxic overlying bottom water.

Contribution of benthic N-loss to the N-deficit in the Arabian Sea

In general, the water column of the central Arabian Sea is believed to be an important sink for fixed nitrogen in global oceans as indicated by a prominent N-deficit (Naqvi, 1994;Naqvi et al., 2006;Ward et al., 2009). Recent studies on the water-column N-loss in the Arabian Sea OMZ could not agree on the dominant pathway, denitrification or anammox, responsible for the N-loss therein, and much variability has been found in the measured rates (Ward et al., 2009;Jensen et al., 2011;Lam et al., 2011). Ward and colleagues (2009) measured pelagic denitrification of up 25.4 nmol N_2 l^{-1} d^{-1} in the central Arabian Sea. In contrast, pelagic N-loss rates measured during the cruise for this study at the same stations on the Pakistan margin (data not shown here) as well as in the central Arabian Sea (Jensen et al., 2011) immediately before this study were very low (0-0.04 nmol N l^{-1} d^{-1}). These direct rate measurements together may suggest that the Arabian Sea harbors distinct regions of seasonally high N-loss (Lam et al., 2011), rather than being an area of uniformly and persistently high N-loss activity throughout the year. While the water column seems to be subject to seasonal variations in N-loss due to the supply of substrates from the surface and removal by sinking particles, benthic N-loss is likely less seasonally dependant, since organic carbon concentrations integrate over a longer period of time. Hence, consistently high benthic N-loss may have contributed significantly to the N-deficit signals in the water column where the OMZ water impinges on the Pakistani margin.

Naqvi and co-workers (2006) calculated that an area of 1.15×10^{12} m^2 of seafloor in the Arabian Sea is affected by oxygen concentrations of < 22 µmol O_2 l^{-1}. Since we measured

N-loss at 4 stations across the OMZ with bottom water O_2 concentrations of 0-23 μmol l^{-1}, an extrapolation of average fluxes to the area estimated by Naqvi et al. appears reasonable. The mean rates measured in the slurry incubations in this study would result in an annual N removal as high as 14.7 Tg N yr^{-1} (range between 12.3 and 17.0 Tg N yr^{-1}). Similar rates via denitrification of 1.1–10.5 Tg N yr^{-1} were estimated for the continental shelves of the Arabian Sea by Schwartz and co-workers (2009). Based on primary production rates, Bange *et al.* (2000) estimated the N-loss from shelf sediments (0-200 m) to be 6.8 Tg N yr^{-1} and as much as 33 Tg N yr^{-1} were attributed to pelagic denitrification. Accordingly, shelf sediments would account for only 17% to the total N-loss in the Arabian Sea. Nonetheless, these estimates did not include sediments at water depths deeper than 200 m, which also contribute to the N-loss in the Arabian Sea. Therefore, sediments likely contribute more to the total N-loss in the Arabian Sea than previously assumed.

Furthermore, N-loss rates measured in the central Arabian Sea of 0.3–0.6 mmol of N m^{-2} d^{-1} (Jensen et al., 2011) are comparable to benthic N-loss rates measured in this study. An extrapolation of these rates to the area of the Arabian Sea to the north of 6°N ($4.93x10^{12}$ m^2 (Bange et al., 2000)) would result in an annual pelagic N-loss of 7.6-15 Tg N yr^{-1}, which is similar to a recently published estimate for pelagic N-loss in the Arabian Sea of 12-16 Tg N yr^{-1} (DeVries et al., 2012). Compared to the mean benthic N-loss calculated from our data (14.7 Tg N yr^{-1}) with only the shelf sediments included, water column and the sediments might contribute more or less equally to the N-loss in the Arabian Sea.

Conclusions

Benthic N-loss due to anammox increased with water depth on the Pakistan margin and the contribution of anammox to total N-loss seemed to co-vary with temperature and nitrate concentrations in the bottom water. Compared to shallow sediments, anammox bacteria seem to be more successful in deeper sediments, as anammox accounted for almost 40% to the total benthic N-loss at 1430 m water depth. The shift from a denitrifier-dominated heterotrophic system in shallow sediments, to a system in which the autotrophic anammox process plays a more important role in sediments at deeper water depths, could also be coupled to the availability of labile organic carbon. Owing to their chemolithoautotrophic lifestyle, anammox bacteria could have a competitive advantage over denitrifiers in deeper sediments due to their lesser dependence on the often seasonally fluctuating primary production in surface waters for sources of electron donor and carbon. Extrapolation from our data suggests that benthic N-loss could account for up to half of the total N-loss in the Arabian Sea as a

whole, and may thus have contributed to the N-deficits in the water column, though further investigations during different seasons are necessary to fully evaluate the role of sediments in the annual marine N-loss. Since human populations and anthropogenic atmospheric N deposition (Duce et al., 2008) have been increasing in the Arabian Sea, primary production therein would likely be enhanced further in the near future, possibly resulting in higher oxygen consumption and thus an expansion of the OMZ. What additional positive and negative feedbacks may ensue, and how the overall nitrogen as well as the intimately linked carbon cycles might respond in this key region of global biogeochemical cycling, cannot be fully evaluated without taking the interacting benthic and pelagic fluxes into due consideration.

Acknowledgements

We are very thankful for the technical support and analyses by G. Klockgether, D. Franzke, M. Meier, I. Vieweg, A. Schipper, S. Kühn and for the excellent cooperation with captain and crew of *R/V Meteor* M74/2. We thank K. Zonneveld and S. Kasten for providing the equipment and fruitful discussions. Funding from DFG-Research Center / Excellence Cluster "The Ocean in the Earth System" (MARUM) and the Max Planck Society are gratefully acknowledged.

References

Abell, G.C.J., Revill, A.T., Smith, C., Bissett, A.P., Volkman, J.K., and Robert, S.S. (2010). Archaeal ammonia oxidizers and nirS-type denitrifiers dominate sediment nitrifying and denitrifying populations in a subtropical macrotidal estuary. Isme Journal 4**,** 286-300.

Altschul, S.F., Madden, T.L., Schaffer, A.A., Zhang, J.H., Zhang, Z., Miller, W., and Lipman, D.J. (1997). Gapped BLAST and PSI-BLAST: a new generation of protein database search programs. Nucleic Acids Research 25**,** 3389-3402.

Bange, H.W., Rixen, T., Johansen, A.M., Siefert, R.L., Ramesh, R., Ittekkot, V., Hoffmann, M.R., and Andreae, M.O. (2000). A revised nitrogen budget for the Arabian Sea. Global Biogeochemical Cycles 14**,** 1283-1297.

Bohlen, L., Dale, A.W., Sommer, S., Mosch, T., Hensen, C., Noffke, A., Scholz, F., and Wallmann, K. (2011). Benthic nitrogen cycling traversing the Peruvian oxygen minimum zone. Geochimica Et Cosmochimica Acta 75**,** 6094-6111.

Braman, R.S., and Hendrix, S.A. (2002). Nanogram nitrite and nitrate determination in environmental and biological materials by vanadium(III) reduction with chemiluminescence detection. Analytical Chemistry 61**,** 2715-2718.

Bulow, S.E., Francis, C.A., Jackson, G.A., and Ward, B.B. (2008). Sediment denitrifier community composition and nirS gene expression investigated with functional gene microarrays. Environmental Microbiology 10**,** 3057-3069.

Byrne, N., Strous, M., Crepeau, V., Kartal, B., Birrien, J.-L., Schmid, M., Lesongeur, F., Schouten, S., Jaeschke, A., Jetten, M., Prieur, D., and Godfroy, A. (2009). Presence and activity of anaerobic ammonium-oxidizing bacteria at deep-sea hydrothermal vents. Isme Journal 3**,** 117-123.

Castro-Gonzalez, M., Braker, G., Farias, L., and Ulloa, O. (2005). Communities of nirS-type denitrifiers in the water column of the oxygen minimum zone in the eastern South Pacific. Environmental Microbiology 7**,** 1298-1306.

Cline, J.D. (1969). Spectrophotometric Determination of Hydrogen Sulfide in Natural Waters. Limnology and Oceanography 14**,** 454-458.

Codispoti, L.A., Brandes, J.A., Christensen, J.P., Devol, A.H., Naqvi, S.W.A., Paerl, H.W., and Yoshinari, T. (2001). The oceanic fixed nitrogen and nitrous oxide budgets: Moving targets as we enter the anthropocene? Scientia Marina 65**,** 85-105.

Dalsgaard, T., Canfield, D.E., Petersen, J., Thamdrup, B., and Acuna-Gonzalez, J. (2003). Anammox is a significant pathway of N_2 production in the anoxic water column of Golfo Dulce, Costa Rica. Nature 422**,** 606-608.

Dalsgaard, T., and Thamdrup, B. (2002). Factors Controlling Anaerobic Ammonium Oxidation with Nitrite in Marine Sediments. Applied Environmental Microbiology 68**,** 3802-3808.

Dalsgaard, T., Thamdrup, B., and Canfield, D.E. (2005). Anaerobic ammonium oxidation (anammox) in the marine environment. Research in Microbiology 156**,** 457-464.

Dang, H., Chen, R., Wang, L., Guo, L., Chen, P., Tang, Z., Tian, F., Li, S., and Klotz, M.G. (2010). Environmental Factors Shape Sediment Anammox Bacterial Communities in Hypernutrified Jiaozhou Bay, China. Applied and Environmental Microbiology 76**,** 7036-7047.

Dang, H., Wang, C., Li, J., Li, T., Tian, F., Jin, W., Ding, Y., and Zhang, Z. (2009). Diversity and Distribution of Sediment NirS-Encoding Bacterial Assemblages in Response to Environmental Gradients in the Eutrophied Jiaozhou Bay, China. Microbial Ecology 58**,** 161-169.

Deutsch, C., Gruber, N., Key, R., Sarmiento, J.L., and Ganachaud, A. (2001). Denitrification and N_2 fixation in the Pacific Ocean. Global Biogeochemical Cycles 15**,** 483-506.

Devol, A.H., Naqvi, S.W.A., and Codispoti, L.A. (2006). "Nitrogen cycling in the suboxic waters of the Arabian Sea," in NATO Science Series IV Earth and Environmental Sciences : 64, Past and Present Water Column Anoxia, ed. L. Neretin. (Amsterdam: IOS Press and Kluwer Academic Publishers in conjunction with the NATO Scientific Affairs Division), 283-310.

Devries, T., Deutsch, C., Primeau, F., Chang, B., and Devol, A. (2012). Global rates of water-column denitrification derived from nitrogen gas measurements. Nature Geosci 5**,** 547-550.

Duce, R.A., Laroche, J., Altieri, K., Arrigo, K.R., Baker, A.R., Capone, D.G., Cornell, S., Dentener, F., Galloway, J., Ganeshram, R.S., Geider, R.J., Jickells, T., Kuypers, M.M., Langlois, R., Liss, P.S., Liu, S.M., Middelburg, J.J., Moore, C.M., Nickovic, S., Oschlies, A., Pedersen, T., Prospero, J., Schlitzer, R., Seitzinger, S., Sorensen, L.L., Uematsu, M., Ulloa, O., Voss, M., Ward, B., and Zamora, L. (2008). Impacts of atmospheric anthropogenic nitrogen on the open ocean. Science 320**,** 893-897.

Engström, P., Dalsgaard, T., Hulth, S., and Aller, R.C. (2005). Anaerobic ammonium oxidation by nitrite (anammox): Implications for N_2 production in coastal marine sediments. Geochimica Et Cosmochimica Acta 69**,** 2057-2065.

Engström, P., Penton, C.R., and Devol, A.H. (2009). Anaerobic ammonium oxidation in deep-sea sediments off the Washington margin. Limnology and Oceanography 54**,** 1643-1652.

Ettwig, K.F., Butler, M.K., Le Paslier, D., Pelletier, E., Mangenot, S., Kuypers, M.M.M., Schreiber, F., Dutilh, B.E., Zedelius, J., De Beer, D., Gloerich, J., Wessels, H., Van Alen, T., Luesken, F., Wu, M.L., Van De Pas-Schoonen, K.T., Den Camp, H., Janssen-Megens, E.M., Francoijs, K.J., Stunnenberg, H., Weissenbach, J., Jetten, M.S.M., and Strous, M. (2010). Nitrite-driven anaerobic methane oxidation by oxygenic bacteria. Nature 464**,** 543-548.

Farías, L., Graco, M., and Ulloa, O. (2004). Temporal variability of nitrogen cycling in continental-shelf sediments of the upwelling ecosystem off central Chile. Deep-Sea Research Part II-Topical Studies in Oceanography 51**,** 2491-2505.

Fossing, H., Gallardo, V.A., Jorgensen, B.B., Huttel, M., Nielsen, L.P., Schulz, H., Canfield, D.E., Forster, S., Glud, R.N., Gundersen, J.K., Kuver, J., Ramsing, N.B., Teske, A., Thamdrup, B., and Ulloa, O. (1995). Concentration and Transport of Nitrate by the Mat-Forming Sulfur Bacterium Thioploca. Nature 374**,** 713-715.

Galloway, J.N., Dentener, F.J., Capone, D.G., Boyer, E.W., Howarth, R.W., Seitzinger, S.P., Asner, G.P., Cleveland, C.C., Green, P.A., Holland, E.A., Karl, D.M., Michaels, A.F., Porter, J.H., Townsend, A.R., and Vöosmarty, C.J. (2004). Nitrogen Cycles: Past, Present, and Future. Biogeochemistry 70**,** 153-226.

Gao, H., Schreiber, F., Collins, G., Jensen, M.M., Kostka, J.E., Lavik, G., De Beer, D., Zhou, H.-Y., and Kuypers, M.M.M. (2009). Aerobic denitrification in permeable Wadden Sea sediments. Isme Jounal 4**,** 417-426.

Gillooly, J.F., Brown, J.H., West, G.B., Savage, V.M., and Charnov, E.L. (2001). Effects of Size and Temperature on Metabolic Rate. Science 293**,** 2248-2251.

Gillooly, J.F., Charnov, E.L., West, G.B., Savage, V.M., and Brown, J.H. (2002). Effects of size and temperature on developmental time. Nature 417**,** 70-73.

Ginestet, P., Audic, J.M., Urbain, V., and Block, J.C. (1998). Estimation of nitrifying bacterial activities by measuring oxygen uptake in the presence of the metabolic inhibitors allylthiourea and azide. Applied and Environmental Microbiology 64**,** 2266-2268.

Glud, R.N., Thamdrup, B., Stahl, H., Wenzhoefer, F., Glud, A., Nomaki, H., Oguri, K., Revsbech, N.P., and Kitazato, H. (2009). Nitrogen cycling in a deep ocean margin sediment (Sagami Bay, Japan). Limnology and Oceanography 54**,** 723–734.

Grasshoff, K., and Johannsen, H. (1972). New Sensitive and Direct Method for Automatic Determination of Ammonia in Sea-Water. Journal Du Conseil 34**,** 516-521.

Grasshoff, K., Kremling, K., and Ehrhardt, M. (1999). Methods of Seawater Analysis,. Weinheim, Germany: Wiley-VCH Verlag GmbH.

Gruber, N. (2004). "The Dynamics of the Marine Nitrogen Cycle and its Influence on Atmospheric CO_2 Variations " in NATO Science Series IV Earth and Environmental Sciences : 40, The Ocean Carbon Cycle and Climate, eds. M. Follows & T. Oguz. (Dordrecht: Kluwer Academic Publishers), 97-148.

Gruber, N., and Sarmiento, J.L. (1997). Global patterns of marine nitrogen fixation and denitrification. Global Biogeochemical Cycles 11**,** 235-266.

Hall, T.A. (1999). BioEdit: a user-friendly biological sequence alignment editor and analysis program for Windows 95/98/NT. Nucleic Acids Symposium Series 41**,** 95-98.

Harhangi, H.R., Le Roy, M., Van Alen, T., Hu, B.-L., Groen, J., Kartal, B., Tringe, S.G., Quan, Z.-X., Jetten, M.S.M., and Op Den Camp, H.J.M. (2012). Hydrazine Synthase, a Unique Phylomarker with Which To Study the Presence and Biodiversity of Anammox Bacteria. Applied and Environmental Microbiology 78**,** 752-758.

Hira, D., Toh, H., Migita, C.T., Okubo, H., Nishiyama, T., Hattori, M., Furukawa, K., and Fujii, T. (2012). Anammox organism KSU-1 expresses a NirK-type copper-containing nitrite reductase instead of a NirS-type with cytochrome cd(1). Febs Letters 586**,** 1658-1663.

Holmes, R.M., Aminot, A., Kerouel, R., Hooker, B.A., and Peterson, B.J. (1999). A simple and precise method for measuring ammonium in marine and freshwater ecosystems. Canadian Journal of Fisheries and Aquatic Sciences 56**,** 1801-1808.

Holtappels, M., Lavik, G., Jensen, M.M., and Kuypers, M.M.M. (2011). "(15)N-Labeling Experiments to Dissect the Contributions of Heterotrophic Denitrification and Anammox to Nitrogen Removal in the Omz Waters of the Ocean," in Methods in Enzymology: Research on Nitrification and Related Processes, Vol 486, Part A, ed. M. Klotz. (San Diego: Elsevier Academic Press Inc.), 223-251.

Jayakumar, D.A., Francis, C.A., Naqvi, S.W.A., and Ward, B.B. (2004). Diversity of nitrite reductase genes (nirS) in the denitrifying water column of the coastal Arabian Sea. Aquatic Microbial Ecology 34**,** 69-78.

Jensen, M.M., Lam, P., Revsbech, N.P., Nagel, B., Gaye, B., Jetten, M.S.M., and Kuypers, M.M.M. (2011). Intensive nitrogen loss over the Omani Shelf due to anammox coupled with dissimilatory nitrite reduction to ammonium. Isme Journal 5**,** 1660-1670.

Jetten, M.S.M., Sliekers, O., Kuypers, M., Dalsgaard, T., Van Niftrik, L., Cirpus, I., Van De Pas-Schoonen, K., Lavik, G., Thamdrup, B., Le Paslier, D., Op Den Camp, H.J.M., Hulth, S., Nielsen, L.P., Abma, W., Third, K., Engstrom, P., Kuenen, J.G., Jorgensen, B.B., Canfield, D.E., Damste, J.S.S., Revsbech, N.P., Fuerst, J., Weissenbach, J., Wagner, M., Schmidt, I., Schmid, M., and Strous, M. (2003). Anaerobic ammonium oxidation by marine and freshwater planctomycete-like bacteria. Applied Microbiology and Biotechnology 63**,** 107-114.

Kartal, B., Koleva, M., Arsov, R., Van Der Star, W., Jetten, M.S.M., and Strous, M. (2006). Adaptation of a freshwater anammox population to high salinity wastewater. Journal of Biotechnology 126**,** 546-553.

Kartal, B., Maalcke, W.J., De Almeida, N.M., Cirpus, I., Gloerich, J., Geerts, W., Op Den Camp, H.J.M., Harhangi, H.R., Janssen-Megens, E.M., Francoijs, K.-J., Stunnenberg, H.G., Keltjens, J.T., Jetten, M.S.M., and Strous, M. (2011). Molecular mechanism of anaerobic ammonium oxidation. Nature 479**,** 127-130.

Kuypers, M.M.M., Lavik, G., Woebken, D., Schmid, M., Fuchs, B.M., Amann, R., Jørgensen, B.B., and Jetten, M.S.M. (2005). Massive nitrogen loss from the Benguela upwelling

system through anaerobic ammonium oxidation. Proceedings of the National Academy of Sciences of the United States of America 102**,** 6478-6483.

Kuypers, M.M.M., Sliekers, A.O., Lavik, G., Schmid, M., Jorgensen, B.B., Kuenen, J.G., Damste, J.S.S., Strous, M., and Jetten, M.S.M. (2003). Anaerobic ammonium oxidation by anammox bacteria in the Black Sea. Nature 422**,** 608-611.

Lam, P., Jensen, M.M., Kock, A., Lettmann, K.A., Plancherel, Y., Lavik, G., Bange, H.W., and Kuypers, M.M.M. (2011). Origin and fate of the secondary nitrite maximum in the Arabian Sea. Biogeosciences 8**,** 1565-1577.

Lam, P., Lavik, G., Jensen, M.M., Van De Vossenberg, J., Schmid, M., Woebken, D., Dimitri, G., Amann, R., Jetten, M.S.M., and Kuypers, M.M.M. (2009). Revising the nitrogen cycle in the Peruvian oxygen minimum zone. Proceedings of the National Academy of Sciences of the United States of America 106**,** 4752-4757.

Li, M., Ford, T., Li, X., and Gu, J.-D. (2011). Cytochrome cd1-Containing Nitrite Reductase Encoding Gene nirS as a New Functional Biomarker for Detection of Anaerobic Ammonium Oxidizing (Anammox) Bacteria. Environmental Science & Technology 45**,** 3547-3553.

Liu, X.D., Tiquia, S.M., Holguin, G., Wu, L.Y., Nold, S.C., Devol, A.H., Luo, K., Palumbo, A.V., Tiedje, J.M., and Zhou, J.Z. (2003). Molecular diversity of denitrifying genes in continental margin sediments within the oxygen-deficient zone off the Pacific coast of Mexico. Applied and Environmental Microbiology 69**,** 3549-3560.

Ludwig, W., Strunk, O., Westram, R., Richter, L., Meier, H., Yadhukumar, Buchner, A., Lai, T., Steppi, S., Jobb, G., Forster, W., Brettske, I., Gerber, S., Ginhart, A.W., Gross, O., Grumann, S., Hermann, S., Jost, R., Konig, A., Liss, T., Lussmann, R., May, M., Nonhoff, B., Reichel, B., Strehlow, R., Stamatakis, A., Stuckmann, N., Vilbig, A., Lenke, M., Ludwig, T., Bode, A., and Schleifer, K.H. (2004). ARB: a software environment for sequence data. Nucleic Acids Research 32**,** 1363-1371.

Marra, J., and Barber, R.T. (2005). Primary productivity in the Arabian Sea: A synthesis of JGOFS data. Progress in Oceanography 65**,** 159-175.

Michotey, V., Mejean, V., and Bonin, P. (2000). Comparison of methods for quantification of cytochrome cd_1-denitrifying bacteria in environmental marine samples. Applied and Environmental Microbiology 66**,** 1564-1571.

Mormile, M.R., Romine, M.F., Garcia, T., Ventosa, A., Bailey, T.J., and Peyton, B.M. (1999). Halomonas campisalis sp nov., a denitrifying, moderately haloalkaliphilic bacterium. Systematic and Applied Microbiology 22**,** 551-558.

Naqvi, S.W.A. (1994). Denitrification Processes in the Arabian Sea. Proceedings of the Indian Academy of Sciences-Earth and Planetary Sciences 103**,** 279-300.

Naqvi, S.W.A., Naik, H., Pratihary, A., D'souza, W., Narvekar, P.V., Jayakumar, D.A., Devol, A.H., Yoshinari, T., and Saino, T. (2006). Coastal versus open-ocean denitrification in the Arabian Sea. Biogeosciences 3**,** 621-633.

Nicholls, J.C., and Trimmer, M. (2009). Widespread occurrence of the anammox reaction in estuarine sediments. Aquatic Microbial Ecology 55**,** 105-113.

Piña-Ochoa, E., Høgslund, S., Geslin, E., Cedhagen, T., Revsbech, N.P., Nielsen, L.P., Schweizer, M., Jorissen, F., Rysgaard, S., and Risgaard-Petersen, N. (2010). Widespread occurrence of nitrate storage and denitrification among Foraminifera and Gromiida. Proceedings of the National Academy of Sciences of the United States of America 107**,** 1148-1153.

Risgaard-Petersen, N., Langezaal, A.M., Ingvardsen, S., Schmid, M.C., Jetten, M.S.M., Op Den Camp, H.J.M., Derksen, J.W.M., Pina-Ochoa, E., Eriksson, S.P., Nielsen, L.P., Revsbech, N.P., Cedhagen, T., and Van Der Zwaan, G.J. (2006). Evidence for complete denitrification in a benthic foraminifer. Nature 443**,** 93-96.

Risgaard-Petersen, N., Nielsen, L.P., Rysgaard, S., Dalsgaard, T., and Meyer, R.L. (2003). Application of the isotope pairing technique in sediments where anammox and denitrification coexist. Limnology and Oceanography-Methods 1**,** 63-73.

Rysgaard, S., Glud, R.N., Risgaard-Petersen, N., and Dalsgaard, T. (2004). Denitrification and anammox activity in Arctic marine sediments. Limnology and Oceanography 49**,** 1493-1502.

Sanger, F., Nicklen, S., and Coulson, A.R. (1977). DNA Sequencing with Chain-Terminating Inhibitors. Proceedings of the National Academy of Sciences of the United States of America 74**,** 5463-5467.

Savage, Vanâ m., Gillooly, Jamesâ f., Brown, Jamesâ h., West, Geoffreyâ b., and Charnov, Ericâ l. (2004). Effects of Body Size and Temperature on Population Growth. The American Naturalist 163**,** 429-441.

Schalk, J., De Vries, S., Kuenen, J.G., and Jetten, M.S.M. (2000). Involvement of a novel hydroxylamine oxidoreductase in anaerobic ammonium oxidation. Biochemistry 39**,** 5405-5412.

Schloss, P.D., Westcott, S.L., Ryabin, T., Hall, J.R., Hartmann, M., Hollister, E.B., Lesniewski, R.A., Oakley, B.B., Parks, D.H., Robinson, C.J., Sahl, J.W., Stres, B., Thallinger, G.G., Van Horn, D.J., and Weber, C.F. (2009). Introducing mothur: Open-Source, Platform-Independent, Community-Supported Software for Describing and Comparing Microbial Communities. Applied and Environmental Microbiology 75**,** 7537-7541.

Schlüter, M. (1990). "Zur Frühdiagenese von organischem Kohlenstoff und Opal in Sedimenten des südlichen und östlichen Weddellmeeres : geochemische Analyse und Modellierung = Early diagenesis of organic carbon and opal in sediments of the southern and eastern Weddell Sea : Geochemical analysis and modelling ", in: Berichte zur Polarforschung (Reports on Polar Research). (Bremerhaven: Alfred Wegener Institute for Polar and Marine Research).

Schott, W., Von Stackelberg, U., Eckhardt, F.J., Mattiat, B., Peters, J., and Zobel, B. (1970). Geologische Untersuchungen an Sedimenten des indisch-pakistanischen Kontinentalrandes (Arabisches Meer). International Journal of Earth Sciences 60**,** 264-275.

Schumacher, S., Jorissen, F.J., Dissard, D., Larkin, K.E., and Gooday, A.J. (2007). Live (Rose Bengal stained) and dead benthic foraminifera from the oxygen minimum zone of the Pakistan continental margin (Arabian Sea). Marine Micropaleontology 62**,** 45-73.

Schwartz, M.C., Woulds, C., and Cowie, G.L. (2009). Sedimentary denitrification rates across the Arabian Sea oxygen minimum zone. Deep Sea Research Part II: Topical Studies in Oceanography 56**,** 324-332.

Seitzinger, S., and Giblin, A. (1996). Estimating denitrification in North Atlantic continental shelf sediments. Biogeochemistry 35**,** 235-260.

Shetye, S., Gouveia, A., and Shenoi, S. (1994). Circulation and water masses of the Arabian Sea. Journal of Earth System Science 103**,** 107-123.

Smith, C.J., Nedwell, D.B., Dong, L.F., and Osborn, A.M. (2007). Diversity and abundance of nitrate reductase genes (narG and napA), nitrite reductase genes (nirS and nrfA), and their transcripts in estuarine sediments. Applied and Environmental Microbiology 73**,** 3612-3622.

Strous, M., Pelletier, E., Mangenot, S., Rattei, T., Lehner, A., Taylor, M.W., Horn, M., Daims, H., Bartol-Mavel, D., Wincker, P., Barbe, V., Fonknechten, N., Vallenet, D., Segurens, B., Schenowitz-Truong, C., Medigue, C., Collingro, A., Snel, B., Dutilh, B.E., Op Den Camp, H.J.M., Van Der Drift, C., Cirpus, I., Van De Pas-Schoonen, K.T., Harhangi, H.R., Van Niftrik, L., Schmid, M., Keltjens, J., Van De Vossenberg, J., Kartal, B., Meier, H., Frishman, D., Huynen, M.A., Mewes, H.W., Weissenbach, J.,

Jetten, M.S.M., Wagner, M., and Le Paslier, D. (2006). Deciphering the evolution and metabolism of an anammox bacterium from a community genome. Nature 440**,** 790-794.

Tamegai, H., Li, L., Masui, N., and Kato, C. (1997). A denitrifying bacterium from the deep sea at 11,000-m depth. Extremophiles 1**,** 207-211.

Thamdrup, B., and Dalsgaard, T. (2002). Production of N_2 through Anaerobic Ammonium Oxidation Coupled to Nitrate Reduction in Marine Sediment. Applied and Environmental Microbiology 68**,** 1312-1318.

Thompson, J.D., Higgins, D.G., and Gibson, T.J. (1994). Clustal-W - Improving the Sensitivity of Progressive Multiple Sequence Alignment through Sequence Weighting, Position-Specific Gap Penalties and Weight Matrix Choice. Nucleic Acids Research 22**,** 4673-4680.

Throback, I.N., Enwall, K., Jarvis, A., and Hallin, S. (2004). Reassessing PCR primers targeting nirS, nirK and nosZ genes for community surveys of denitrifying bacteria with DGGE. Fems Microbiology Ecology 49**,** 401-417.

Tiquia, S.M., Masson, S.A., and Devol, A. (2006). Vertical distribution of nitrite reductase genes (nirS) in continental margin sediments of the Gulf of Mexico. Fems Microbiology Ecology 58**,** 464-475.

Trimmer, M., and Engström, P. (2011). "Distribution, Activity, and Ecology of Anammox Bacteria in Aquatic Environments," in Nitrification, eds. B. Ward, D. Arp & M. Klotz. (Washingtopn: American Society for Microbiology), 201-235.

Trimmer, M., and Nicholls, J.C. (2009). Production of nitrogen gas via anammox and denitrification in intact sediment cores along a continental shelf to slope transect in the North Atlantic. Limnology and Oceanography 54**,** 577-589.

Van De Vossenberg, J., Rattray, J.E., Geerts, W., Kartal, B., Van Niftrik, L., Van Donselaar, E.G., Damste, J.S.S., Strous, M., and Jetten, M.S.M. (2008). Enrichment and characterization of marine anammox bacteria associated with global nitrogen gas production. Environmental Microbiology 10**,** 3120-3129.

Ward, B.B., Devol, A.H., Rich, J.J., Chang, B.X., Bulow, S.E., Naik, H., Pratihary, A., and Jayakumar, A. (2009). Denitrification as the dominant nitrogen loss process in the Arabian Sea. Nature 461**,** 78-81.

Wiggert, J.D., Hood, R.R., Banse, K., and Kindle, J.C. (2005). Monsoon-driven biogeochemical processes in the Arabian Sea. Progress in Oceanography 65**,** 176-213.

Woulds, C., Schwartz, M.C., Brand, T., Cowie, G.L., Law, G., and Mowbray, S.R. (2009). Porewater nutrient concentrations and benthic nutrient fluxes across the Pakistan margin OMZ. Deep Sea Research Part II: Topical Studies in Oceanography 56**,** 333-346.

Supplementary table 1: Range of similarities (%) between the different clusters identified in the NirS phylogenetic trees, based on amino acid sequences.

	Denitrifier or Kuenenia-like									*Scalindua-like*			
	D1	D2	D3	D4	D5	D6	D7	*K. stutt.*	*M. oxy.*	S1	S2	S3	*S. pro*
D1													
D2	82-54												
D3	82-60	76 56											
D4	70-47	71-53	70-54										
D5	74-51	70-55	70-56	72-55									
D6	59-38	60-47	58-44	62-47	63-48								
D7	58-38	58-43	59-41	58-46	61-45	66-48							
Kuenenia stuttgartiensis (K. stutt.)	61-48	60-53	61-54	62-55	62-53	60-51	73-38						
Methylomirabilis oxyfera (M. oxy.)	58-42	58-49	55-45	59-52	60-54	62-47	69-42	56					
S1	62-39	61-42	57-39	63-44	66-47	66-46	60-44	61-51	64-56				
S2	61-41	62-44	57-40	65-43	68-48	65-49	63-44	61-50	66-54	94-57			
S3	66-38	62-37	59-36	65-38	67-44	65-41	63-42	59-44	64-49	85-52	84-50		
Scalindua profunda (S. pro.)	60-49	61-52	57-47	64-54	65-57	64-56	62-45	51	60	94-77	95-77	82-64	

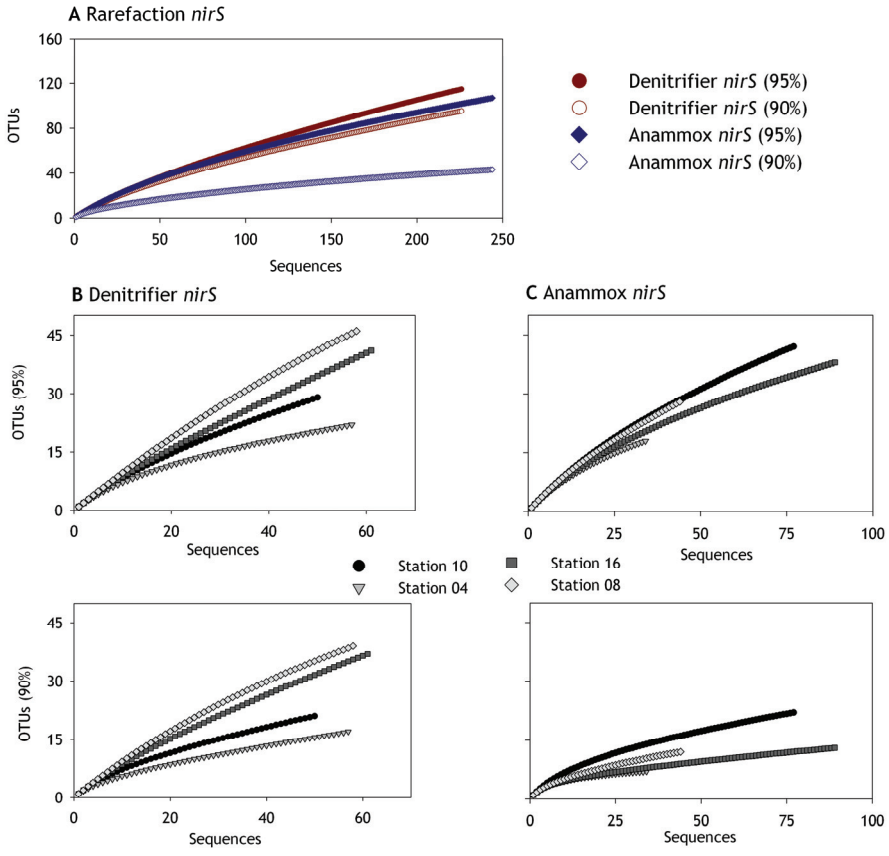

Supplementary Figure 1: Rarefaction curves for denitrifier and anammox (Scalindua) *nirS* sequences based on 95% and 90% nucleotide sequences cut offs. a) shows rarefaction curves over all sampled stations, b) shows the denitrifier *nirS* rarefaction curves separately for each sampled station and c) the corresponding curves for anammox (Scalindua) *nirS*.

Chapter III

Extensive nitrogen loss from permeable sediments off North West Africa

Sokoll, Sarah[1], Moritz Holtappels[1], Gaute Lavik[1], Stefan Sommer[2], Tobias Goldhammer[3] and Marcel M. M. Kuypers[1]

[1]Max Planck Institute for Marine Microbiology, Bremen, Germany

[2]GEOMAR Helmholtz Centre for Ocean Research, Kiel, Germany

[3]MARUM-Center for Marine Environmental Sciences, University of Bremen, Bremen, Germany

Abstract

The upwelling area off North Western (NW)-Africa is characterized by a high primary productivity, resulting in high particle export to subsurface waters and high nitrate concentrations in the bottom water. On the shelf off NW-Africa sandy sediments are widely distributed. So far, anthropogenically eutrophied regions with sandy sediments were shown to exhibit high nitrogen (N)-loss via denitrification. However, not much is known about benthic N-loss from permeable sediments in upwelling and thus naturally eutrophied regions. To investigate benthic N-loss, ^{15}N slurry incubation experiments were performed at 16 stations in different sediment layers during two research cruises, to Cape Blanc (April 2010) and the coast of Senegal and Mauritania (March/April 2011). Permeable sandy sediments in this area were found from ~50 m down to ~500 m water depth. The contribution of anammox (anaerobic ammonium oxidation) to the total N-loss was below 32% in sandy sediments but increased to 73 % at 3000 m water depth.

Potential benthic denitrification rates in the permeable shelf sediments ranged from 0.07 up to 0.79 μmol N cm^{-3} d^{-1} and were amongst the highest rates so far reported for marine sediments. Surprisingly, denitrification rates were detected to 8 cm sediment depth and did not decrease with sediment depth suggesting a deep penetration of nitrate into the sediment by porewater advection as well as bioirrigation and biotubation. In contrast, potential denitrification rates in muddy sediments of the continental slope (3000 m water depth) were low (0.02 μmol N cm^{-3} d^{-1}) and restricted to a zone from 4-8 cm below the sediment surface. Our results show a correlation of median grain size with water depth and denitrification rates for the permeable sediments. This correlation was used to model an N-loss of 1.9×10^{11} mol N yr^{-1} from the Mauritanian and Senegalese shelf, which is roughly five times more than previously estimated. Considering that 70% of the continental shelf areas are covered by sandy sediments our results indicate that permeable sediments significantly contribute to the global benthic N-loss.

Introduction

Sediments are important for the nitrogen (N)-cycling in the oceans, because 50-70% of marine N-loss is generally attributed to the sediments (Codispoti et al. 2001; Gruber 2004; Codispoti 2007). The continental shelf area, 70% of which is covered by sandy permeable sediments (Emery 1968), plays a key role in this benthic N-loss. However, little is known about N-cycling processes in sandy sediments as in former times N-loss was assumed to occur mainly in muddy, diffusively dominated sediments (Lohse et al. 1996; Vance-Harris and Ingall 2005). Recently this paradigm has been overturned by research taking into account the impacts of advective flow (Cook et al. 2006; Rao et al. 2007; Gao et al. 2010). In fact coastal sandy sediments from mid latitudes have now been identified as sites of extremely high N-loss, and appear responsible for most of the N removal in these areas (Cook et al. 2007; Gao et al. 2012). Therefore sandy sediments seem to play an important role in global N-loss, despite this studies are still scarce and are restricted to a few locations: the Wadden Sea (Cook et al. 2006; Cook et al. 2007; Gao et al. 2010; Gao et al. 2012), the South Atlantic bight (Rao et al. 2007; Rao et al. 2008), the Gulf of Mexico (Gihring et al. 2010) and Eastern Australia (Evrard et al. 2012; Kessler et al. 2012).

In the mid latitude regions where high N-loss has been reported from sandy sediments, nitrate and organic matter is supplied from the anthropogenically eutrophied water column. Advective flow transports these substrates into the permeable sediments, which act as natural biofilters (Andersen and Helder 1987; Huettel and Rusch 2000; Boudreau et al. 2001; Huettel et al. 2003). N-loss mainly occurs at these sandy sites through canonical denitrification, the reduction of nitrate to N_2. Although anaerobic ammonium oxidation (anammox) to N_2 also occurs in sediments, so far it has not been shown to contribute substantially to N-loss in coastal permeable sediments (e. g. Gao 2012, Gihring 2010). However, few studies of permeable sediments have been undertaken in water depths >100 m and none of these have looked for anammox. As the contribution of anammox to the benthic N-loss generally increases with water depth (Engström et al. 2009; Trimmer and Nicholls 2009; Bohlen et al. 2011; Sokoll et al. 2012), we cannot exclude that it may become more important in deeper continental shelf sediments.

To date no experimental studies on N-loss in permeable sandy sediments have been carried out in low latitude, upwelling areas. In these areas high primary productivity is fuelled by high nutrient inputs originating from deeper waters. The NW-African coast is one of the most productive upwelling systems (Carr 2002) and large areas of the seafloor are covered by sandy sediments, especially off Senegal and northern Mauritania (Lutze and Coulbourn 1984;

Holz et al. 2004). Furthermore the water column off Mauritania is permanently oxic (>22 µmol L^{-1} (Helly and Levin 2004) and therefore N-loss does not occur in the water column (which is the case at other Eastern Boundary upwelling areas). The permeable nature of the sediments off the Mauritanian coast combined with high nitrate concentrations (>15 µmol L^{-1}) in the bottom water and high export production, make this region as potentially important in global benthic N-loss as mid latitude anthropogenically eutrophied sediments.

Currently NW-African shelf sediments in waters <200 m deep are believed to be responsible for a N_2 production via denitrification of 1.7 x 10^{11} mol N yr^{-1} and thus 0.5-1.5% of the global marine N-loss (Seitzinger and Giblin 1996; Codispoti et al. 2001; Gruber 2004; Codispoti 2007). However, this estimate is based on a modelling study (Seitzinger and Giblin 1996) and does not take into account the role of advective processes in permeable sediments for N-loss. Therefore it is likely to be an underestimate of the N_2 production. Moreover, this study also neglected the influence of anammox, which may be important in this region as anammox bacteria have been quantified within the sediment and become more abundant with increasing water depth (Jaeschke et al. 2010).

Here, we present measurements of benthic denitrification and anammox rates using ^{15}N-stable isotope incubation experiments. N-loss was determined at several stations in sediments off Senegal und Mauritania at water depths ranging from 50 to ~3000 m. Moreover, denitrification rates were modelled for the sandy sediments on the entire shelf off Mauritania and Senegal.

Material and Methods

Water column sampling and nutrient analysis

Sampling was conducted during two cruises to the Western African Shelf. In April 2010 a cruise to Cape Blanc at the border off Mauritania and Western Sahara was conducted with *R/V Poseidon* (P398, Table 1). In March/April 2011 a cruise went to the shelf off Senegal and Mauritania with *R/V Maria S. Merian* (MSM17/4, Table 1). Dissolved oxygen, salinity and temperature in the water column were measured with a conductivity-temperature-depth (CTD) system, equipped with an oxygen sensor (Sea Bird Electronics). Oxygen concentration was calibrated against Winkler titration. Water samples for nutrient analyzes were taken with a CTD-rosette. Ammonium and nitrite were measured fluorometrically and photometrically on board (Grasshoff and Johannsen 1972; Holmes et al. 1999). Samples were immediately frozen

and stored at -20°C for determination of phosphate with an autoanalyzer (TRAACS 800, Bran & Luebbe) in an on-shore laboratory.

Sediment sampling and porewater analysis

Sediment cores were taken with a multi-corer (MUC) or during benthic lander deployments (BIGO)(Sommer et al. 2008). The retrieved cores were processed within a few hours. Procedures of porewater extraction and analysis as well as porewater data for cruise MSM 17/4 will be published elsewhere (Dale et al. submitted to GCA). Briefly, porewaters were extracted either by rhizons® (cruise P398, MSM17/4) or by slicing the sediment in an argon atmosphere (MSM17/4). Sediment slices were subsequently centrifugued at max. 4500 G for 20 min and the supernatant porewater filtered with 0.2 µm cellulose acetate Nuclepore® filters. Aliquots of porewater were diluted with O_2-free artificial seawater prior to analysis when necessary. Ammonium (NH_4^+) was measured according to Grasshoff et al. (1999) and nitrate (NO_3^-) was measured chromatographically or with a chemoluminescence NO_x analyzer (Thermo Environmental Instruments Inc. (Braman and Hendrix 2002)). Porosity was calculated from the weight loss of wet sediment during freeze-drying, assuming a dry solid density of 2 g cm^{-3} (Böning et al. 2004). Concentrations of organic carbon and nitrogen were determined by combustion/gas chromatography (Carlo Erba NA-1500 CNS analyzer) of dried sediment samples after acidification with 10% hydrochloric acid.

Grain size analysis and permeability calculation

From the upper layer (0-2cm), sediment was collected for grain size and permeability analysis. Grain size distribution was measured with a Laser Diffraction Particle Size Analyzer (Beckman Coulter) LS200 for 92 size classes from 0.4 to 2000 µm. Measurements were performed after pre-treatment of the samples with H_2O_2 to remove organic compounds. All pre-treatments and the grain-size measurements were carried out in the laboratories of MARUM, Bremen. The lognormal distribution of the grain size diameter was used to calculate sediment permeability using the empirical relation ship of Krumbein and Monk (1943).

^{15}N incubation experiments

Sediment for incubation experiments was sampled by a MUC using plastic liners of 10 cm Ø. The sediment cores were cut in 2 cm layers to a depth of 6, 8 or 12 cm and prepared for incubation in air-tight bags as described in detail before (Gao et al. 2010; Sokoll et al. 2012).

Briefly, the sediment slices were transferred to bags, which were subsequently sealed carefully. To the air-tight bags 200-300 ml of the core overlying bottom water was added with a syringe though a glass port. The water contained either in situ concentrations of O_2 or was degassed prior to the addition. ^{15}N substrate (sodium-$^{15}NO_3$, $^{15}NH_4$-sulfate, Sigma-Aldrich) was added with a 1 ml syringe through the stopper into the bags to final concentrations of 64-88 µmol L^{-1} (cruise MSM17/4) and 230 µmol L^{-1} (during cruise P398). In experiments for determination of denitrification, $^{15}NO^{3-}$ was added, while for anammox $^{15}NH_4^+$, $^{14}NO_2^-$ and allylthiourea (ATU, to a concentration of 86 µmol L^{-1}) were added and is believed to inhibited ammonia oxidation (Ginestet et al. 1998). Occurrence of nitrification was expected in parallel experiments with oxygenated bottom water and without added ATU, however no $^{30}N_2$ production was observed in any of the bags with $^{15}NH_4^+$ addition. Therefore coupled nitrification-denitrification can be excluded as a source of $^{29}N_2$ in the $^{15}NH_4^+$ incubations and all $^{29}N_2$ was assumed to originate from anammox activity. Presumably high oxygen respiration quickly consumed the entire oxygen at the beginning of the experiment, thus preventing the occurrence of significant N_2 production by coupled nitrification-denitrification and only anaerobic processes could be determined.

The bags were incubated at *in situ* temperature in the dark and gently mixed prior to the subsampling. Unfortunately a cold room was not available during cruise P398, therefore the incubation temperature was slightly higher (~20°C) compared to the *in situ* temperature (~14°C). After 0, 3, 6, 12, 24 h (cruise MSM17/4) or 0, 6, 12, 24, 36 (cruise P398) subsamples (~6 ml) of the incubation were taken with a syringe. Subsamples were transferred to a gastight glass vial (exetainer, Labco) and killed with 100 µL of a saturated mercuric chloride solution. The exetainers were stored at room temperature in the dark until further processing. A headspace of 1 ml was introduced into the exetainers prior to the measurement of $^{28,\ 29,\ 30}N_2$ using gas chromatography-isotopic ratio mass spectrometry (VG Optima Micromass) as described in detail by previous publications (Kuypers et al. 2005; Holtappels et al. 2011). N_2 production rates were calculated from the linear increase of $^{29}N_2$ and $^{30}N_2$ over the first 6 hours of the incubation. Denitrification rates (D) were calculated according to Thamdrup and Dalsgaard (2002):

$$D = \frac{p^{30}N_2}{(F_{NO_3^-})^2}$$

where $p^{30}N_2$ denotes the $^{30}N_2$ production measured in experiment 1 and F_{NO3-} is the ratio of $^{15}NO_3^-$ over the total NO_3^-. Anammox rates (A) were calculated according to:

$$A = \frac{p^{29}N_2}{(F_{NH_4^+})^2}$$

where $p^{29}N_2$ denotes the $^{29}N_2$ production measured in experiment 2 and F_{NH4+} is the ratio of $^{15}NH_4^+$ over the total NH_4^+. The labeling percentage (F_N) of either nitrate or ammonium, ranged between 1 and 0.6.

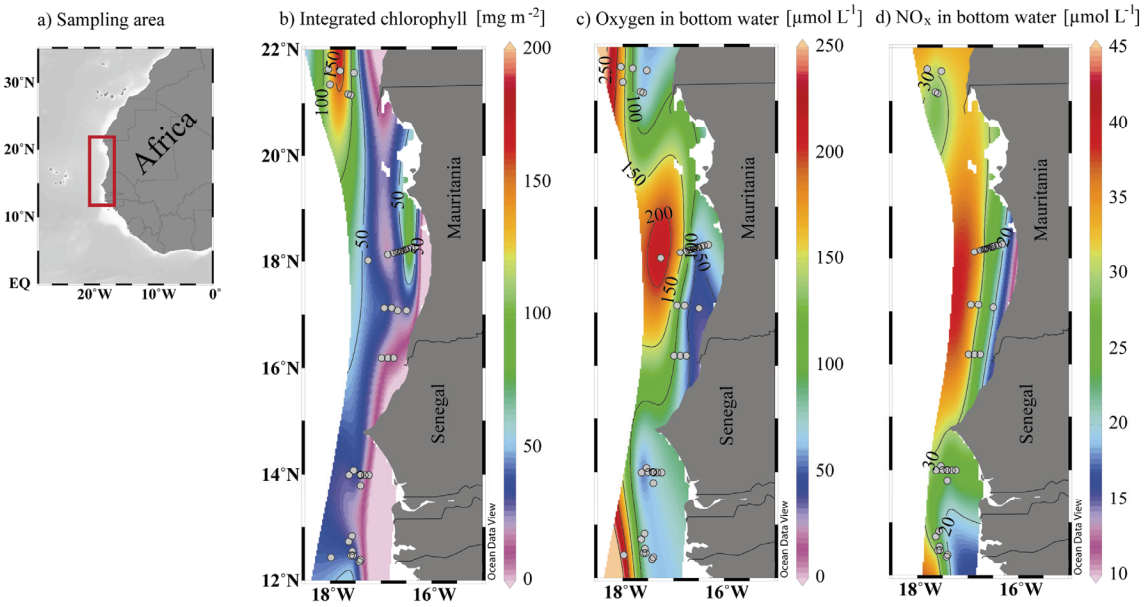

Figure 1: Sampling area (a), chlorophyll concentration (b), oxygen (c) and NO_x (nitrate and nitrite) concentrations (d) in the bottom water off Mauritania and Senegal. Samples taken during P398 (April 2010, 21°-22°N) are plotted together with samples taken during MSM17/4 (March/April 2011, 12°-18°N).

Results

Water column and porewater geochemistry

At the Mauritanian and Senegalese continental shelf, an OMZ was detected during cruise P398 in April 2010 and MSM 17/4 in March/April 2011. In general, oxygen concentrations in the bottom water (BW) at the investigated stations were generally >50 µmol L^{-1} during both cruises (Table 1, Figure 1+2 a). At the shallow stations on the shelf between 50 and 500 m, oxygen in the BW was low (50-80 µmol L^{-1}), indicating the intercept of the seafloor with a pronounced OMZ with the seafloor at this depth interval. At stations deeper than 500 m, oxygen was higher (>80 µmol L^{-1}) indicating the lower boundary of the OMZ around this depth. Nitrate concentrations in the BW increased with water depth from 19 at 50 m to a maximum 37 µmol NO_3^- L^{-1} at 780 m and was slightly lower (32 µmol NO_3^- L^{-1}) at ~3000 m (Figure 2 a).

Table 1: Characteristics and parameters of water column and sediment at the investigated station

Cruise	St.	Water depth	Lat.	Lon.	O_2 in BW	NO_3^- in BW	Porosity surface	Median grain size	Permeability	Sediment classification	C-org	Integration depth	Denitrification rates		Integrated rates		Total N-loss	An
													surface	mean	Den	An		
	no	[m]	[°N]	[°W]	[µmol L^{-1}]			[µm]	[m^2]		[%]	[cm]	[nmol cm^{-3} d^{-1}]		[mmol N m^{-2} d^{-1}]			[%]
P398 April 2010	14102	485	21°34.2	17°31.5	67.8	30.3	n. d.	149.1	7.2×10^{-12}	fine sand	1.15	^{R}4.0	65.9	155.9	6.1	2.8	8.9	31.5
	14103	855	21°36.2	17°48.2	101.4	32.2	n. d.	35.0	2.8×10^{-13}	impermeable	3.82	^{R}4.0	269.7	241.4	10.4	4.7	15.1	31.1
	14105	259	21°08.9	17°35.6	60.2	27.5	n. d.	102.3	4.6×10^{-12}	fine sand	1.97	^{R}1.5	347.9	323.8	5.2	1.2	6.4	18.8
	14107	361	21°10.2	17°38.7	58.1	27.8	n. d.	513.0	9.8×10^{-11}	medium sand	1.67	^{R}6.0	232.7	269.7	16.5	n. d.	16.5	n. d.
MSM17 March/ April 2011	326	2778	12°26.3	17.58.8	230.1	n.d.	n. d.	9.9	1.8×10^{-14}	impermeable	2.51	n. i.	11	59	n. i.	n. i.	n. i.	n. i.
	330	781	12°28.3	17°35.3	80.2	36.7	0.91	20.7	3.9×10^{-14}	impermeable	3.69	1.0	793.8	495.1	7.9	0.4	8.3	4.8
	342	54	12°50.0	17°33.8	81.0	20.6	0.44	256.2	2.6×10^{-11}	medium sand	0.11	0.5	265.4	278.5	2.7	0.4	3.1	12.9
	366	81	13°60.0	17°24.0	68.5	22.6	0.63	387.1	4.2×10^{-11}	medium sand	1.28	^{R}2.5	614.1	697.2	15.8	2.5	18.3	13.7
	380	91	16°11.5	16°45.0	61.2	24.4	0.54	123.2	6.0×10^{-12}	fine sand	0.73	1.0	241.8	285.4	2.4	0.7	3.1	22.6
	410	96	18°15.3	16°27.0	58.8	24.7	0.60	262.8	1.4×10^{-11}	fine sand	1.25	^{R}1.5	754.4	759.5	11.3	0.7	12	5.8
	450	416	18°12.5	16°35.6	53.0	30.5	0.66	77.5	3.3×10^{-12}	fine sand	1.30	0.5	462.3	398.7	2.3	1	3.3	30.3
	496	787	18°11.3	16°39.3	95.9	33.8	0.85	n. d.	n. d.	n. d.	n. d.	0.5	167	126.2	0.8	0.1	0.9	11.1
	522	3024	18°13.0	18°32.0	214.7	32.2	0.82	24.5	4.9×10^{-14}	impermeable	1.02	5.5	2.5	13.3	0.6	1.6	2.2	72.7
	529	77	18°16.3	16°24.0	62.6	23.6	0.58	157.5	6.6×10^{-12}	fine sand	0.45	^{R}1.5	313.1	277.7	4.7	0.2	4.9	4.1
	552	174	18°14.3	16°31.0	56.6	26.4	0.70	104.5	4.2×10^{-12}	fine sand	1.50	0.5	301.9	267.1	1.5	0.2	1.7	11.8
	554	53	18°17.4	16°19.2	55.9	19.4	0.50	179.4	6.5×10^{-12}	fine sand	0.81	^{R}0.5	288.9	267.1	1.4	0.03	1.43	2.1

Den: denitrification
An: anammox
BW: bottom water
R: pore water samples taken with rhizones, other samples were taken by slicing and centrifugation
n. d. not determined
n. i. not integrated
*samples not degassed

Porewater ammonium concentrations were low at the sediment surface and increased with sediment depth (Figure 3). The highest ammonium concentration measured was 65 µmol L^{-1} at 7 cm sediment depth St. 554 (174 m). At some stations, ammonium was undetectable in the surface layer and increased below 3, 2 and 5 cm depth (St. 14102, 10403 and 14107, respectively, Table 1, Figure 3). Nitrate and nitrite concentrations (NO_x) in the porewater usually decreased with sediment depth, with exception of the deep station 522 (~3000 m), where a maximum of NO_x (36 µmol L^{-1}) was found at 1.5 cm. NO_x was detectable to a depth of 5 or even 8 cm at some of the stations, while at other stations nitrate was depleted within the first 2.5 cm (Table 1, Figure 3).

The porosity, grain size and permeability of the sediment increased with water depth (Table 1, Figure 2 b+c). In sediments between 50 m and 400 m water depth, porosity ranged between 0.4 and 0.7, whereas sediments below 780 m were characterized by higher porosities (0.8 to 0.9). The median grain diameters in the sediments of the shallow stations (50-500 m) ranged from 77.5 to 513 µm, such that calculated permeabilities were between 3.3 x 10^{-12} and 9.8 x 10^{-11} m^2. The shallow sediments are therefore characterized as medium to fine sands. In contrast, sediments below 780 m had median grain size distribution of 9.9-35.0 µm and were thus characterized as impermeable (< 2.8 x 10^{-13} m^2). The organic carbon content in the surface sediment layer was lowest (0.11%) in sediment at 50 m water depth and increased with water depth to 3.8% at ~800 m, while at ~3000 m organic carbon was lower (1.1-2.5%).

Measured potential nitrogen loss rates

Nitrogen loss due to denitrification and anammox in sediments were measured in slurry incubation experiments amended with ^{15}N compounds. $^{30}N_2$ production in experiments amended with $^{15}NH_4^+$ was minor for the time-points taken for rate calculation, therefore coupled nitrification-denitrification was insignificant in the experiments, as was outlined in the Material and Methods section. Potential denitrification rates at the deepest station (3024 m depth, St. 522) increased from 2.5 nmol N cm^{-3} d^{-1} at the surface to 22.1 nmol N cm^{-3} d^{-1} at a sediment depth of 4-8 cm (Figure 3) and to 18.3 nmol N cm^{-3} d^{-1} at a sediment depth of 8-12 cm. At the same station, anammox rates increased from 0 at the surface to 81.6 nmol N cm^{-3} d^{-1} at 4-8 cm and decreased again to 17.1 nmol N cm^{-3} d^{-1} at a sediment depth of 8-12 cm.

At water depths between 53 and 858 m, volumetric denitrification rates were much higher than at the deep station and ranged between 65.9 and 794 nmol N cm^{-3} d^{-1} (Figure 3). Surprisingly, denitrification rates did not decrease within the analyzed sediment depths

(6-8 cm) at most of the stations. At most of the shallow stations, anammox rates were considerably lower than denitrification rates and ranged between 5.3 nmol N cm^{-3} d^{-1} (St. 554) and 201 nmol N cm^{-3} d^{-1} (St. 449, Figure 3).

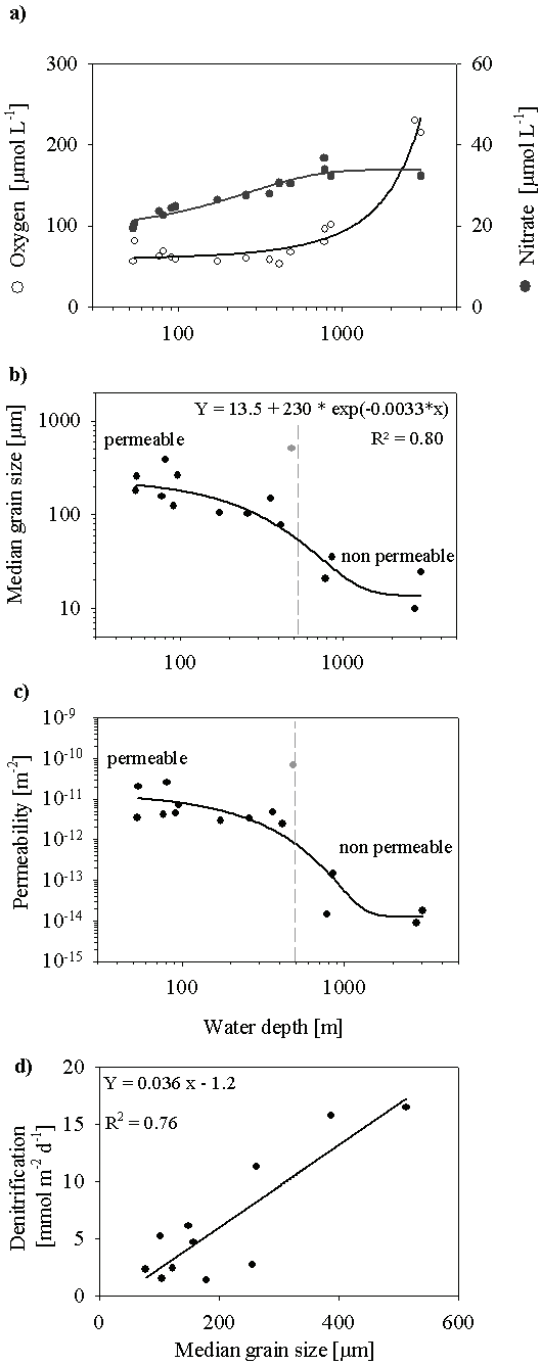

Figure 2: Correlations of different parameters. Bottom water oxygen and NO_x (a), median grain size (b), permeability of sediment (c) with water depth and correlation of NO_3^- penetration depth with median grain size (d) and denitrification rates (e). Grey areas in (b) and (c) mark the non permeable sediments.

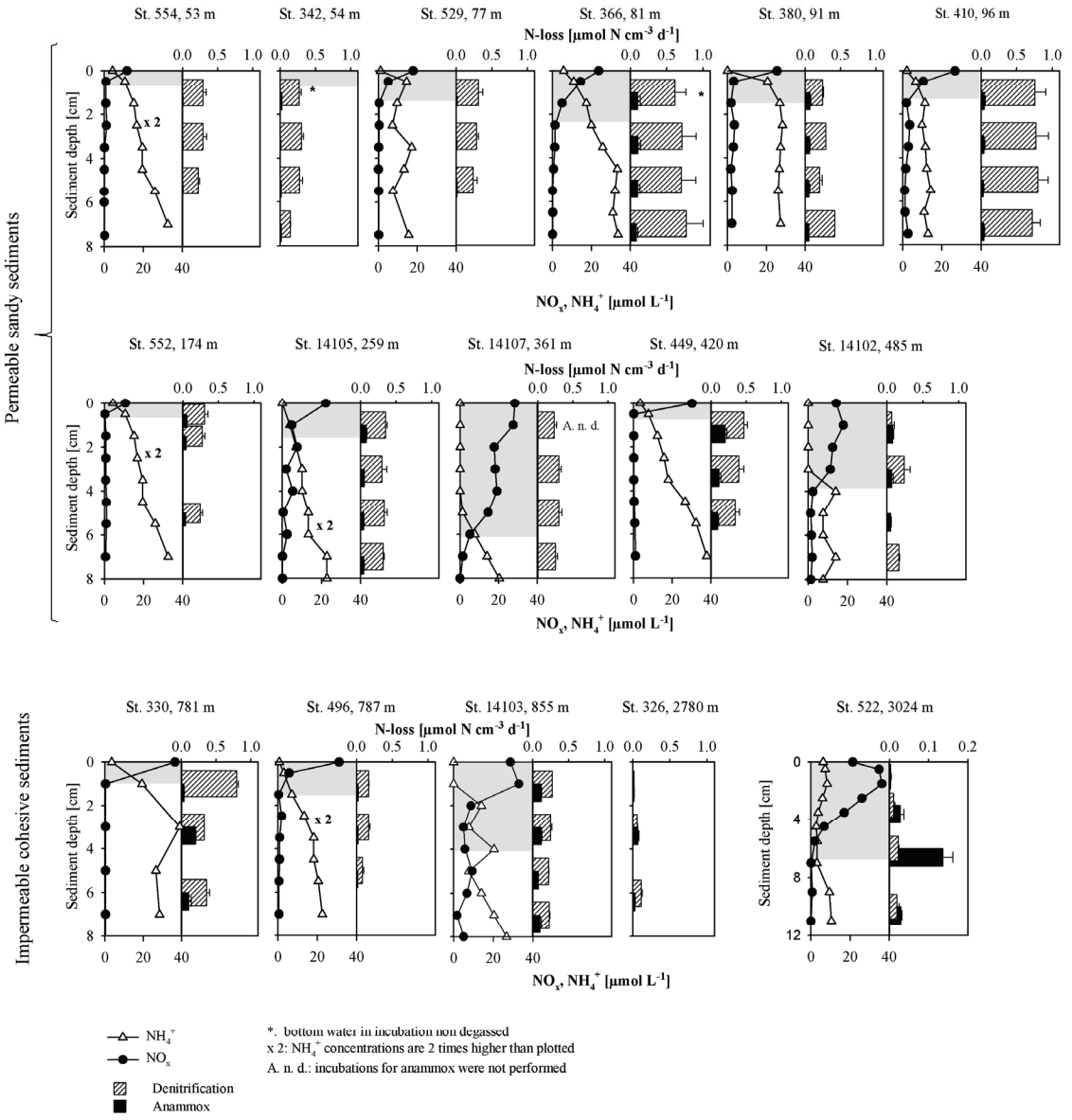

Figure 3: N-loss rates along with porewater profiles of NO_x and ammonium. Stations are ordered according to water depths, such that stations from cruise P398 (14102, 14103, 14105, 14107) are plotted in between stations from MSM17. Please note the axis change for the N-loss rates for different stations and the higher ammonium concentrations at stations 554, 552, 14105 and 496. The grey areas mark the integration depth.

Integrated rates

The volumetric rates from the slurry incubation experiments were integrated over the NO_3^- penetration depth in the sediments (Table 1, Figure 4). At the deep station (3000 m, St. 522), integrated rates were 0.6 mmol N m^{-2} d^{-1} for denitrification and 1.6 mmol N m^{-2} d^{-1} for

anammox, respectively. Therefore anammox contributed 73% to the N-loss at the deep station (Table 1).

In cohesive sediments at water depths between 780 and 855 m, integrated denitrification rates were higher (0.8-10.4 mmol N m^{-2} d^{-1}) with a smaller anammox contribution (5-31%) than at 3000 m (Table 1, Figure 4). In the permeable sediments below a water depth of 700 m, integrated denitrification rates ranged from 1.4 to 15.8 mmol N m^{-2} d^{-1}, with anammox contributing 2-32% to the total N_2 production. In permeable sediments, integrated denitrification rates showed a significant correlation with median grain size (i. e. R^2 = 0.76; Figure 2 d).

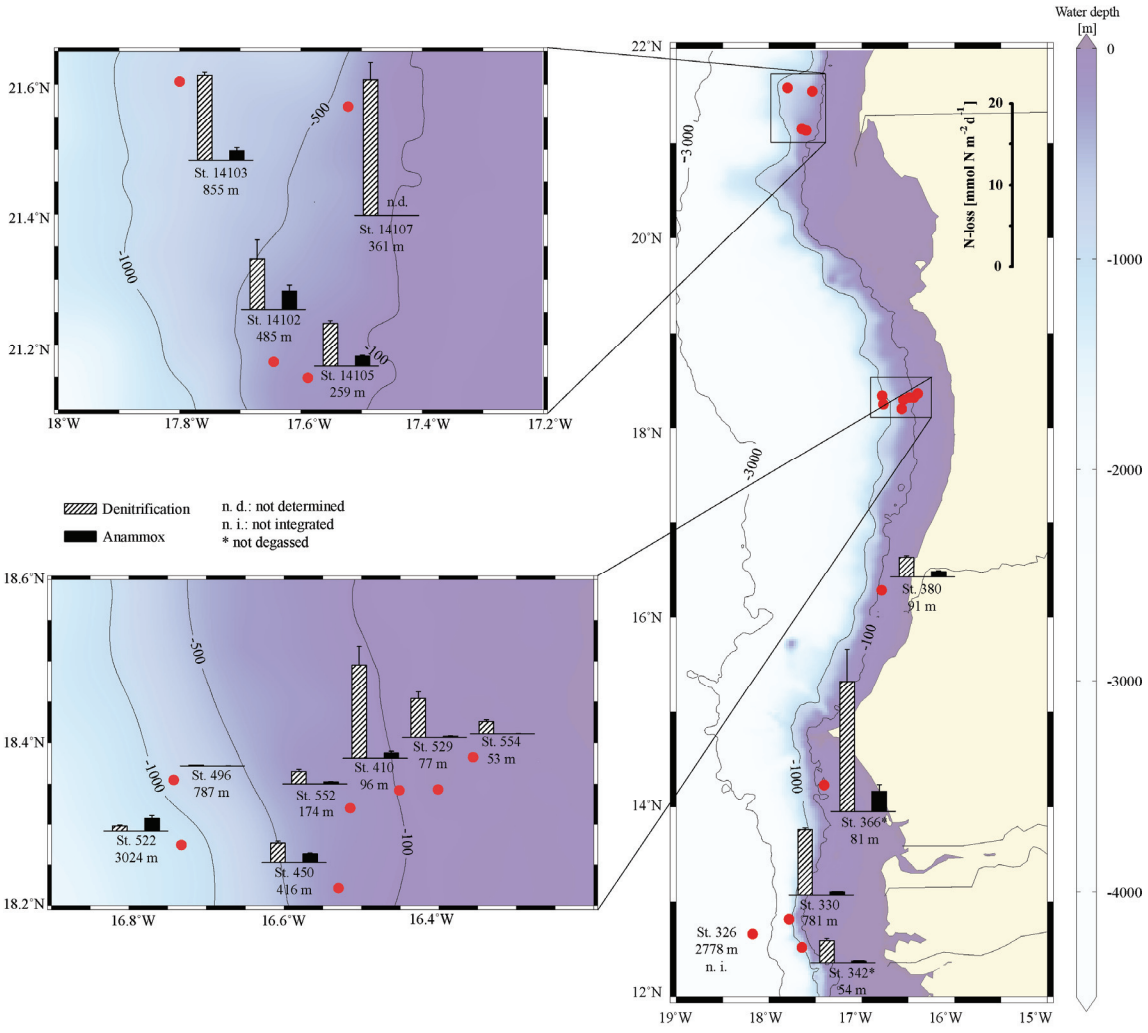

Figure 4: Integrated rates of denitrification and anammox. Rates for St. 326 were not integrated due to the lack of information of the NO_3^- penetration depth. Rates at St. 342 were integrated to a depth of 0.5 cm although NO_3^- penetration depth was unknown.

Discussion

The concentrations of ^{15}N substrates in slurry incubations were significantly above the respective *in situ* concentrations of nitrate and ammonium. Therefore, the volumetric rates have to be considered as potential rates. However, no lag phase in the production of labeled N_2 was observed, indicating constant rates from the beginning of the experiment and no adaptation to higher substrate concentrations in the course of the experiment. Additionally, it was shown by Gao and co-workers (2010) that slurry incubation experiments integrated to the nitrate penetration depth were similar to the core percolation method. In this study N-loss via anammox and denitrification was measured amongst a wide range of water depths with very diverse sediment and bottom water characteristics such as porosity, median grain size, permeability, and bottom water concentrations of O_2 and NO_3^- (Table 1).

Benthic N-loss rates in impermeable slope sediments

At the deepest investigated station (St. 522, 3000 m), low bio-irrigation due to low abundance of benthic fauna and the cohesive nature of the sediments results in a system controlled by diffusive transport. This diffusion limitation leads to stable redox conditions and to a zonation of microbial substrate transformation processes in the sediment. The zonation of the N-loss processes is in line with the porewater profiles, which suggest that the sediment surface at this station is oxygenated. Thus mineralization and nitrification take place in the surface and produce a NO_x maximum at 1.5 cm sediment depth. NO_x concentrations decrease along with the increase of N-loss rates.

At St. 522 potential denitrification rates of up to 22 nmol N cm^{-3} d^{-1} were measured (Figure 3). These rates are half of what was measured off the Washington margin (41 nmol N cm^{-3} d^{-1}) at a comparable water depth using the same method (Engström et al. 2009). In contrast, anammox rates at St. 522 were twice as high (82 nmol N cm^{-3} d^{-1}) as those measured by Engström at al. (2009) off the Washington margin (43 nmol N cm^{-3} d^{-1}). The depth integrated contribution of anammox to the benthic N-loss was ~72% at St 522 of Mauritania. At this station, the high activity of anammox bacteria in deeper sediment layers is in line with the molecular analysis by Jaeschke and co-workers (2010) who found the highest abundance of anammox bacteria based on ladderane lipids and 16S analysis at comparable water depths and sediment layers on the continental margin off Senegal.

The increase of anammox contribution with water depth has been reported by various other studies and has often been attributed to the lower organic carbon supply and higher NO_3^- concentrations at depth (Engström et al. 2009; Trimmer and Nicholls 2009; Bohlen et al.

2011; Sokoll et al. 2012). In principle, high NO_3^- concentrations and decreased denitrification rates due to decreased organic carbon supply could result in incomplete denitrification and thus enhanced NO_2^- availability for the anammox bacteria. However, off Mauritania organic carbon content in the surface sediment increased with water depth (Table 1) corresponding to the decrease in sediment grain size. This could suggest that slow growing autotrophic anammox bacteria find more favorable conditions in sediments which are less permeable and bioturbated, but are instead characterized by a more stable redox zonation. In contrast, heterotrophic denitrifier seem better adapted to dynamic redox conditions such as the pulse-like supply of various substrates caused by dynamic porewater advection and bioturbation. Denitrification as the dominant N-loss process in permeable sediments was also observed in previous studies (Gao et al. 2012)

Benthic N-loss rates in permeable shelf sediments

In contrast to the zonation at the deep station, N_2 production rates were high throughout the investigated sediment layers at the shallower stations and the decrease of the potential N-loss activity with sediment depth was very little. The lack of zonation suggests that the shallow stations are very dynamic and presumably influenced by advective transport of bottom water and bioirrigation. In general, volumetric denitrification rates were very high at the shallower stations. At St. 410 (96 m water depth), rates of 0.8 µmol cm^{-3} d^{-1} were measured, which is more than two orders of magnitude higher than the denitrification rates measured at St. 522 (0.003 µmol cm^{-3} d^{-1}, 3000 m). This difference in activity presumably reflects the different NO_x transport conditions, which change from advective porewater transport in permeable and shallow sediments to a diffusion limited transport in cohesive sediments at the deep station. Increased denitrification may also be stimulated by the flux of labile organic matter that is expected to be enhanced at shallow stations compared to deep stations. The volumetric denitrification rates measured in these permeable sediments are extremely high. These rates are above those measured for intertidal Wadden Sea sediments (0.26 µmol cm^{-3} d^{-1}), which were so far amongst the highest reported benthic denitrification rates (Gao et al. 2010).

Impact of advective transport on porewater nitrate concentrations and benthic N-loss

At the stations off Cape Blanc, NO_x was detected down to a sediment depth of 4-8 cm (St. 14102, 14103, 14105, 14107). Similarly, at some of the shallow stations off Mauritania and Senegal NO_x was detected in the first 1-2 cm of the sediment (St. 366, 410, 529, 496) while at other stations NO_x was depleted within 0.5 cm of the sediment (St. 380, 554, 552, 449, 330).

Porewater profiles in the same area by a different study suggest a similar nitrate penetration into the sediment of ~1.5-3.5 cm at water depths of 330 and 500 m (Jaeschke et al. 2010).

Samples for porewater nitrate concentrations were taken from sediment cores in which advective porewater transport was absent. The reduced porewater transport in combination with high denitrification rates can change the porewater concentrations within short time periods. Denitrification rates of approximately 0.2 μmol cm^{-3} d^{-1}, measured in the permeable shelf sediments, would remove ~10 μmol L^{-1} NO_3^- within 72 minutes if NO_3^- transport is shut down completely, e. g. during core storage before porewater extraction. The nitrate penetration depths presented here are therefore conservative estimates. Similar observations have been made by Rao and co-workers (2007), who detected high denitrification rates without high porewater NO_x concentrations.

Based on the permeable nature of the sandy sediment at the shallow stations, advective transport of nitrate rich bottom water into the sediment can be expected (Huettel et al. 1998). Indeed, in the surface layers of stations 14107, 14102 and 14103, NH_4^+ and NOx concentrations similar to those in the bottom water were found down to 4 cm depth indicating advective transport of bottom water. Furthermore, coarse grained and more permeable sediment should facilitate the advective exchange of bottom- and porewater. Advective porewater flow at these depths can be induced by current-topography-interactions and by bio-irrigation. Bio-irrigation in permeable sediments significantly enhances the affected sediment volume compared to cohesive muddy sediments (Meysman et al. 2006a; Meysman et al. 2006b; Volkenborn et al. 2010). At some stations (e. g. 410, 450) a rich benthic macrofauna community and high density of burrow holes was observed in the sampled sediment and documented by an Ocean Floor Observation System (OFOS; Pfannkuche unpublished data). Additionally, other studies report a high number of polychaetes in the investigated area (Le Loeuff and von Cosel 1998). The dense macrofauna populations at these stations suggest a significant impact of bioirrigation on the sediment biogeochemistry and indeed, several NO_x profiles exhibit local concentration maxima at greater sediment depth (St. 380, 410, 14105, 496 and 14103).

Areal benthic N-loss from permeable sediments

The N_2 production rates from slurry incubations were integrated down to the nitrate penetration depth, which was conservatively estimated from the nitrate porewater profiles. The areal rates of denitrification for the Mauritanian and Senegalese shelf ranged from 0.6 to 16.5 mmol N m^{-2} d^{-1} (Table 1). In general, denitrification rates tend to increase with organic

carbon content in the sediment and integrated chlorophyll concentrations in the water column, but correlation was poor ($R^2 \leq 0.2$). Highest areal denitrification rates were calculated for St. 14107 (361 m) at Cape Blanc (16.5 mmol N m^{-2} d^{-1}, Figure 4) and for St. 366 (81 m) further south (15.8 mmol N m^{-2} d^{-1}). Both stations (St. 366 and 14107) exhibit a deep penetration of nitrate, resulting in high denitrification rates. Therefore factors like median grain size and permeability seem to be the main regulators for the turnover of organic matter and nitrate via denitrification. Indeed, areal denitrification rates in sandy sediments significantly correlate with median grain size (Figure 2 e). Areal denitrification rates increase from 1.4 mmol N m^{-2} d^{-1} at 50 m to a maximum of 11.8 mmol N m^{-2} d^{-1} at 96 m (St. 410, Figure 4) and decrease with water depth. Interestingly, St. 410 is characterized by a high abundance of burrow holes and benthic fauna, which suggest a high pumping activity and substrate transport into deeper sediment layers.

At most of the stations off Mauritania, denitrification rates were higher than the rates measured in permeable subtidal sediments in the eastern Atlantic (0.25-1.5 mmol N m^{-2} d^{-1} (Rao et al. 2007)). The highest denitrification rates off Mauritania (16.7 mmol N m^{-2} d^{-1}) were similar to the highest rates measured in the Wadden Sea (25.3 mmol N m^{-2} d^{-1}(Gao et al. 2012)) and at the Australian coast (16.1 mmol N m^{-2} d^{-1}(Santos et al. 2012)). In fact, the majority of the stations off Mauritania exhibited areal denitrification rates comparable to the intertidal Wadden Sea (3.5-7.2 mmol N m^{-2} d^{-1} (Gao et al. 2010)).

Modelled N-loss from the Mauritanian and Senegalese shelf

The denitrification rates measured in permeable sediments were extrapolated to an entire shelf area of 84.150 km^2, enclosed by the Latitudes 12° and 22° North, the coastline and the 500 m depth isoline, which defines the transition from permeable to non permeable sediments (Figures 2 b and c). The area was extracted from a bathymetry map with 1 minute spatial resolution (http://www.ngdc.noaa.gov). We applied the empirical relationship between water depth and median grain size (Figure 2 b) to derive a spatial grain size distribution. Subsequently, the observed linear relation between median grain size and denitrification rates was used to estimate denitrification rates within this area (Figure 5). The N-loss due to canonical denitrification from the sandy sediment of this broad shelf area amounts in total to 5.1×10^8 mol N d^{-1} ($\pm$ 9.7×10^7 mol N d^{-1}, derived from the standard error of the slope of the linear regression). Neglecting seasonal variability this would result in a yearly denitrification rate of 1.9×10^{11} mol N yr^{-1}. Seitzinger and Giblin (1996) modeled a similar benthic denitrification rate of 1.7×10^{11} mol N yr^{-1} for the NW-African shelf but for an area five times

as large (between 0-45°N and <200 m water depth). First, in contrast to Seitzinger and Giblin, who used primary production as a proxy for organic matter input to model denitrification rates, our model was based on a proxy for advective transport conditions (i.e. median grain size), which also reflects the increasing relevance of mass transport conditions for process rates in sandy sediment that was recognized in recent years. Second, our model is based on denitrification rate measurements that consider advective porewater transport in contrast to Seitzinger and Giblin (1996) who used diffusion limited rates.

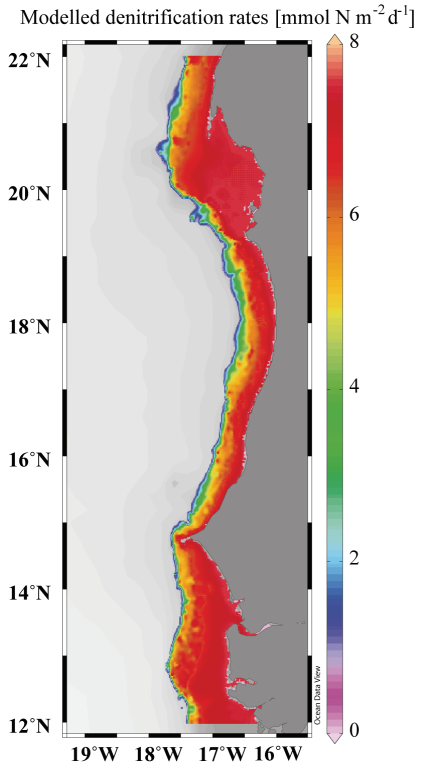

Figure 5: Modelled N-loss by denitrification. Modelled for the Mauritanian and Senegalese shelf to a depth of 500 m based on the correlations of water depth and grain size as well as grain size and denitrification rates.

Conclusions

Our results from the upwelling region off Mauritania and Senegal show that anammox is the dominant N-loss process in impermeable slope sediments at ~3000 m. Since deep sediments are covering most of the seafloor, anammox could be very widespread and an important N-loss process in the deep sea. The continental shelf of Mauritania and Senegal to a water depth of ~500 m is covered by permeable sediments. High potential for denitrification was for the first time measured and verified in this study for these permeable sediments and for sandy

sediments in a major upwelling region in general. In these naturally eutrophied waters high velocity currents may not only be responsible for the lack of an organic sediment toplayer, as in other Eastern Boundary upwelling regions (e. g. Peru, Namibia) but also for the missing imprint of the N-loss on the N:P ratio in form of a N-deficit in the bottom water.

Moreover, high denitrification potential was also measured in sediments from mid-range water depths (~800 m), that were so far not considered as important N-sinks at the Mauritanian shelf. The sediments at these water depths are highly bioturbated. Bioturbation and bioirrigation on the margin presumably provides substrate such as nitrate and organic matter to deeper sediment layers and fueling denitrification activity deep in the sediment. In summary, favorable conditions such as high primary production and organic matter export, fast advective porewater transport, high abundance of benthic fauna lead to extensive N-loss from permeable sediments off Mauritania and Senegal. Intensified upwelling expected in the future for this region might further fuel benthic N-loss by denitrification due to higher organic carbon export from the surface. Considering their widespread occurrence, subtidal sandy sediments might play an important but so far largely neglected role in marine N-loss.

Acknowledgements

For excellent collaboration and mug-deployment during cruise P398 and MSM17/4 the authors like to thank K. Zonneveld, G. Versteegh, O. Pfannkuche, R. Schneider, P. Martinez, T. Treude and V. Bertics. We also like to thank the captain and crews of *RV* Poseidon and *RV* Maria S. Merian for co-operation. Moreover, we are very thankful for the porewater extraction and analysis by L. Bohlen, A. Noffke and A. Bleyer and for the permission from the Mauritanian and Senegalese authorities to access their national waters. We also like to thank the assistance of J. Füssel, T. Kalvelage and H. Marchant as well as K. Thieme and I. Boosmann for their GC-IRMS measurements. The analysis of the grain size by C. Winter and his students improved this study and is thoughtfully acknowledged. For the measurements of TOC we are grateful to G. Klockgether and T. Kanli. Funding for this project came from the Max Planck Society and the Center of Environmental Science (MARUM) at the University of Bremen.

References

Andersen, F. O. and W. Helder (1987). "Comparison of oxygen microgradients, oxygen flux rates and electron-transport system activity in coastal marine-sediments." Marine Ecology Progress Series 37(2-3): 259-264.

Bohlen, L., A. W. Dale, S. Sommer, T. Mosch, C. Hensen, A. Noffke, F. Scholz and K. Wallmann (2011). "Benthic nitrogen cycling traversing the Peruvian oxygen minimum zone." Geochimica Et Cosmochimica Acta 75(20): 6094-6111.

Böning, P., H. J. Brumsack, M. E. Bottcher, B. Schnetger, C. Kriete, J. Kallmeyer and S. L. Borchers (2004). "Geochemistry of Peruvian near-surface sediments." Geochimica Et Cosmochimica Acta 68(21): 4429-4451.

Boudreau, B. P., M. Huettel, S. Forster, R. A. Jahnke, A. McLachlan, J. J. Middelburg, P. Nielsen, F. Sansone, G. Taghon, W. Van Raaphorst, I. Webster, J. M. Weslawski, P. Wiberg and B. Sundby (2001). "Permeable marine sediments: Overturning an old paradigm." Eos, Transactions American Geophysical Union 82(11): 133-136.

Braman, R. S. and S. A. Hendrix (2002). "Nanogram nitrite and nitrate determination in environmental and biological materials by vanadium(III) reduction with chemiluminescence detection." Analytical Chemistry 61(24): 2715-2718.

Carr, M. E. (2002). "Estimation of potential productivity in Eastern Boundary Currents using remote sensing." Deep-Sea Research Part II-Topical Studies in Oceanography 49(1-3): 59-80.

Codispoti, L. A. (2007). "An oceanic fixed nitrogen sink exceeding 400 Tg Na-1 vs the concept of homeostasis in the fixed-nitrogen inventory." Biogeosciences 4(2): 233-253.

Codispoti, L. A., J. A. Brandes, J. P. Christensen, A. H. Devol, S. W. A. Naqvi, H. W. Paerl and T. Yoshinari (2001). "The oceanic fixed nitrogen and nitrous oxide budgets: Moving targets as we enter the anthropocene?" Scientia Marina 65: 85-105.

Cook, P. L. M., F. Wenzhoefer, S. Rysgaard, O. S. Galaktionov, F. J. R. Meysman, B. D. Eyre, J. Cornwell, M. Huettel and R. N. Glud (2006). "Quantification of denitrification in permeable sediments: Insights from a two-dimensional simulation analysis and experimental data." Limnology and Oceanography-Methods 4: 294-307.

Cook, P. L. M., F. Wenzhöfer, R. N. Glud, F. Janssen and M. Huettel (2007). "Benthic solute exchange and carbon mineralization in two shallow subtidal sandy sediments: Effect of advective pore-water exchange." Limnology and Oceanography 52(5): 1943-1963.

Emery, K. O. (1968). "Relict sediments on continental shelves of world." AAPG Bulletin 52(3): 445-464.

Engström, P., C. R. Penton and A. H. Devol (2009). "Anaerobic ammonium oxidation in deep-sea sediments off the Washington margin." Limnology and Oceanography 54(5): 1643-1652.

Evrard, V., R. Glud and P. M. Cook (2012). "The kinetics of denitrification in permeable sediments." Biogeochemistry: 1-10.

Gao, H., M. Matyka, B. Liu, A. Khalili, J. E. Kostka, G. Collins, S. Jansen, M. Holtappels, M. M. Jensen, T. H. Badewien, M. Beck, M. Grunwald, D. de Beer, G. Lavik and M. M. M. Kuypers (2012). "Intensive and extensive nitrogen loss from intertidal permeable sediments of the Wadden Sea." Limnology and Oceanography 57(1): 185-198.

Gao, H., F. Schreiber, G. Collins, M. M. Jensen, J. E. Kostka, G. Lavik, D. de Beer, H.-y. Zhou and M. M. M. Kuypers (2010). "Aerobic denitrification in permeable Wadden Sea sediments." Isme Jounal 4(3): 417-426.

Gihring, T. M., A. Canion, A. Riggs, M. Huettel and J. E. Kostka (2010). "Denitrification in shallow, sublittoral Gulf of Mexico permeable sediments." Limnology and Oceanography 55(1): 43-54.

Ginestet, P., J. M. Audic, V. Urbain and J. C. Block (1998). "Estimation of nitrifying bacterial activities by measuring oxygen uptake in the presence of the metabolic inhibitors allylthiourea and azide." Applied and Environmental Microbiology 64(6): 2266-2268.

Grasshoff, K. and H. Johannsen (1972). "New sensitive and direct method for automatic determination of ammonia in sea-water." Journal Du Conseil 34(3): 516-521.

Grasshoff, K., K. Kremling and M. Ehrhardt (1999). Methods of Seawater Analysis,. Weinheim, Germany, Wiley-VCH Verlag GmbH.

Gruber, N. (2004). The dynamics of the marine nitrogen cycle and its influence on atmospheric CO_2 variations NATO Science Series IV Earth and Environmental Sciences : 40, The Ocean Carbon Cycle and Climate. M. Follows and T. Oguz. Dordrecht, Kluwer Academic Publishers: 97-148.

Helly, J. J. and L. A. Levin (2004). "Global distribution of naturally occurring marine hypoxia on continental margins." Deep-Sea Research Part I-Oceanographic Research Papers 51(9): 1159-1168.

Holmes, R. M., A. Aminot, R. Kerouel, B. A. Hooker and B. J. Peterson (1999). "A simple and precise method for measuring ammonium in marine and freshwater ecosystems." Canadian Journal of Fisheries and Aquatic Sciences 56(10): 1801-1808.

Holtappels, M., G. Lavik, M. M. Jensen and M. M. M. Kuypers (2011). ^{15}N-labeling experiments to dissect the contributions of heterotrophic denitrification and anammox to nitrogen removal in the OMZ waters of the ocean. Methods in Enzymology: Research on Nitrification and Related Processes, Vol 486, Part A. M. Klotz. San Diego, Elsevier Academic Press Inc. 486: 223-251.

Holz, C., J. B. W. Stuut and R. Henrich (2004). "Terrigenous sedimentation processes along the continental margin off NW Africa: implications from grain-size analysis of seabed sediments." Sedimentology 51(5): 1145-1154.

Huettel, M., H. Roy, E. Precht and S. Ehrenhauss (2003). "Hydrodynamical impact on biogeochemical processes in aquatic sediments." Hydrobiologia 494(1-3): 231-236.

Huettel, M. and A. Rusch (2000). "Transport and degradation of phytoplankton in permeable sediment." Limnology and Oceanography 45(3): 534-549.

Huettel, M., W. Ziebis, S. Forster and G. W. Luther (1998). "Advective transport affecting metal and nutrient distributions and interfacial fluxes in permeable sediments." Geochimica Et Cosmochimica Acta 62(4): 613-631.

Jaeschke, A., B. Abbas, M. Zabel, E. C. Hopmans, S. Schouten and J. S. S. Damste (2010). "Molecular evidence for anaerobic ammonium-oxidizing (anammox) bacteria in continental shelf and slope sediments off northwest Africa." Limnology and Oceanography 55(1): 365-376.

Kessler, A. J., R. N. Glud, M. B. Cardenas, M. Larsen, M. F. Bourke and P. L. M. Cook (2012). "Quantifying denitrification in rippled permeable sands through combined flume experiments and modeling." Limnology and Oceanography 57(4): 1217-1232.

Krumbein, W. C. and G. D. Monk (1943). "Permeability as a function of the size parameters of unconsolidated sand." Transactions of the American Institute of Mining and Metallurgical Engineers 151: 153-163.

Kuypers, M. M. M., G. Lavik, D. Woebken, M. Schmid, B. M. Fuchs, R. Amann, B. B. JØrgensen and M. S. M. Jetten (2005). "Massive nitrogen loss from the Benguela upwelling system through anaerobic ammonium oxidation." Proceedings of the National Academy of Sciences of the United States of America 102(18): 6478-6483.

Le Loeuff, P. and R. von Cosel (1998). "Biodiversity patterns of the marine benthic fauna on the Atlantic coast of tropical Africa in relation to hydroclimatic conditions and paleogeographic events." Acta Oecologica-International Journal of Ecology 19(3): 309-321.

Lohse, L., H. T. Kloosterhuis, W. van Raaphorst and W. Helder (1996). "Denitrification rates as measured by the isotope pairing method and by the acetylene inhibition technique in continental shelf sediments of the North Sea." Marine Ecology Progress Series 132(1-3): 169-179.

Lutze, G. F. and W. T. Coulbourn (1984). "Recent benthic foraminifera from the continental-margin of Northwest Africa - community structure and distribution." Marine Micropaleontology 8(5): 361-401.

Meysman, F. J. R., E. S. Galaktionov, B. Gribsholt and J. J. Middelburg (2006a). "Bioirrigation in permeable sediments: Advective pore-water transport induced by burrow ventilation." Limnology and Oceanography 51(1): 142-156.

Meysman, F. J. R., O. S. Galaktionov, B. Gribsholt and J. J. Middelburg (2006b). "Bio-irrigation in permeable sediments: An assessment of model complexity." Journal of Marine Research 64(4): 589-627.

Rao, A. M. F., M. J. McCarthy, W. S. Gardner and R. A. Jahnke (2007). "Respiration and denitrification in permeable continental shelf deposits on the South Atlantic Bight: Rates of carbon and nitrogen cycling from sediment column experiments." Continental Shelf Research 27(13): 1801-1819.

Rao, A. M. F., M. J. McCarthy, W. S. Gardner and R. A. Jahnke (2008). "Respiration and denitrification in permeable continental shelf deposits on the South Atlantic Bight: N_2 : Ar and isotope pairing measurements in sediment column experiments." Continental Shelf Research 28(4-5): 602-613.

Santos, I. R., B. D. Eyre and R. N. Glud (2012). "Influence of porewater advection on denitrification in carbonate sands: Evidence from repacked sediment column experiments." Geochimica Et Cosmochimica Acta 96: 247-258.

Seitzinger, S. and A. Giblin (1996). "Estimating denitrification in North Atlantic continental shelf sediments." Biogeochemistry 35(1): 235-260.

Sokoll, S., M. Holtappels, P. Lam, G. Collins, M. Schlüter, G. Lavik and M. M. M. Kuypers (2012). "Benthic nitrogen loss in the Arabian Sea off Pakistan." Frontiers in Microbiology 3(395).

Sommer, S., M. Turk, S. Kriwanek and O. Pfannkuche (2008). "Gas exchange system for extended in situ benthic chamber flux measurements under controlled oxygen conditions: First application - Sea bed methane emission measurements at Captain Arutyunov mud volcano." Limnology and Oceanography-Methods 6: 23-33.

Thamdrup, B. and T. Dalsgaard (2002). "Production of N_2 through anaerobic ammonium oxidation coupled to nitrate reduction in marine sediment." Applied and Environmental Microbiology 68(3): 1312-1318.

Trimmer, M. and J. C. Nicholls (2009). "Production of nitrogen gas via anammox and denitrification in intact sediment cores along a continental shelf to slope transect in the North Atlantic." Limnology and Oceanography 54(2): 577-589.

Vance-Harris, C. and E. Ingall (2005). "Denitrification pathways and rates in the sandy sediments of the Georgia continental shelf, USA." Geochemical Transactions 6(1): 12-18.

Volkenborn, N., L. Polerecky, D. S. Wethey and S. A. Woodin (2010). "Oscillatory porewater bioadvection in marine sediments induced by hydraulic activities of Arenicola marina." Limnology and Oceanography 55(3): 1231-1247.

Chapter IV

Intense biological phosphate uptake in the sub-euphotic zone of upwelling areas

Sarah Sokoll[1], Timothy G. Ferdelman[1], Moritz Holtappels[1], Tobias Goldhammer[2], Sten Littmann[1], Morten H. Iversen[2] and Marcel M. M. Kuypers[1]

[1]Max Planck Institute for Marine Microbiology, Bremen, Germany

[2]MARUM-Center for Marine Environmental Sciences, University of Bremen, Bremen, Germany

First Paragraph

The benthic boundary layer (BBL) is a particle-rich transition zone between the water column and sediments where remineralization of sinking organic matter and nutrient exchange from sediments releases dissolved phosphate (P_i), a key nutrient, to the water column. Although P_i is known to be particle reactive, microbial turnover and incorporation of P_i into particles in the BBL and the sub-euphotic zone in general is virtually unexplored. We investigated incorporation of phosphorus (P) into particles in the sub-euphotic water column and BBL in the Mauritanian and Namibian upwelling regions using $^{33}PO_4^{3-}$ labeling experiments combined with sequential extraction (SEDEX) of ^{33}P (Ruttenberg 1992; Goldhammer et al. 2010) and nano scale secondary ion mass spectrometry (nanoSIMS) analysis of ^{33}S (decay product of ^{33}P)-enriched particles. Our experiments show biological uptake of P_i ostensibly linked to organic carbon remineralization. In oxygenated waters off Mauritania and Namibia P-uptake rates in the BBL were rapid (4.3 and 29.7 nmol P L^{-1} d^{-1}) and biologically controlled. Comparison of P_i-uptake and oxygen consumption rates off Mauritania indicated that almost all P_i was released by aerobic respiration of organic matter in the sub-euphotic water column. In anoxic waters, rapid exchange of ^{33}P with P_i on iron-rich particles (within 0.5 h) masked likewise high rates of biotic P-uptake. This P_i associated with iron-rich particles in the anoxic Namibian shelf waters may provide an additional pool of biologically available P_i. This study provides mechanistic insight into the biotic and abiotic regulation of P concentrations and eventually N:P ratios in continental shelf water masses.

Main

Phosphorus (P) is one of the major elements (carbon, nitrogen, phosphorus) that is essential for all living organisms on earth and ultimately limits global primary production in the ocean on geological time-scales (Tyrrell 1999). While the mean oceanic concentration of P_i is 2.25 µmol L^{-1} (Delaney 1998), most surface waters are depleted in P_i (<<1 µmol L^{-1}) due to the assimilation by phytoplankton in the euphotic zone. P-uptake has been studied extensively in these P_i limited areas (Perry and Eppley 1981; Thingstad et al. 1993; Tanaka et al. 2003; van den Broeck et al. 2004; Duhamel et al. 2007; Zubkov et al. 2007; Casey et al. 2009; Sohm and Capone 2010), as P_i concentrations can regulate the degree of primary production as well as the community structure of the primary producers. In contrast, P-uptake, the degree of internal cycling of P, and the influence of abiotic particles on the bioavailability of P in the deep waters and the BBL are practically unknown and P-uptake processes in the BBL have not been considered in oceanic P-cycling (Delaney 1998; Benitez-Nelson 2000; Paytan and McLaughlin 2007).

In high productive upwelling areas, reduced ventilation and remineralization of organic matter can lead to a severe decrease of oxygen, resulting in low oxygen concentrations in the water column – so-called oxygen minimum zones (OMZs). High P_i concentrations in the BBL of OMZs are usually attributed to the flux of P from sediments to the water column (Ingall and Jahnke 1994). Nevertheless, mechanisms of microbial uptake, particulate P formation, and adsorption might "trap" P in the BBL, and effectively enhance total P concentrations in laterally advected or upwelled shelf OMZ waters.

We investigated P-incorporation into particles in the lower water column and BBL of two shelf OMZs. The Namibian and Mauritanian shelf sites are coastal upwelling zones characterized by high primary productivity and particle export flux (Figure 1) (Wefer and Fischer 1993; Carr 2002). Two of the three investigated stations (St. 477 Mauritania and St. 13 Namibia) had low dissolved oxygen concentrations (~60-80 µmol O_2 L^{-1}) and P_i concentrations of up to 2.3 µmol L^{-1} in the BBL (Figure 1). At St. 2 on the Namibian shelf north of Walvis Bay the water column was anoxic from 90 m down to the seafloor and P_i concentrations reached 4.9 µmol L^{-1} at the seafloor. We performed $^{33}PO_4^{3-}$ incubations on water samples from the water column and BBL to examine P uptake. The distribution of ^{33}P into different chemically defined organic and inorganic fractions was investigated using SEDEX (Ruttenberg 1992; Goldhammer et al. 2010). Particles and individual cells were analyzed for ^{31}P and ^{33}S (decay product of ^{33}P) using a secondary ion mass spectrometer (nanoSIMS) to determine their enrichment in ^{33}P.

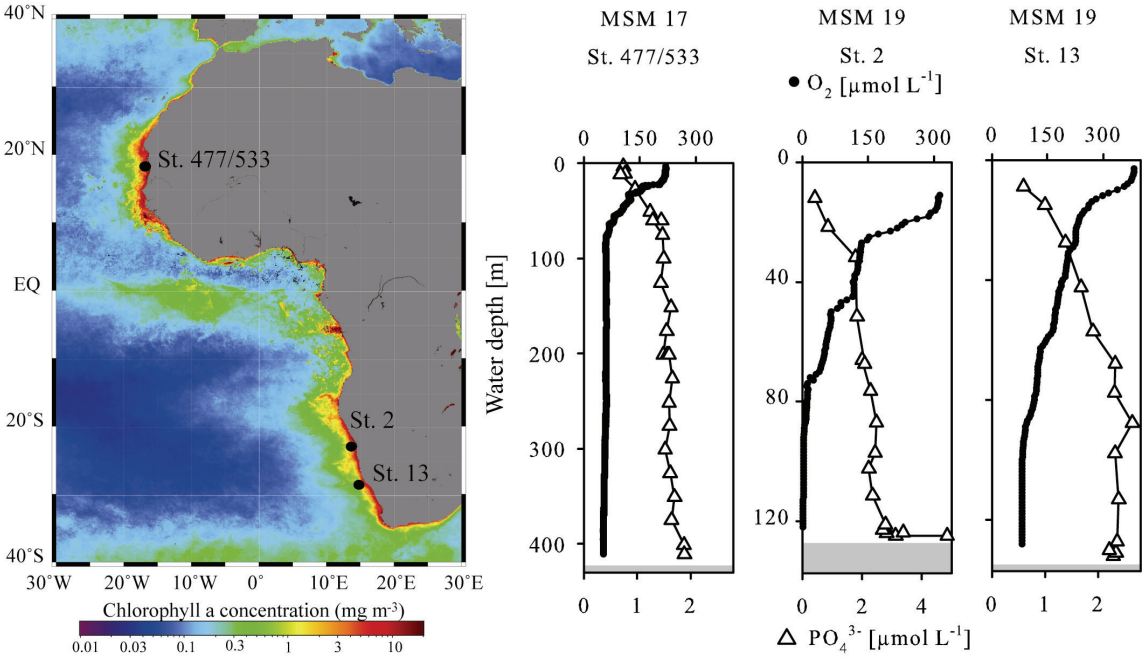

Figure 1: Annual chlorophyll a concentration in 2011, oxygen and phosphate profiles at the three sampled stations off Mauritania (MSM17) and off Namibia (MSM19). Water samples were taken either by a CTD-rosette or a bottom water sampler. The grey areas in the profiles depict the seafloor. Chlorophyll map was downloaded from http://oceancolor.gsfc.nasa.gov/.

Uptake of P_i in oxic waters

Enrichment of ^{33}P in particles (>0.2 µm) over time was observed in all incubations with oxygenated bottom water and ranged from 4‰ off Namibia to 21‰ off Mauritania (Figure 2 A, B and D). The time-course incubations showed an initial delay (up to ~30 h) in ^{33}P incorporation into particles followed by a linear increase and reached a plateau after 30 h in some of the incubations (Figure 2 B and D, SI). Samples treated with azide exhibited negligible (<8 nmol P L^{-1}) uptake over the course of the experiment, suggesting that ^{33}P-uptake was biologically mediated (Figure 2 A, B, D).

P_i pools and turnover

Analytical speciation of the incorporated ^{33}P into chemically defined fractions using the SEDEX procedure (see SI) showed that ^{33}P accumulated predominately in the adsorbed/ iron bound fraction (34-67%) and in the organic fraction (25-63%) with minor accumulation in the apatite fractions (2-22%) (Figure 3 B, SI Figure 2 A and C). We are confident that the ^{33}P extracted from the organic fraction represents cellular ^{33}P, as application of the procedure to the azide controls yielded no significant accumulation in the organic fraction (adsorption accounted for ≥ 92%). Microorganisms also appear to have some further effect on

P-adsorption itself, since at St. 477 and in the BBL of Mauritania, adsorption of ^{33}P in azide controls was considerably lower than in live incubations (Figure 3 B, SI Figure 2), which is consistent with adsorption processes known from algae in the surface waters (Sanudo-Wilhelmy et al. 2004).

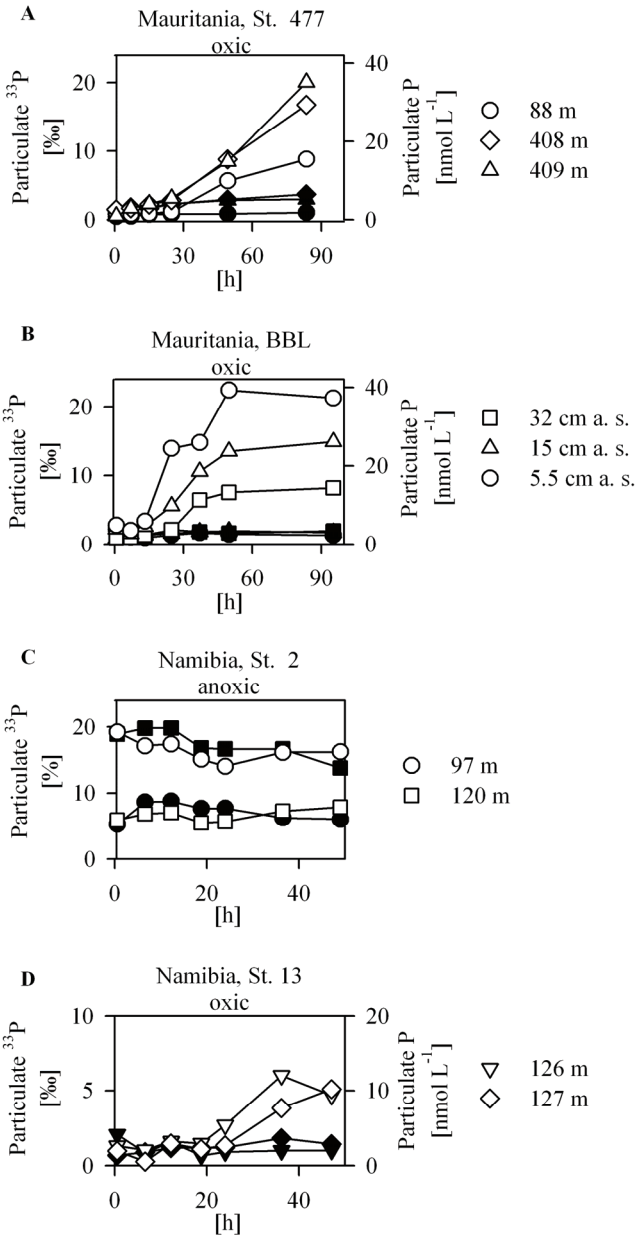

Figure 2: Phosphorus in the particulate fraction (>0.2 µm) determined from ^{33}P incubations. Particulate phosphorus calculated for A: St. 477 off Mauritania, B: BBL off Mauritania, C: St. 2 (anoxic) off Namibia, D: St 13 (oxic) off Namibia. Incubations were run at in situ O_2 concentrations. Closed symbols represent controls amended with sodium azide.

The ^{33}P-uptake and SEDEX ^{33}P extractions demonstrated that P-uptake in the sub-euphotic oxygenated water column was primarily a biotic process (Figure 3, SI Figure 2 A, B and D). The recovery of some ^{33}P from the "detrital" fraction, subsequent to the organic extraction, is somewhat surprising, since formation of a significant amount of detrital P in the course of the experiment would not be expected. Uptake into the detrital fraction, however, appears to be biologically controlled. Therefore, we suggest that the treatment of HCl might also recover some resistant biotic P, such as cellular poly-P. The increase of ^{33}P uptake into the detrital fraction towards the seafloor (Figure 3 B) suggests a higher poly-Pi production close to the sediment, perhaps due to surplus substrate availability in the BBL (Kornberg et al. 1999).

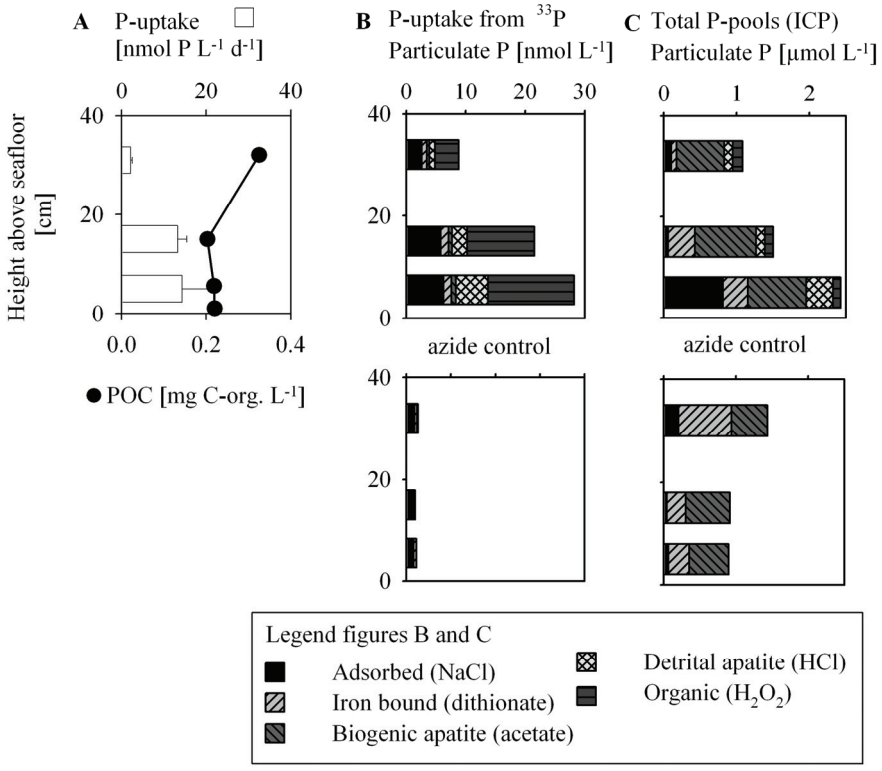

Figure 3: P-uptake rates and different P-pools in the bottom water off Mauritania. A: Profiles of P-uptake and POC, B: ^{33}P-uptake into different P pools, C: Total P in different P-fractions. Samples were taken with a BBL-profiler. POC: particulate organic carbon**.**

The uptake and distribution of ^{33}P contrasts with the distribution of phosphorus in the particulate fraction as determined from the SEDEX extractable P in samples from the Mauritanian BBL (Figure 3 A and C). P was variably distributed among the adsorbed pool

(0.06-0.81 µmol P L^{-1}), organic (0.10 and 0.13 µmol P L^{-1}), iron-bound P (0.07-0.37 µmol P L^{-1}), and detrital (0.11-0.36 µmol P L^{-1}) fractions. In contrast to the ^{33}P results, biogenic apatite P comprised the largest pool of P (0.67-0.84 µmol P L^{-1}). In the azide controls, a smaller amount of P was recovered from the detrital and organic fractions, compared to live incubation, suggesting a degradation of organic and detrital material and dissolution of P in the azide controls.

Anoxic waters

In contrast to the oxic stations, uptake of ^{33}P onto particles at the anoxic station off Namibia (St. 2) was immediate (<0.5 h). A further increase of ^{33}P on particles over time was not observed (shown for 97 and 120 m, Figure 2 C), but rather some of the incubations exhibited what appeared to be desorption of ^{33}P from the particles. ^{33}P uptake at St. 2 was an order of magnitude higher compared to the oxic stations. In contrast to the oxic stations, most of the ^{33}P was recovered from the adsorbed pool in both live incubations (74 to 99%) and azide controls (≥99%). Together these results suggest an additional mechanism of P-uptake in the anoxic samples. We attribute this to a rapid exchange of ^{33}P with ^{31}P adsorbed on iron oxides (SI). We assume that rapid exchange of ^{33}P into the adsorbed pools resulted in near equilibrium distribution of ^{33}P between the dissolved and adsorbed pools. Knowing the specific activity of the dissolved pools (2.3 – 5.1 GBq mol^{-1}) we calculate that exchangeable 92-360 nmol P L^{-1} of easily exchangeable P exists at the anoxic sites, values which agree well with the amount of total ^{33}P extracted from the adsorbed/iron oxide fractions at St. 2 (SI Figure 2). The eventual fate of this exchangeable particulate phosphate remains unknown.

At the anoxic station we also observed ^{33}P uptake into the organic fraction, which was even greater (up to 20 nmol P L^{-1}) than at the oxic stations (up to 15 nmol P L^{-1}), and which was also inhibited by azide (SI Figure 2). Recoveries of ^{33}P from biogenic apatite (0.9 and 4.0 nmol P L^{-1}) and detrital apatite (0.9 and 15.6 nmol P L^{-1}) were also greater at the anoxic station off Namibia, compared to the oxic stations (SI Figure 2 B). These enhanced extents of biotic P-uptake in the anoxic waters at St. 2 correlate with the greater bacterial abundances observed at St. 2 (SI Table 2). In summary, biotic uptake of P occurs also in the anoxic waters, but is, in part, masked by the extremely rapid exchange of ^{33}P into a large pool of P_i that was abiotically adsorbed onto particles in the anoxic Namibian shelf waters. Both pools, biotic and abiotic, of particulate P are actively cycling in the anoxic shelf waters, and can be transported to the sediments or offshore where P may become biologically available.

Nanoscale analysis of individual particles with nanoSIMS and EDX

The results of the NanoSIMS analyses of single particles are consistent with the ^{33}P uptake and SEDEX and support biotic P uptake in waters at the oxic stations and abiotic exchange in the anoxic waters (Figure 4, SI Figure 2). Samples from incubation experiments at St. 13 and 2 off Namibia were analyzed with nanoSIMS for the presence of organic material ($^{12}C^{14}N$), phosphorus (^{31}P), iron oxides ($^{56}Fe^{16}O$), sulfur (^{32}S) and the decay product of ^{33}P (^{33}S: natural abundance of 0.0078). At the oxic St. 13, most of the particles were organic in nature ($^{12}C^{14}N$) (Figure 4). At the anoxic St. 2, some particles which were enriched in $^{33}S/^{32}S$ and were not associated with organic material (Figure 4). Some of the enriched particles in the anoxic sample were high in $^{56}Fe^{16}O$ content, suggesting that iron-oxides might be responsible for a rapid P-uptake.

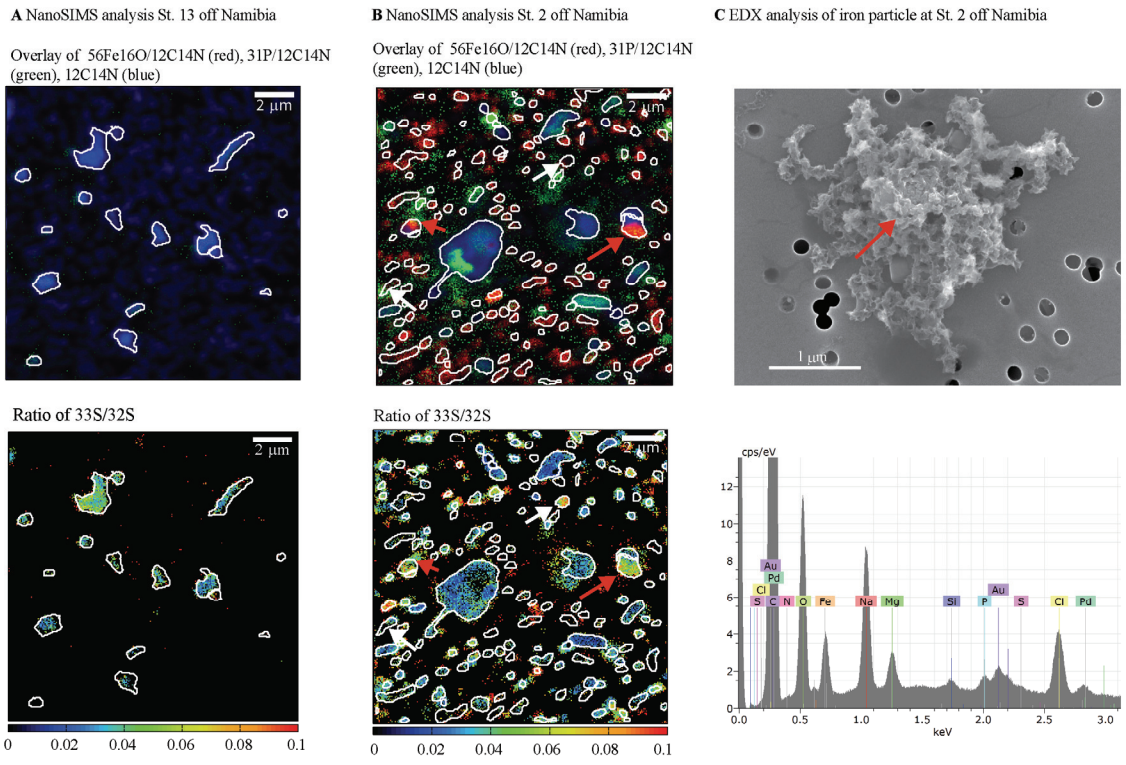

Figure 4: Nanoscale analysis of particles and cells with nanoSIMS and EDX. A: nanoSIMS analysis at St. 13 off Namibia. B: nanoSIMS analysis at St. 2 off Namibia, red arrows: 33S/32S enriched particles with high iron content, white arrows: 33S/32S enriched particles without high content of organic carbon or iron. C: EDX analysis of iron particle found at the St. 2 off Namibia.

EDX analysis confirmed the presence of amorphous particles rich in iron and phosphorus (Figure 4). These particles could be of biotic origin and might be responsible for the fast exchange of ^{33}P and ^{32}P on the surfaces, which lead to the rapid equilibration with ^{33}P in the anoxic waters. The adsorption of Pi onto iron-oxyhydroxides and concurrent resuspension of the particles in the BBL may cause a trapping of P in the BBL of Namibia and leading to enhanced primary productivity and a focusing of P sequestration in upwelling dominated continental shelf sediments (Slomp and van Cappellen 2007).

Uptake rates

Calculated P-uptake rates for the linear increase of particulate P after the lag phase for the live incubations of oxic waters are uniform throughout the water column of Mauritania and Namibia (SI Figure 1). In the BBL of Mauritania the rates tend to increase towards the seafloor (Figure 3). In general, our P-uptake rates (2.1 to 29.8 nmol P L^{-1} d^{-1}) were in the same range as uptake rates measured in surface waters (3-5 m) on a transect from Cape Verde to Barbados in the Atlantic (2.9-317 nmol P L^{-1} d^{-1}; Sohm and Capone, (2010)). Consistent with total uptake rates, recovery of ^{33}P from the organic fraction with SEDEX increased towards the seafloor (Figure 3 B) in the BBL off Mauritania, although bacterial abundances did not increase towards the seafloor (SI Table 2). This could be due to an increase of cellular P-uptake activity within the BBL (SI Table 2), and be attributed to enhanced metabolic activity of bacteria living attached to particles.

P_i regeneration from organic matter and P-turnover

Cellular P-uptake occurs at similar rates as P mineralization from sinking organic matter, based on oxygen consumption rates. It can be estimated that up to ~7.3 nmol P L^{-1} d^{-1} can be regenerated from sinking particulate organic material on the Mauritanian shelf, using oxygen consumption rates determined for the sub-euphotic water column (0.3 to 1 µmol O_2 L^{-1} d^{-1} Holtappels, unpublished data). Given an O_2:P ratio of 138 (Redfield et al. 1963) and assuming a growth efficiency of heterotrophic bacteria of 30% of the respiration rate, we calculated a P-uptake of 0.7 to 2.1 nmol P L^{-1} d^{-1}. This rate is similar to our experimentally determined ^{33}P uptake (~5 nmol P L^{-1} d^{-1}) into the organic fraction.

Calculated turnover rates for the P fractions in the BBL of Mauritania from the total amount of P_i and uptake of ^{33}P (SI Table 3), indicate that the organic fraction has a turnover of about 15 d. Overall, a complete turnover of the dissolved P in the sub-euphotic water column is approximately 300 days (in comparison the P-turnover times in the surface ocean

can be as short as 2 h (Tanaka et al. 2003)). P in sinking organic matter is mineralized in the water column, while nearly equivalent amounts are taken up as microbial biomass. Effectively, phosphate released upon microbial remineralization of organic matter is transferred back into a sinking particulate organic fraction by microorganism.

Biogeochemical Implications

Our experimental study highlights the intense cellular P_i turnover and efficient P_i enrichment that occurs in both oxic and anoxic sub-euphotic waters. However, rapid surface adsorption of P_i and a strong association to iron-rich pools may additionally influence P_i concentrations in the anoxic bottom waters of high productivity shelf ecosystems. Elucidating these controls is important, because P_i concentrations in the sub-euphotic water column are used to estimate N:P ratios, and eventually N-deficits in OMZs. High P_i concentrations in anoxic waters from trapping of P_i onto inorganic and organic particles may bias these N-deficits, such that the N-loss is actually lower than assumed by the N:P ratio. This may be of importance when considering the consequences of the climate induced alteration of larger-scale circulation patterns. Global conceptual models of P-cycling usually focus on P-uptake and recycling in P_i limited waters (specifically, the euphotic zone), and on remineralization of P from organic matter in the subsurface water column and sediments (Delaney 1998; Benitez-Nelson 2000; Paytan and McLaughlin 2007). However, P-uptake in the sub-euphotic zone and the BBL have not yet been considered in such models of P-cycling. As oxygen minimum zones in the oceans are projected to expand and intensify in future scenarios of global change (Stramma et al. 2008), it can be expected that P-cycling, the mechanisms of P-uptake, and general P availability undergo significant alterations in these areas. For example, recent observations of intensified upwelling off NW-Africa could result in increased microbial activity in the sub-euphotic waters due to higher primary production and organic matter supply to the BBL (McGregor et al. 2007). Our experimental study highlights intense cellular P_i turnover and efficient P_i enrichment in the sub-euphotic water column, which may be of importance when considering the consequences of the rapid alteration of larger-scale circulation patterns. Models predict greater accumulation and burial of P on continental shelves with slower ocean circulation (Slomp and van Cappellen 2007); our results suggest a mechanism for the transport of particles with low C:P ratios to the sediments.

Material and Methods

Sampling (Figure 1, SI Table) was conducted at the shelf off Mauritania (MSM17/4, March/April 2011 St. 477/533) and Namibia (MSM19/1c, October 2011, St. 2 and St. 13). Water samples were taken with a CTD-rosette (St. 477, 2, 13), a bottom water sampler (St. 477, 2, 13) or a BBL-profiler (St. 533) (Holtappels et al. 2011a). Samples for incubation ^{33}P incubation experiments were directly transferred into 250 ml Serum bottles avoiding oxygen contamination and closed with a gastight stopper as described in detail previously (Holtappels et al. 2011b). For all incubation experiments, abiotic controls with 2 ml of a saturated azide solution were run simultaneously. Oxygen concentrations in the incubations were kept at *in situ* levels. Subsamples of 10 ml were taken with a syringe and the volume replaced with a mixture of air/N_2 according to the oxygen concentration in the individual incubation and the portions of air and N_2 were calculated according to the solubilities of O_2 (Garcia and Gordon 1992) and N_2 (Hamme and Emerson 2004) in sea water and the proportion of both gases in air. All experiments were incubated at *in situ* temperature in the dark and permanently stirred.Subsamples were filtered through 0.2 µm polycarbonate filters (GTTP, Millipore) and measured in a liquid scintillation counter (Packard Tri-Carb 2900TR). Samples were taken at 0, 6, 12, 24, 36, 49, 86 h (MSM17/4) or every 6 h during a 48 h incubation (MSM19/1). The radioactivities were converted into P concentrations and P-uptake (SI).

Subsamples for analysis at a secondary iron mass spectrometer (nanoSIMS) and for the SEDEX extraction were taken at the end of the incubation. Extraction of different fractions of the particulate P was performed according to the sequential P_i extraction (SEDEX) developed by Ruttenberg (1992). Some modifications had been introduced to the protocol to adjust the extraction method to the filter samples (SI). Dissolved P and Fe concentration in the extracts were measured at an inductively coupled plasma optical emission spectrometer (Varian Vista Pro) radial plasma observation. The ^{33}P radioactivity was measured in the different extractants of SEDEX and converted into P according to Eq. 1 to correct for the different labeling percentages in the incubations (Figures 2 and 3).

Samples taken after 48 h of incubation at St. 13 and 2 off Namibia were analyzed with secondary ion mass spectrometer (nanoSIMS) type 50 l (Cameca) for 12C14N, 31P, 56Fe16O, 32S and 33S (decay product of 33P) after 6 months of decay. The resulting images of the nanoSIMS analysis were analyzed with Look@NanoSIMS (Polerecky et al. 2012). Samples were analyzed a scanning electron microscope Quanta FEG 250 (FEI) energy dispersive X-rayspectroscopy (EDS) with a double detector system (XFlash 6/30, Bruker Nano GmbH).

Acknowledgements

We are sincerely thankful for the technical assistance of G. Klockgether, K. Imhoff, G. Schüssler, D. Franzke, S. Lilienthal, J. Füssel and S. Pape. We highly appreciate the discussions with P. Lam and G. Lavik and their suggestions for experimental development. For excellent co-operation we thank captain and crew of cruises MSM17/4 and MSM19/1 on *R/V* Maria S. Merian as well as the cruise leaders O. Pfannkuche and M. Zabel. This project was funded by the DFG-Research Center / Excellence Cluster "The Ocean in the Earth System" (MARUM), BMWF and the Max Planck Society.

References

Benitez-Nelson, C. R. (2000). "The biogeochemical cycling of phosphorus in marine systems." Earth-Science Reviews 51(1-4): 109-135.

Carr, M. E. (2002). "Estimation of potential productivity in Eastern Boundary Currents using remote sensing." Deep-Sea Research Part II-Topical Studies in Oceanography 49(1-3): 59-80.

Casey, J. R., M. W. Lomas, V. K. Michelou, S. T. Dyhrman, E. D. Orchard, J. W. Ammerman and J. B. Sylvan (2009). "Phytoplankton taxon-specific orthophosphate (Pi) and ATP utilization in the western subtropical North Atlantic." Aquatic Microbial Ecology 58(1): 31-44.

Delaney, M. L. (1998). "Phosphorus accumulation in marine sediments and the oceanic phosphorus cycle." Global Biogeochemical Cycles 12(4): 563-572.

Duhamel, S., T. Moutin, F. van Wambeke, B. van Mooy, P. Rimmelin, P. Raimbault and H. Claustre (2007). "Growth and specific P-uptake rates of bacterial and phytoplanktonic communities in the Southeast Pacific (BIOSOPE cruise)." Biogeosciences 4(6): 941-956.

Garcia, H. E. and L. I. Gordon (1992). "Oxygen solubility in seawater: Better fitting equations." Limnology and Oceanography 37(6): 1307-1312.

Goldhammer, T., V. Brüchert, T. G. Ferdelman and M. Zabel (2010). "Microbial sequestration of phosphorus in anoxic upwelling sediments." Nature Geoscience 3(8): 557-561.

Hamme, R. C. and S. R. Emerson (2004). "The solubility of neon, nitrogen and argon in distilled water and seawater." Deep-Sea Research Part I-Oceanographic Research Papers 51(11): 1517-1528.

Holtappels, M., M. M. M. Kuypers, M. Schlueter and V. Bruchert (2011a). "Measurement and interpretation of solute concentration gradients in the benthic boundary layer." Limnology and Oceanography-Methods 9: 1-13.

Holtappels, M., G. Lavik, M. M. Jensen and M. M. M. Kuypers (2011b). ^{15}N-labeling experiments to dissect the contributions of heterotrophic denitrification and anammox to nitrogen removal in the OMZ waters of the ocean. Methods in Enzymology: Research on Nitrification and Related Processes, Vol 486, Part A. M. Klotz. San Diego, Elsevier Academic Press Inc. 486: 223-251.

Ingall, E. and R. Jahnke (1994). "Evidence for enhanced phosphorus regeneration from marine-sediments overlain by oxygen depleted waters." Geochimica Et Cosmochimica Acta 58(11): 2571-2575.

Kornberg, A., N. N. Rao and D. Ault-Riche (1999). "Inorganic polyphosphate: A molecule of many functions." Annual Review of Biochemistry 68: 89-125.

McGregor, H. V., M. Dima, H. W. Fischer and S. Mulitza (2007). "Rapid 20th-century increase in coastal upwelling off northwest Africa." Science 315(5812): 637-639.

Paytan, A. and K. McLaughlin (2007). "The oceanic phosphorus cycle." Chemical Reviews 107(2): 563-576.

Perry, M. J. and R. W. Eppley (1981). "Phosphate-uptake by phytoplankton in the central north pacific-ocean." Deep-Sea Research Part a-Oceanographic Research Papers 28(1): 39-49.

Polerecky, L., B. Adam, J. Milucka, N. Musat, T. Vagner and M. M. M. Kuypers (2012). "Look@NanoSIMS – a tool for the analysis of nanoSIMS data in environmental microbiology." Environmental Microbiology 14(4): 1009-1023.

Ruttenberg, K. C. (1992). "Development of a Sequential Extraction Method for Different Forms of Phosphorus in Marine-Sediments." Limnology and Oceanography 37(7): 1460-1482.

Sanudo-Wilhelmy, S. A., A. Tovar-Sanchez, F. X. Fu, D. G. Capone, E. J. Carpenter and D. A. Hutchins (2004). "The impact of surface-adsorbed phosphorus on phytoplankton Redfield stoichiometry." Nature 432(7019): 897-901.

Slomp, C. P. and P. van Cappellen (2007). "The global marine phosphorus cycle: sensitivity to oceanic circulation." Biogeosciences 4(2): 155-171.

Sohm, J. A. and D. G. Capone (2010). "Zonal differences in phosphorus pools, turnover and deficiency across the tropical North Atlantic Ocean." Global Biogeochemical Cycles 24(2): GB2008.

Stramma, L., G. C. Johnson, J. Sprintall and V. Mohrholz (2008). "Expanding oxygen-minimum zones in the tropical oceans." Science 320(5876): 655-658.

Tanaka, T., F. Rassoulzadegan and T. F. Thingstad (2003). "Measurements of phosphate affinity constants and phosphorus release rates from the microbial food web in Villefranche Bay, northwestern Mediterranean." Limnology and Oceanography 48(3): 1150-1160.

Thingstad, T. F., E. F. Skjoldal and R. A. Bohne (1993). "Phosphorus cycling and algal-bacterial competition in Sandsfjord, Western Norway." Marine Ecology-Progress Series 99(3): 239-259.

Tyrrell, T. (1999). "The relative influences of nitrogen and phosphorus on oceanic primary production." Nature 400(6744): 525-531.

van den Broeck, N., T. Moutin, M. Rodier and A. Le Bouteiller (2004). Seasonal variations of phosphate availability in the SW Pacific Ocean near New Caledonia. 268: 1-12.

Wefer, G. and G. Fischer (1993). "Seasonal patterns of vertical particle flux in equatorial and coastal upwelling areas of the eastern Atlantic." Deep Sea Research Part I: Oceanographic Research Papers 40(8): 1613-1645.

Zubkov, M. V., I. Mary, E. M. S. Woodward, P. E. Warwick, B. M. Fuchs, D. J. Scanlan and P. H. Burkill (2007). "Microbial control of phosphate in the nutrient-depleted North Atlantic subtropical gyre." Environmental Microbiology 9(8): 2079-2089.

Supplementary information

Material and Methods

Water samples

Dissolved oxygen and temperature in the water column were measured with a conductivity-temperature-depth (CTD) system, equipped with an oxygen sensor (Sea Bird Electronics) calibrated against Winkler titration. Samples for P_i analysis were frozen and stored at -20°C for measurement in an autoanalyzer (TRAACS 800, Bran & Luebbe) in an on-shore laboratory.

For determination of particulate carbon (POC), water column samples were filtered through pre-combusted glas-fibre filters (GFF, Whatman), washed with filtered seawater or MilliQ and kept at -20°C until analysis. Analysis of POC was performed by combustion/gas chromatography (Carlo Erba NA-1500 CNS or HEREAUS-CHN analyzer) after acidification. Samples for DAPI staining were fixed with 2% paraformaldehyde (final concentration), filtered through 0.2 µm polycarbonate filters (GTTP, Millipore), frozen and stored at -20°C until analysis.

^{33}P incubation experiments

^{33}P-uptake was determined in incubation experiments with water samples in 250 ml serum bottles. For all incubation experiments, abiotic controls with 2 ml of a saturated azide solution were run simultaneously. Azide inhibits the respiration activity and catalytic oxidases inhibiting the cytochrome-c oxidase-and binding to the O_2 reduction site (Keilin 1936; Fei et al. 2000). Oxygen in the incubations was kept at in situ levels. After a pre-incubation of ~20 minutes at *in situ* temperature, the carrier-free $H_2{}^{33}PO_4$ label (Hartmann Analytic) was added directly to the incubations (final concentration 2-10 kBq ml^{-1}) and incubations mixed on a 15x magnetic stirrer (~130 min^{-1}, IKA). Immediately after label addition (T0), subsamples were taken with a syringe and the volume replaced with a mixture of air/N_2 according to the oxygen concentration in the individual incubation. The portions of air and N_2 were calculated according to the solubilities of O_2 (Garcia and Gordon 1992) and N_2 (Hamme and Emerson 2004) in sea water and the proportion of both gases in air. All experiments were incubated at *in situ* temperature in the dark and permanently stirred.

Subsamples of 10 ml were taken at each time-point with a syringe and filtered through 0.2 µm polycarbonate filters (GTTP, Millipore) on a 12 x filtration system (Millipore). The filters were rinsed with 15 ml of sterile filtered seawater. Subsequently, filters were transferred to 20 ml scintillation vials (Perkin Elmer) and 5 ml of the sterile filtered seawater

as well as 14 ml of Lumasafe Plus scintillation liquid (Perkin Elmer) were added to the vials. For determination of the total radioactivity at T0, 1 ml of the incubation liquid was diluted with 4 ml filtered seawater before the addition of 14 ml scintillation liquid. Radioactivity was measured in a liquid scintillation counter (Packard Tri-Carb 2900TR). Backgrounds were determined from blank filters and subtracted. The radioactivities (A) were converted into P concentrations in the particulate fraction ($P_{particulate}$; µmol P_{part} L^{-1}) using Equation 1, (specific activity of ^{33}P: 5.1 x 10^{-18} mol Bq^{-1}).

$$\left[P_{particulate}\right] = \frac{A_{P-particle}}{A_{P-total}} \times \left[PO_4^{3-}\right] \quad \text{Eq. 1}$$

where $A_{P\text{-}particulate}$ is the activity (Bq L^{-1}) on the filter normalized to volume, $A_{P\text{-}total}$ is the total activity normalized to volume of ^{33}P (Bq L^{-1}) measured at the start of the experiment, and (PO_4^{3-}) is the measured concentration of dissolved phosphate (µmol P_{diss} L^{-1}) at the start of the experiment. (Specific activities of ^{33}P in the experiments ranged from 1.5 to 5.1 GBq mol^{-1}). The P-uptake rates were calculated from the increase of radioactivity in the particulate fraction over the period of time, t, that $P_{particulate}$ increased in a linear fashion (i.e. the lag times were not include in *t* at the oxic station experiments (Figures 3, SI Figure 1).

$$P-uptake = \frac{\left[P_{particulate}\right]}{t} \quad \text{Eq. 2}$$

Subsamples for analysis at a secondary iron mass spectrometer (nanoSIMS) were taken at the beginning (T0) and at the end of the experiment. 30 ml of the incubation were fixed with 1% paraformaldehyde (final concentration), filtered through a gold-palladium coated 0.2 µm polycarbonate filter (GTTP, Millipore) and washed with 30 ml of sterile filtered seawater. Filters were air-dried, frozen and kept at -20 °C until analysis. Samples for the SEDEX extraction were taken at the end of the incubation. The remaining incubation liquid (~100 ml) was filtered through 0.2 µm polycarbonate filters (GTTP, Millipore) and fixed with 2% glutaraldehyde (Electron Microscopy Sciences). The filters were washed with 30 ml filtered seawater, frozen and stored until extraction at -20°C.

Extraction of particulate P fractions

Extraction of different fractions of the particulate P was performed according to the sequential P_i extraction (SEDEX) developed by Ruttenberg (1992) with some modification. The volume of the extractant was reduced to 20 ml and centrifugation after every extraction and washing step was done for 30 min at 4500 x g to increase the pelletizing of the particles. The following solutions with different incubation times were used to extract the various P_i fractions: 0.46 M

NaCl according to Jensen and Thamdrup (1993), 30 min (adsorbed fraction), CDB-buffer, 6 h (citrate-sodium-dithionate-bicarbonate buffer, iron fraction), 1 M Na-acetate, 4 h (apatite fraction) 0.1 M HCl, 16 h (detrital fraction), 7 ml of 32% H_2O_2, 24 h (organic fraction). The H_2O_2 was decomposed in a water bath at 60-70°C. After every extraction solution, besides HCl, the filter and particles were washed for 30 min shaking with 20 ml 0.46 M NaCl and centrifuged for 30 min at 4500 x g. The radioactivity in all extractants and washing steps was analyzed in a 5 ml subsample with 14 ml Lumasafe Plus scintillation fluid (Perkin Elmer) in a liquid scintillation counter (Packard Tri-Carb 2900TR). The radioactivity or rather the P content of the whole filtered volume was calculated according to the previously described calculation.

Results and discussion

Water column chemistry

In April 2011, oxygen concentrations on the shelf off Mauritania (St. 477/533) decreased sharply from ~160 µmol O_2 L^{-1} at ~ 30 m to ~60 µmol O_2 L^{-1} at 75 m and remained almost constant towards the seafloor at 410 m (Figure 1). At the same station, P_i concentrations doubled from 0.7 µmol P L^{-1} at the surface to 1.5 µmol L^{-1} at 75 m and slightly increased further to 1.9 µmol L^{-1} in the bottom water. Phosphate concentrations in the water columns off Africa were inversely related to oxygen concentrations within the water column due to the remineralization of organic matter and possibly some P_i reflux from the sediments (Figure 1).

In October 2011 oxygen concentrations off Walvis Bay (St. 2) were at the detection limited from 90 m downwards. Phosphate concentrations at St. 2 increased from 0.4 µmol P_i L^{-1} at the surface to 2.3 µmol P_i L^{-1} at 76 m and further increased to 4.9 µmol L^{-1} at the seafloor (125 m). However, anoxic conditions were found at a station off Walvis Bay (St. 2), an area formerly known to exhibit anoxic conditions in the water column e. g. (Lavik et al. 2009). Further south (St. 13) oxygen decreased to ~80 µmol O_2 L^{-1} at 100 m and remained constant to the seafloor (128 m).

At St. 13 concentrations of P_i increased from 0.6 µmol P L^{-1} at the surface to 2.3 µmol L^{-1} in the BBL. At the anoxic station off Namibia, P_i concentrations in the BBL were >1 µmol L^{-1} higher than at the oxic station further south (St. 13, Figure 1). The excess P_i probably originated from dissolution of iron oxyhydroxides in the sediments under anoxic conditions and diffusion of P_i into the water column. The assumption that P_i is released from the sediment is supported by the extreme high P_i concentrations of 4.9 µmol L^{-1} at the seafloor of St. 2 (Figure 1). Particulate organic carbon (POC) in general was highest at the surface

(Figure SI 1) and varied between 0.053 and 0.344 mg C-org L^{-1} amongst the incubation depths of the different stations (Table 2). Similarly, turbidity was also high in the surface, decreased with depth within the water column and increased again towards the seafloor (SI Figure 1). Cell numbers counted by DAPI staining were between 2.2 x 10^5 and 1.9 x 10^6 cells ml^{-1} amongst the stations (SI Table 2). Other studies e.g. in the Barent Sea (Thomsen et al. 1994) also observed that POC did not increase in the bottom water, instead particulate organic matter decreased towards the seafloor. The discrepancies between turbidity and POC in the bottom water shows that the turbidity results from resuspended sediment particles, instead of organic material.

P_i-uptake kinetics

The P_i-uptake curves included a lag, a linear increase and a stationary phase, typical for growth curves. However, artificial growth in the incubations should have been prevented by the *in situ* temperature, dark incubation and the small amount of ^{33}P (≈pmol) added as tracer to background concentrations of P >1.8 µmol L^{-1}. More likely, exchange and equilibrium processes of $^{31}PO_4^{3-}$ and $^{33}PO_4^{3-}$ on particle and cell surfaces or in the periplasm might have influenced the uptake kinetics. Therefore we assume that the initial lag phase is the time it takes to reach the equilibrium of $^{31}P/^{33}P$ on particle and cell surfaces. The linear increase of particulate-P would then represent the actual uptake of P_i into the cells, since no linear increase of particulate-P was observed in the azide controls (Figure 2, A+B). Furthermore, if we assume a constant uptake of P_i by microorganisms through a constitutive P transporter system, the inner-cellular pool of P_i is exchanged with the ambient pool of P_i and thus we would expect to reach equilibrium of $^{33}P/^{31}P$ in the incubation experiments after a certain period of time. This equilibrium of inner-cellular and extracellular P could explain the stationary phase after ~48 h in some of the incubations. Interestingly, Thingstad and colleagues (1993) found that turnover of phosphorus in bacteria took ~50 h in a Norwegian Fjord. However, the fact that particle density or aggregate quality affects P-uptake can not be excluded and how exactly the equilibrium is reached needs to be further investigated to explain the kinetics of the P-uptake in the sub-euphotic water column.

Influence of oxygen conditions on the Pi-uptake

In some experiments oxygen concentrations were manipulated, while in others the oxygen concentrations were kept at or close to *in situ* concentrations. In some incubations oxygen concentration were manipulated to investigate the influence of different oxygen conditions on

P-uptake. To lower the oxygen concentrations, samples were degassed with N_2 gas for 15 min, while to increase O_2 conditions, samples air was introduced into the samples with aquarium pumps. P-uptake rates in the BBL off Mauritania were the highest in the incubation with saturated oxygen at 5.5 cm above the seafloor, but the effect of oxygen seems to be minor and there was no difference between oxic and hypoxic incubations. Interestingly, the oxygen manipulation experiments in our study showed that oxygen conditions had only little influence on the P-uptake, suggesting an adaptation of the organisms to different oxygen concentrations.

Exchange of P_i on iron oxides at the anoxic station

A possible mechanism for the rapid formation of particulate P in the anoxic samples could be the formation of iron-oxyhydroxides as a result of oxygen introduction into the samples during sample preparation and the adsorption of P_i onto the particles, since P_i has been shown to adsorb within minutes onto iron-particles (Ruttenberg and Sulak 2011). However, oxygen concentrations in the incubations were at the detection limit (<1 µmol L^{-1}) and therefore formation of iron oxides most likely too slow to cause the rapid adsorption of the radiolabel (Roden et al. 2004; Emerson et al. 2010). Rapid exchange of ^{33}P and ^{31}P after addition of the radiolabel on the particle surfaces until equilibrium might have caused the immediate uptake of ^{33}P onto the particles. Since the oxygen conditions in the water column were presumably to low to support formation of iron oxides, these particles could be iron oxides, which have not been dissolved under anoxic conditions. A different possibility could be the biotic production of iron oxides by microaerophilic Fe(II)-oxidation or coupled nitrate reduction to Fe(II)-oxidation. Biotic iron particles were shown to be very effective in adsorbing P_i, likely due to a high surface availability of the amorphous particles (Rentz et al. 2009). The different origin of the iron oxides might also explain why the P_i is exchanged on the surfaces of the particles in the anoxic water, whereas P_i seems to be less exchanged on iron oxides in oxic waters, although the amount of particulate iron in the extract was similar. Moreover, ^{33}P might have diffused into exopolymer particles. After drying the particles with a high water content during sample preparation, salt crystals together with ^{33}P might have precipitated and resulted in a high recovery of ^{33}P in the adsorbed fraction. This idea might be supported by the electron images, which showed sodium-chloride crystals in a dark spot, which could have been dried organic material.

References

Emerson, D., E. J. Fleming and J. M. McBeth (2010). Iron-Oxidizing Bacteria: An Environmental and Genomic Perspective. Annual Review of Microbiology, Vol 64, 2010. Palo Alto, Annual Reviews. 64: 561-583.

Fei, M. J., E. Yamashita, N. Inoue, M. Yao, H. Yamaguchi, T. Tsukihara, K. Shinzawa-Itoh, R. Nakashima and S. Yoshikawa (2000). "X-ray structure of azide-bound fully oxidized cytochrome c oxidase from bovine heart at 2.9 A resolution." Acta Crystallographica Section D 56(5): 529-535.

Garcia, H. E. and L. I. Gordon (1992). "Oxygen solubility in seawater: Better fitting equations." Limnology and Oceanography 37(6): 1307-1312.

Hamme, R. C. and S. R. Emerson (2004). "The solubility of neon, nitrogen and argon in distilled water and seawater." Deep-Sea Research Part I-Oceanographic Research Papers 51(11): 1517-1528.

Jensen, H. S. and B. Thamdrup (1993). "Iron-bound phosphorus in marine-sediments as measured by bicarbonate-dithionite extraction." Hydrobiologia 253(1-3): 47-59.

Keilin, D. (1936). "The Action of Sodium Azide on Cellular Respiration and on some Catalytic Oxidation Reactions." Proceedings of the Royal Society of London. Series B, Biological Sciences 121(822): 165-173.

Lavik, G., T. Stuehrmann, V. Bruechert, A. van der Plas, V. Mohrholz, P. Lam, M. Mussmann, B. M. Fuchs, R. Amann, U. Lass and M. M. M. Kuypers (2009). "Detoxification of sulphidic African shelf waters by blooming chemolithotrophs." Nature 457(7229): 581-U86.

Rentz, J. A., I. P. Turner and J. L. Ullman (2009). "Removal of phosphorus from solution using biogenic iron oxides." Water Research 43(7): 2029-2035.

Roden, E. E., D. Sobolev, B. Glazer and G. W. Luther (2004). "Potential for microscale bacterial Fe redox cycling at the aerobic-anaerobic interface." Geomicrobiology Journal 21(6): 379-391.

Ruttenberg, K. C. (1992). "Development of a Sequential Extraction Method for Different Forms of Phosphorus in Marine-Sediments." Limnology and Oceanography 37(7): 1460-1482.

Ruttenberg, K. C. and D. J. Sulak (2011). "Sorption and desorption of dissolved organic phosphorus onto iron (oxyhydr)oxides in seawater." Geochimica Et Cosmochimica Acta 75(15): 4095-4112.

Thingstad, T. F., E. F. Skjoldal and R. A. Bohne (1993). "Phosphorus cycling and algal-bacterial competition in Sandsfjord, Western Norway." Marine Ecology-Progress Series 99(3): 239-259.

Thomsen, L., G. Graf, V. Martens and E. Steen (1994). "An instrument for sampling water from the benthic boundary-layer." Continental Shelf Research 14(7-8): 871-882.

SI Table 1: Sampled stations for this study. CTD: conductivity-temperature-depth-rosette, BWS: bottom water sampler. BBL: BBL-profiler

St.	Cruise	Shelf	Water depth [m]	Lat	Long	Date 2011	Gear
477	MSM17/4	Mauritania	410	18°12.40 N	16°35.50 W	27.03.	CTD BWS
533 (BBL)	MSM17/4	Mauritania	410	18°12.98 N	16°35.51 W	04.04.	BBL
2	MSM19/1c	Namibia	125	23°00.00 S	14°07.00 E	13.10.	CTD BWS
13	MSM19/1c	Namibia	128	28°30.00 S	15°45.00 E	17.10.	CTD BWS

SI Table 2: Particulate organic carbon (POC), cell numbers and cell specific P uptake in the different incubation depths. A. s.: above seafloor.

St.	Incubation depth	POC [mg C-org L^{-1}]	Cell numbers [cells ml^{-1}]	Cellular uptake [mol P $cell^{-1}$]
477	88 m	0.053	2.8×10^5	2.5×10^{-19}
	260 m	0.076	2.7×10^5	4.7×10^{-19}
	408 m	0.194	/	/
	409 m	0.121	/	/
	409.2 m	0.262	2.2×10^5	6.6×10^{-19}
533 (BBL)	32 cm a.s	0.325	5.2×10^5	8.4×10^{-20}
	15 cm a. s.	0.203	5.2×10^5	5.4×10^{-19}
	5.5 cm a. s	0.217	5.2×10^5	5.7×10^{-19}
2	97 m	0.098	9.3×10^5	/
	120 m	0.105	1.1×10^6	/
	123 m	0.089	1.6×10^6	/
	124 m	0.344	1.9×10^6	/
13	66 m	0.061	1.0×10^6	4.0×10^{-18}
	125 m	0.063	9.5×10^5	4.3×10^{-18}
	126 m	0.153	6.7×10^5	3.2×10^{-18}
	127 m	0.229	8.3×10^5	4.7×10^{-18}

SI Table 3: Turnover of different P pools in the BBL of Mauritania. Calculated from the reservoir of P, the ^{33}P uptake rates and the distribution of ^{33}P over the different fraction. a . s. : above seafloor.

Depth [cm]	P turnover in different fractions [d]				
	Adsorbed	Iron bound	Apatite	Detrital	Organic
32 cm a.s	164	367	6440	520	141
15 cm a. s.	17	450	2288	76	16
5.5 cm a. s	256	507	2193	133	15

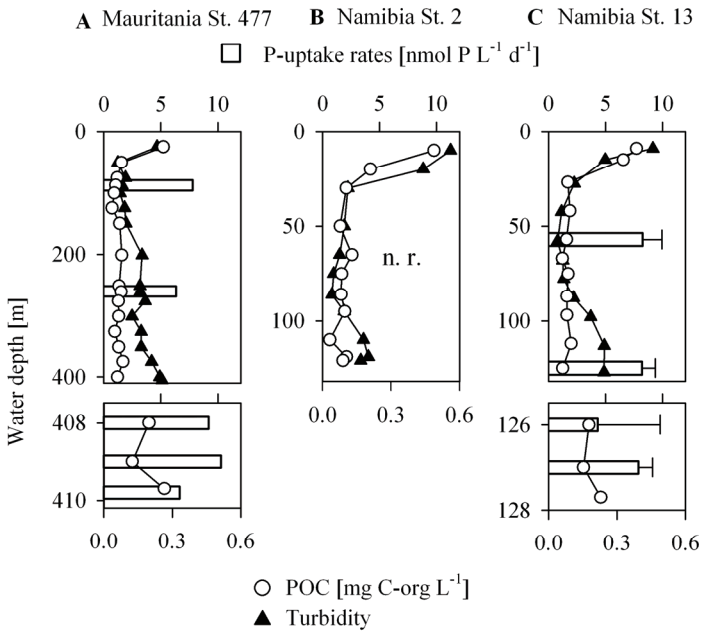

SI Figure 1: Turbidity, particulate organic carbon and P-uptake rates off Mauritania and Namibia. A: P-uptake rates of the oxic St. 477 (Mauritania), B: Turbidty and POC at the anoxic station off Namibia, C: P-uptake at oxic St. 13 (Namibia). POC: particulate organic carbon. n. r. rates could not be calculated due to rapid adsorption of the radiolabel.

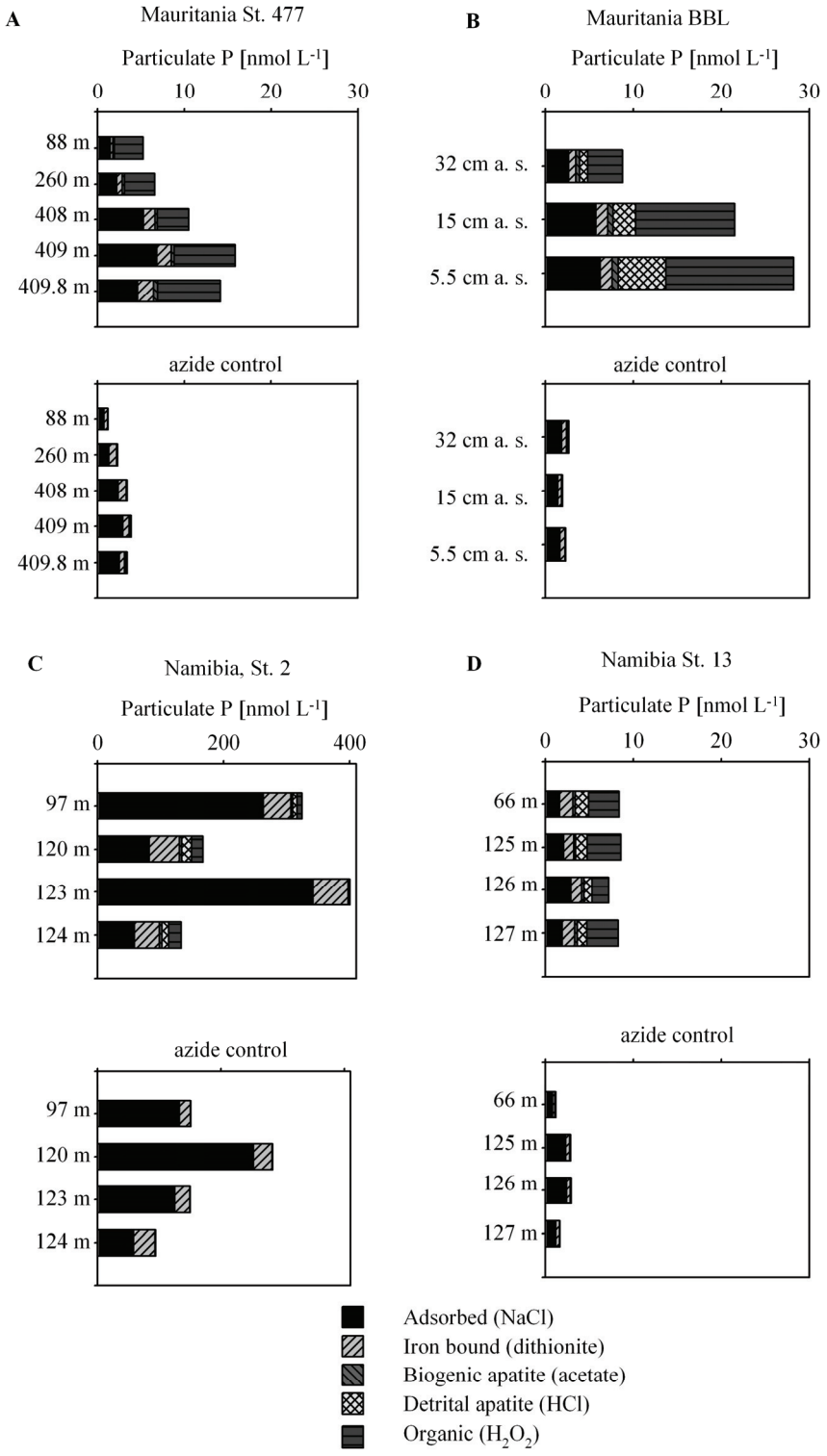

SI Figure 2: Phosphorus recovery from different P pools. Samples for the sequential P extraction were collected at the end of the ^{33}P experiments and the radioactivity in the different solutions was converted to P, incubations at in situ O_2. A and B: oxic station off Mauritania, water column and bottom water samples, samples in B were taken with a BBL-profiler. C: Oxic station off Namibia. D: Anoxic station off Namibia.

Chapter V

Iron and phosphorus dynamics in bottom waters under variable redox conditions

Sokoll, Sarah, Timothy G. Ferdelman and Moritz Holtappels

Max Planck Institute for Marine Microbiology, Bremen, Germany

Abstract

High primary production often results in increased respiration and O_2 consumption in the water column. In the Baltic Sea high primary production is paired with poor ventilation leading to seasonal anoxia. Changing oxygen concentrations lead to very dynamic iron (Fe) and phosphorus (P) cycling, due to the affinity of P to adsorb to Fe-oxyhydroxides. We investigated the dynamic fluxes of P and Fe between the particulate and dissolved fraction in the bottom water and between bottom water and sediment using long term (12 d) radiotracer (^{33}P, ^{55}Fe) incubation experiments. Baltic Sea sediment cores with overlying water were kept under variable redox conditions. One core was kept oxic continuously, while oxygen conditions in another core were changed from oxic to anoxic. The results suggest that due to a dissolution and formation of Fe-P particles, the radiotracers disappeared faster into the sediment when the oxygen conditions changed. Initial results also suggest that use of ^{55}Fe or ^{33}P tracers might be used to disentangle mechanisms regulating P and Fe fluxes and uptake onto particles during oxic-anoxic perturbations in coastal marine sediments.

Introduction

The Baltic Sea is an inland sea covering an area of 377 000 km^2 whose watershed falls within a heavily populated area (Elmgren 2001). The Baltic Sea consist of several basins that are connected to each other, while the only outflow and exchange region with marine water of the North Sea lays in the north of Denmark. Based on the topography and the high riverine inflow, salinities in the Baltic Sea increase from freshwater in the Finish Basin to marine at Skagerrak, Denmark. In summer, density stratification builds up a stable thermocline, which allows primary production based on the shallow mixing depth. Since tides are too low in the Baltic Sea to cause any mixing, wind is the only mechanisms to erode the thermocline. The eutrophic character of the Baltic Sea is largely created by the increased anthropogenic nutrient input, in earlier days it used to be oligotrophic. This high primary production in the surface causes anoxic and sulfidic conditions in the deep basins and in summer sometimes in shelf areas as well (Figure 1 a). The Baltic Sea is only sporadic ventilated by inflow from the North Sea and thus deep waters of the Baltic Sea episodically comprise one of the largest dead zones of the world (Diaz and Rosenberg 2008).

Phosphorus (P) and iron (Fe) are both essential nutrients for primary producers. The cycling of these two nutrients are tightly coupled du to the affinity of phosphate (P_i) to adsorb to particles. In the oxic marine environments, P_i would adsorb to Fe-oxyhydroxides, while under reducing conditions, most Fe-oxyhydroxides would dissolve and P would desorb. This shuttle has been described for the Baltic and Black Sea, to explain anomalies in the P profile (Shaffer 1986; Jilbert and Slomp 2013). Sediment can act as a sink for P in different forms such as Fe-oxyhydroxides, carbonate fluorapatite (CFA), Mn-Ca-carbonates and Fe(II)-phosphates such as vivianite ($Fe_3(PO_4)_2 \cdot 8(H_2O)$). However, most burial of P in the Baltic Sea occurs as organic P (Mort et al. 2010). Increased anoxia leads to less P burial and enhanced P flux from the sediments to the water column and enhanced primary production (Conley et al. 2009). It has been even suggested that the decrease of the oxygen concentrations in the water column from 1970-2000 is a more important factor for the increase of P in the water column than the human input of P into the Baltic Sea (Conley et al. 2002).

Other studies also related the diffusion of P into the water column from anoxic/sulfidic sediments by pyrite formation into water column to enhanced nutrient concentration and algal blooms (Rozan et al. 2002). High P and ammonium concentration due to sulfidic conditions in sediments are even thought to cause harmful algal blooms (Ma et al. 2006). Therefore it is important to know, how P_i and Fe concentrations in the water column react to fast oxygen changes. Already in 1997, incubation experiments with Baltic Sea sediments have been

performed (Gunnars and Blomqvist 1997). These experiments showed the flux of P and Fe out of the sediment under anoxic conditions in the water column. However, how the P is scavenged onto the Fe-particles has not been investigated. To investigate scavenging of P we incubated Baltic Sea sediments and the overlying water using the radiolabels ^{55}Fe and ^{33}P. By changing the oxygen conditions in the overlying water the dynamic response to changing redox conditions was investigated.

Material and Methods

Long term (12 day) incubation experiments with the radiolabels ^{33}P and ^{55}Fe were performed with two sediment cores collected from 21 m depth near the monitoring station B1, which is located at the transition of the Swedish fjord 'Himmerfjärden' and the Baltic Sea (Figure 1 A). A site description can be found at the website of the monitoring project (www2.ecology.su.se). Sediment cores of 10 cm diameter were sampled on Nov. 18, 2011 using a multicorer. The sediment was muddy and by the time of the experiment a black precipitate had developed a couple of centimeters below the sediment surface, even though cores were kept at 4°C with oxygen introduction by a aquarium pump into the overlying water (ca. 1 L) until the start of the experiment. To place optode spots (PreSens) in the plastic liners, the overlying water was carefully removed. The optode spots were place in the liners (Figure 1 B) and connected with a computer to read the oxygen concentrations. The overlying water was carefully filled back into the cores without disturbing the surface of the cores. A temperature sensor was placed in the overlying water of one of the cores. Magnetic stirrers were placed in the overlying water and the water stirred at a very low rate, without disturbing the sediment.

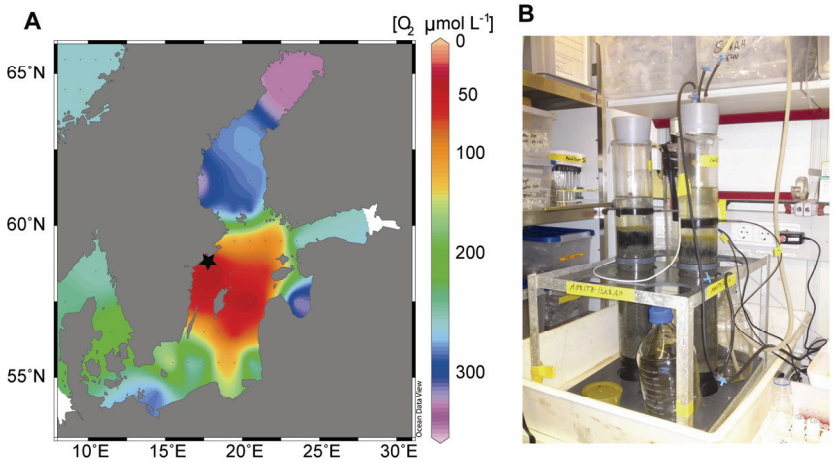

Figure 1: Oxygen concentrations in the bottom water (A), incubation set-up (B). Oxygen concentrations in A were taken from World Ocean Atlas 2009. The black star in A marks the sampling area.

Before the addition of the radiolabels, cores were closed until the overlying water was anoxic. At the time, the overlying water was anoxic, radiolabels of iron (^{55}Fe, Perkin Elmer) and phosphate ($H^{33}PO_4^{2-}$, Hartman Analytics) were added into the overlying water. The ^{55}Fe was reduced prior to addition with dithionite and ascorbic acid. Concentrations of the radiolabel in the overlying water at the beginning were 80-120 kBq L^{-1} for ^{55}Fe and ~2 MBq L^{-1} for ^{33}P. Incubations were run at 4°C in a dark room. After addition of the radiolabel, the cores were opened to allow oxygen to diffusive into the overlying water. Oxygen conditions in Core 1 were kept oxic, while the oxygen conditions in Core 2 were alternated between oxic and anoxic conditions (Figure 2).

Over a period of several days, the overlying water of the cores was subsampled and directly filtered to obtain dissolved concentrations. The overlying water was monitored for bulk radioactivity, particulate radioactivity (>0.2 µm), dissolved radioactivity (<0.45 µm), total phosphate, dissolved phosphate (<0.45 µm), total and dissolved iron as Fe^{2+} and total Fe over a period of time. Radioactivity was analyzed in scintillation vial with Lumasafe Plus scintillation fluid (Perkin Elmer) in a liquid scintillation counter (Packard Tri-Carb 2900TR). The radioactivity was back calculated to the time of label addition assuming exponential decay. To differentiate between ^{55}Fe and ^{33}P, the radioactivities were measured again after the decay of ^{33}P to derive ^{55}Fe. The difference of total minus ^{55}F was assumed to be ^{33}P. Phosphate concentrations were analyszed with a modified molybdenum blue method (Murphy and Riley 1962; Hansen and Koroleff 1999). Iron concentrations were determined with ferrozine (Viollier et al. 2000). After the incubation experiments, pore waters were taken with rhizones and the pore waters analyzed for radioactivities of ^{55}Fe and ^{33}P as well as iron and P_i concentrations. Porewater were taken with rhizones after the cores were oxic for several days and the porewater analyzed for the aforementioned elements and radioactivities.

Results

Radioactive tracers were used to investigate the Fe and P dynamics in the sediment overlying water column in the Baltic Sea. Before tracer addition and beginning of the experiment on the 6.12.2011, sediment cores were closed and the oxygen decreased to the detection limit (Figures 2 A, F). One of the cores (Core 1) was opened and it took two days to reach the saturation (~380 µmol L^{-1}). This core was kept oxic over the entire experiment. The other

core (Core 2) was opened as well, but only until oxygen reached 84 μmol L^{-1}, when the core was closed and oxygen dropped back to anoxic conditions. Core 2 was kept anoxic for four days, before it was again oxygenated to almost saturation concentrations for ~2 days. Thereafter Core 2 was sealed and became anoxic.

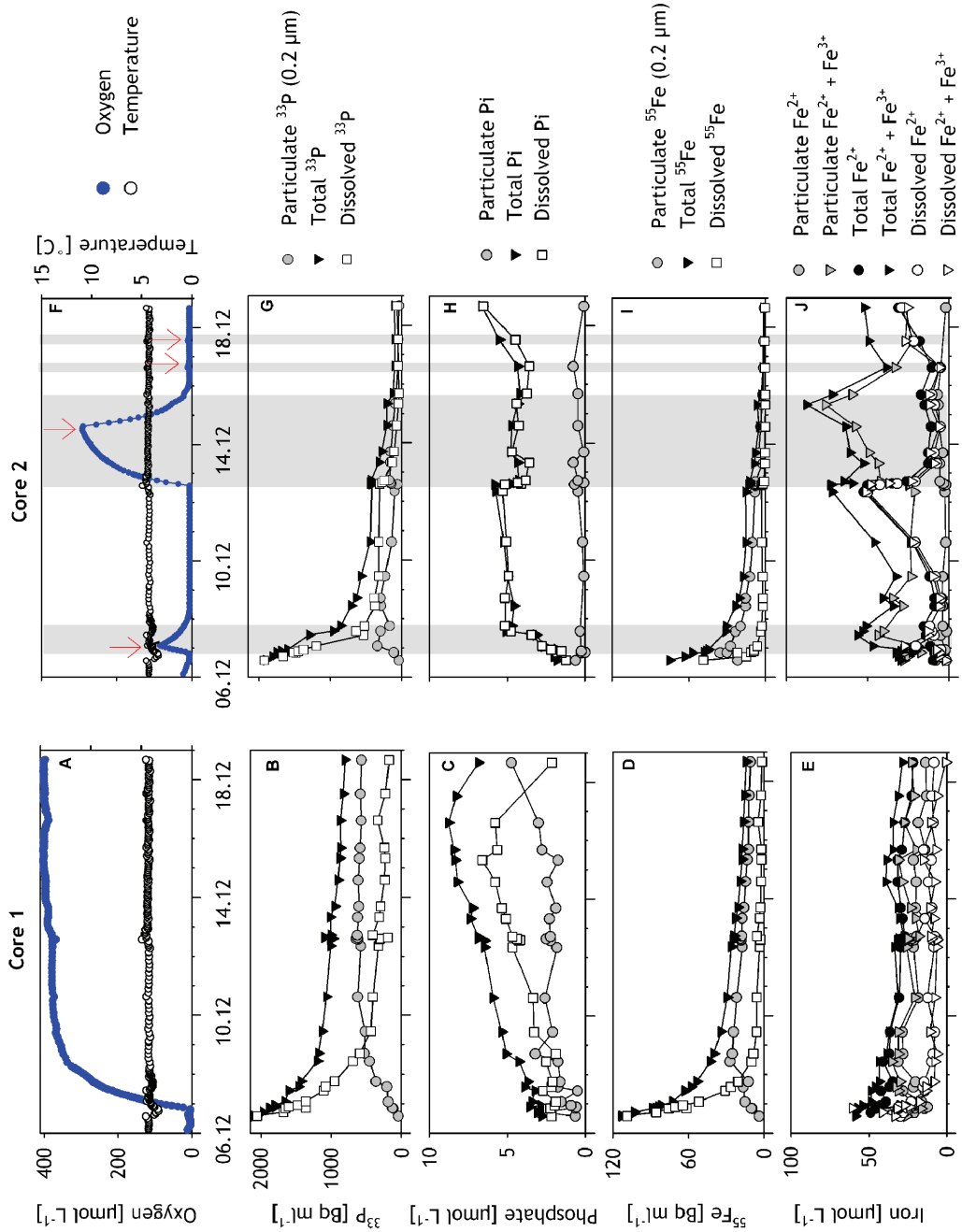

Figure 2: Time series of the incubation experiment. Core 1 was the core with oxic conditions after label additions and oxygen concentrations in Core 2 were varied by opening and closing the lid of the core. The grey areas in Core 2 depict the anoxic phases in the incubation.

The procedure was repeated twice however with low oxygen concentrations of 10 µmol L^{-1}. Total ^{33} P in the overlying water in both cores decreased exponentially over the course of the experiment (Figures 2 B, G). In Core 1 total ^{33}P dropped from ~2000 to 1200 Bq mL^{-1} in the first two days. Then the decrease slowed down and 800 Bq mL^{-1} were reached at the end of the incubation. In Core 2 total ^{33}P decreased fast in the first 1.5 days from ~2000 to ~800 Bq mL^{-1}. After this initial rapid decrease, the rate decrease during the anoxic phase slowed and dropped to 400 Bq mL^{-1} on day 6. During the following oxic phase, total ^{33}P decreased slightly faster to 100 Bq mL^{-1} on day 8, a level which was kept until the end. Particulate (0.2 µm) ^{33}P in Core 1 increased during the first four days, reached 600 Bq mL^{-1} and stayed at this level until the end of the incubation. Particulate radioactivity in Core 2 increased during the first day of incubation to ~300 Bq mL^{-1}. During the anoxic phase, particulate ^{33}P decreased to ~50 Bq mL^{-1}. The following oxic phase resulted in an increase of particulate ^{33}P to ~170 Bq mL^{-1}. With a decrease of oxygen, particulate ^{33}P decreased and reached ~40 Bq mL^{-1}at the end of the incubation.

In contrast to ^{33}P, total P_i increased over the course of the experiment in Core 1 from 2.8 to 8.8 µmol L^{-1} before it dropped slightly to 6.9 µmol L^{-1} at the end of the experiment (Figure 2 C). Similarly, dissolved (0.45 µm) P_i increased from 2.1 to ~6 µmol L^{-1}, before it dropped at end to 2.2 µmol L^{-1} and thus particulate P_i (0.45 µm) increased from 0.6 to 4.7 µmol L^{-1} at end. In Core 2 however, the difference of dissolved and total P_i was minor during the entire incubation (Figure 2 H), suggesting that the fraction of particulate P_i (0.45 µm) was minor (<0.7 µmol L^{-1}). In the initial oxic phase total P_i in Core 2 increased from 1.8 to 5.0 µmol L^{-1}. At anoxic conditions, P_i remained nearly in steady state at ~4.7 µmol L^{-1} and slightly increased towards the end of the anoxic phase to 5.7 µmol L^{-1}. With the onset of oxic conditions, P_i dropped to 4.3 µmol L^{-1} and remained again in steady state until the onset of anoxia where P_i finally increased to 6.6 µmol L^{-1}.

In both cores, most of the ^{55}Fe was present in particulate form, probably due to formation of iron-oxyhydroxides (Figures 2 D, I). In Core 1, ^{55}Fe dropped to half (from 110 to 40 Bq mL^{-1}) within the first two days and further decreased to 14 Bq mL^{-1} at the end of the incubation. Particulate ^{55}Fe increased from 3.7 Bq mL^{-1} at the begging to a maximum of ~27 Bq mL^{-1} and decreased to 10 Bq mL^{-1} at the end of the incubation. In Core 2, total ^{55}Fe decreased from 75 to 30 Bq mL^{-1} at the anoxic phase and to 23 Bq mL^{-1} at the beginning of the oxic phase. Total ^{55}Fe dropped further to 12 Bq mL^{-1} in the oxic and to 1.4 Bq mL^{-1} at the end. After the initial phase, most of the ^{55}Fe was particulate (>0.2 µm), which firstly increased form 22 to 35 Bq mL^{-1}. With anoxia, particulate ^{55}Fe decreased to 16 Bq mL^{-1}, further

decreased to ~8 Bq mL^{-1} at the end of the oxic phase and <1 Bq mL^{-1} at the end of the incubation. Hence dissolved (0.45 µm) ^{55}Fe decreased from 35 Bq mL^{-1} at the beginning to 4 Bq mL^{-1} at the end of the anoxic phase and further decreased to <1 Bq mL^{-1} at the end of the incubation.

Interestingly, in Core 1 almost all of the particulate iron seemed to be present as Fe^{2+} and accounts for around half of the iron fraction, the total iron decreased from 60 to 43 µmol L^{-1} after two days and further to ~30 µmol L^{-1} at the end of the experiment (Figure 2 E). Dissolved iron also in form of Fe^{2+}, dropped from ~30 to 14 µmol L^{-1} until the end. In Core 2, iron concentrations are varying much more than in Core 1 (Figure 1 J). Total Fe increased in the oxic phase at the beginning of the experiment from 30 to 56 µmol L^{-1} and dropped during the subsequent decrease of oxygen to 32 µmol L^{-1}. Thereafter, in the anoxic phase, total Fe increased again to 72 µmol L^{-1}. After another introduction of oxygen, total Fe dropped again to 52 µmol L^{-1} and increased with the decrease of oxygen to a maximum of 87 µmol L^{-1}. After this increase, total Fe concentration decreased to 38 µmol L^{-1} and was slightly higher (51 µmol L^{-1}) at the end of the incubation. Comparison with the Total Particulate Fe (TPFe = particulate Fe^{2+} + Fe^{3+}) showed that most of the iron was particulate at the beginning (28 µmol L^{-1} compared to 30 µmol L^{-1} of TPFe) and further increased to 43 µmol L^{-1} during the first oxic period. Then TPFe dropped to 24 µmol L^{-1} in the anoxic period while the dissolved fraction was strongly increasing. At the onset of the next oxic period, TPFe rapidly increased by 20 µmol L^{-1}. After a short plateau, TPFe increased further to 75 µmol L^{-1} at the end of the oxic phase. In the following anoxic period, TPFe dropped to ~26 µmol L^{-1} while the dissolved fraction increased again.

Porewater taken from Core 2 after the overlying water was oxic for several days revealed distinct profiles for both ^{33}P and ^{55}Fe relative to one another and to non-radiocative dissolved P and Fe (Figure 3). ^{55}Fe and ^{56}Fe exhibited activity and concentration maxima, respectively, in the same sediment layer centere near 3 cm depth. In contrast, a peak in ^{33}P activity was offset slightly deeper (4-5 cm) and not coupled to the concentration of ^{31}P, which increased from below.

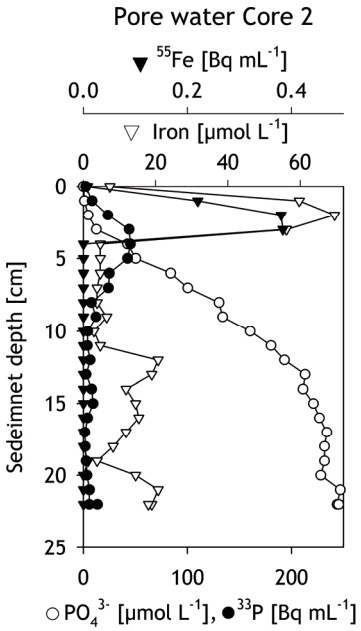

Figure 3: Porewater of Core 2: Porewater was taken after the incubation an the overlying water was oxic for several days.

Discussion

In both cores, the radioactive tracers ^{33}P and ^{55}Fe show a significantly different temporal evolution compared to the bulk concentrations of P and Fe. The reason for this is the strong initial disequilibrium of tracer concentrations between water and sediments, which leads to a strong diffusive flux into the sediment at the start of the experiment and to exponentially decreasing concentrations over time (Figures 2 B, D, G, I). Although this diffusive flux to a certain extent masks the response of tracer concentrations upon changing redox conditions, the temporal evolution of the dissolved and particulate fraction of ^{33}P and ^{55}Fe reveals some interesting aspects.

In the oxic core (Core 1) it took 3 days until the particulate fraction of ^{55}Fe built up from zero to 30 Bq ml^{-1} (Figure 2 D). Thereafter the particulate ^{55}Fe remained as the principal fraction and continuously decreased until the end of the experiment. The slow transformation of ^{55}Fe from the dissolved into the particulate phase suggests that oxidation of the added $^{55}Fe(II)$ is strongly delayed most likely from complexation by dissolved organic compounds. Bulk particulate Fe concentrations were high but variable (15-30 µmol L^{-1}, Figure 2 E) throughout the experiment. Nevertheless, no immediate scavenging of the added dissolved ^{33}P was observed. Instead, it took 4 days for the particulate ^{33}P activity to increase from zero to

600 Bq ml^{-1} (Figure 2 B). Thereafter the ^{33}P activity stayed constant until the end of the experiment. The slow increase of the particulate ^{33}P suggests a slow exchange of desorbed or biologically incorporated ^{33}P and ^{31}P until they reflect the ratio of dissolved ^{33}P and ^{31}P in the water column. It was observed that the sum of particulate (>0.2 µm) and dissolved (<0.45 µm) was higher than total P_i, however, which suggests that some P_i ended up in a fraction of 0.45-0.2 µm that could be either small bacteria or iron particles, both of which occur in that size range.

In Core 1, most of the ^{33}P in the water column was found in the particulate fraction (Figure 2 B), while most of the bulk P was present in the dissolved phase (Figure 2 C). This indicates that ^{33}P and ^{31}P were not in steady-state with respect to particulate and dissolved phases. Sulfidic conditions within the sediments could have enhanced P_i flux from the sediment to the water column. From the increase of bulk P_i of ~5 µmol L^{-1} within 10 days (Figure 2 C) a P_i efflux of 100 µmol m^{-2} d^{-1} can be calculated. Using Redfield stoichiometry (1:138 for P:O_2) results in an O_2 uptake of 13 mmol m^{-2} d^{-1} which is in the range of previously measured O_2 uptake at this station (Holtappels pers. com.).

In Core 2, most P_i was present in the dissolved phase (Figure 2 H). The concentration of particulate bulk P_i were significantly lower compared to Core 1, although concentrations of particulate bulk Fe were high throughout the experiment (Figure 2 J). During the long period of anoxic conditions (days 2 to 6), bulk P_i concentrations remained constant. With the subsequent onset of oxic conditions a drop of total P_i concentration of 2 µmol L^{-1} was observed, which corresponded with a rapid increase of particulate Fe and decrease of dissolved Fe by 20 and 26 µmol L^{-1}, respectively (Figure 2 J). Besides the rapid shift from the dissolved to the particulate phase, total Fe concentrations dropped significantly. In summary this suggests a rapid scavenging of dissolved P by a rapidly precipitated and sedimented Fe fraction, while the remaining particulate Fe is not involved in any formation of particulate P. The shift to oxic conditions was also reflected by a decrease of total ^{33}P and ^{55}Fe concentrations until a new steady state is reached (Figure 2 G, I). The depletion of ^{33}P and ^{55}Fe in the porewaters at the sediment water interface also mirrors this shift (Figure 3).

In conclusion, incubations of sediments and overlying water reveal far more complex interactions between P and Fe phases which are likely regulated not only by the abundance of oxygen but also by the presence of dissolved organics and the specific structure of the particulate iron. Although the initial dynamic flux of ^{33}P and ^{55}Fe from water column to sediment is strongly masking the bulk exchange fluxes, radiotracer incubations are useful to

observe the dynamic shifts between dissolved and particulate phases. Further studies should include a thorough analysis of suspended particles.

Acknowledgements

We thank V. Brüchert for the opportunity to take the sediment cores. The study was funded by the Max-Planck Society and MARUM-Center of Marine Environmental Sciences.

References

Conley, D. J., S. Bjorck, E. Bonsdorff, J. Carstensen, G. Destouni, B. G. Gustafsson, S. Hietanen, M. Kortekaas, H. Kuosa, H. E. M. Meier, B. Mueller-Karulis, K. Nordberg, A. Norkko, G. Nuernberg, H. Pitkanen, N. N. Rabalais, R. Rosenberg, O. P. Savchuk, C. P. Slomp, M. Voss, F. Wulff and L. Zillen (2009). "Hypoxia-related processes in the Baltic Sea." Environmental Science & Technology 43(10): 3412-3420.

Conley, D. J., C. Humborg, L. Rahm, O. P. Savchuk and F. Wulff (2002). "Hypoxia in the Baltic Sea and basin-scale changes in phosphorus biogeochemistry." Environmental Science & Technology 36(24): 5315-5320.

Diaz, R. J. and R. Rosenberg (2008). "Spreading dead zones and consequences for marine ecosystems." Science 321(5891): 926-929.

Elmgren, R. (2001). "Understanding human impact on the Baltic ecosystem: Changing views in recent decades." Ambio 30(4-5): 222-231.

Gunnars, A. and S. Blomqvist (1997). "Phosphate exchange across the sediment-water interface when shifting from anoxic to oxic conditions - an experimental comparison of freshwater and brackish-marine systems." Biogeochemistry 37(3): 203-226.

Hansen, H. P. and F. Koroleff (1999). Determination of nutrients. Methods of Seawater Analysis, Third Edition. K. K. K. Grasshoff, & M. Ehrhardt, Wiley, 1999: 159-228.

Jilbert, T. and C. P. Slomp (2013). "Iron and manganese shuttles control the formation of authigenic phosphorus minerals in the euxinic basins of the Baltic Sea." Geochimica et Cosmochimica Acta 107(0): 155-169.

Ma, S., E. B. Whereat and G. W. Luther, III (2006). "Shift of algal community structure in dead end lagoons of the Delaware Inland Bays during seasonal anoxia." Aquatic Microbial Ecology 44(3): 279-290.

Mort, H. P., C. P. Slomp, B. G. Gustafsson and T. J. Andersen (2010). "Phosphorus recycling and burial in Baltic Sea sediments with contrasting redox conditions." Geochimica Et Cosmochimica Acta 74(4): 1350-1362.

Murphy, J. and J. P. Riley (1962). "A modified single solution method for the determination of phosphate in natural waters." Analytica Chimica Acta 27(0): 31-36.

Rozan, T. F., M. Taillefert, R. E. Trouwborst, B. T. Glazer, S. F. Ma, J. Herszage, L. M. Valdes, K. S. Price and G. W. Luther (2002). "Iron-sulfur-phosphorus cycling in the sediments of a shallow coastal bay: Implications for sediment nutrient release and benthic macroalgal blooms." Limnology and Oceanography 47(5): 1346-1354.

Shaffer, G. (1986). "Phosphate pumps and shuttles in the Black-Sea." Nature 321(6069): 515-517.

Viollier, E., P. W. Inglett, K. Hunter, A. N. Roychoudhury and P. Van Cappellen (2000). "The ferrozine method revisited: Fe (II)/Fe (III) determination in natural waters." Applied Geochemistry 15(6): 785-790.

Conclusions and perspectives

Marine primary production and the community structure of primary producers are determined by the availability of energy and the key nutrients C, N, P and Fe. In the ocean, sinking organic particles act as "biological carbon pump" and transport carbon to depth (Raven and Falkowski 1999). During transport to the seafloor, organic matter is remineralized and nutrients dissolve into the water column, resulting in a concentration increase of dissolved N and P-compounds with depth. How microorganisms further transform these nutrients in water column and sediment is in parts not always well constrained. This study investigated benthic microbial N-loss processes and biologically mediated formation of particulate phosphorus in the sediment and water column of upwelling regions. The experimental approaches applied and developed in the course of the studies allowed for a detailed examination of microbially controlled processes in surface sediments (chapter II+III) or the immediately overlying water column (benthic boundary layer, chapter IV+V) and related to specific particulate fractions (chapter IV). Experimental approaches include direct rate measurements and allowed to correlate microbial activity to gene abundance (chapter II) or environmental parameters (chapter III), which even could be used to predict and extrapolate process rates to larger areas.

N-loss in diffusive sediments and the decreasing importance of denitrification with depth

Via ^{15}N incubation experiments, it was shown that benthic N-loss affect N-budgets in the Arabian Sea (Chapter II) and off Mauritania (Chapter III). The Arabian Sea harbors 5% of the global marine primary production, although this area covers only 1% of the surface ocean. Large fluxes of organic matter together with the poor ventilation of the water column have resulted in a permanent OMZ in the Arabian Sea. Formerly it has been believed that pelagic denitrification in the central Arabian Sea is the most important mechanism for N_2 production (Ward et al. 2009). In the recent years, it has been shown that pelagic N-loss in the Arabian Sea is rather patchy and dominated by anammox (Jensen et al. 2011; Lam et al. 2011). The results in chapter II suggest that benthic N-loss accounts for 50% of the total N-loss in the Arabian Sea and might therefore contribute significantly to the N-deficit in the water column. Anammox is an important N-loss process in the Arabian Sea, not only in the water column, but also in the sediments. Rate measurements in the Arabian Sea showed a decrease of benthic denitrification rates with an increase in water depth, while benthic anammox rates increased, and thus contribution of anammox to N-loss increased to 40% at ~1400 m. This was further supported by quantification of the functional *nirS* genes (chapter II). An even more pronounced increase of anammox contribution was found in the sediments off

Mauritania (chapter III), where anammox contributed up to 80% to the N-loss at 3000 m water depth. In contrast, denitrification was dominant in shallow sandy sediments, where redox conditions are highly dynamic. The combined results of chapter II and III suggest that the slow-growing anammox bacteria prefer stable redox conditions and low concentrations of organic carbon, while denitrifiers are better adapted to more dynamic redox conditions that result from pulse like organic carbon input and variable nitrate concentrations as found in shallow and sandy sediments. The high diversity of the denitrifiers might be the way, how this community adapts to the different environmental conditions.

Therefore, further investigations should aim to understand how denitrification is adapted at the cellular and community levels to the pulse-like supply of organic carbon. In ^{15}N incubation experiments, organic carbon supply and activity measurements on the process level could be paired with molecular methods (such as RT-qPCR and FISH) and single cell techniques (such as nanoSIMS analysis). Active members of the community could be further studied and gene expression of functional genes such as *nirS* in different denitrifying communities could be linked to carbon input or changing redox conditions. With this approach would not only be the activity of the denitrifying community be studied, but activity could be linked to sub-groups of the denitrifiers to understand the reaction to pulse-like supply of substrates.

The role of the permeability for denitrification

Permeable, sandy sediments are widely distributed on the shelf off Mauritania (Holz et al. 2004), and are typical of the most common type of shelf sediment facies that cover 70% of the global shelf regions (Emery 1968). In contrast to cohesive sediments, permeable sediments off Mauritania allow fast advective transport of substrates to deeper sediment layers, which is reflected by the increased nitrate penetration depths (chapter III). Consequently, permeable sediments off Mauritania revealed an extremely high potential for denitrification (up to 16.5 mmol N m^{-2} d^{-1}) which was up to an order of magnitude higher than in the Arabian Sea (chapter II). Moreover, a significant correlation was found between grain size distribution and benthic denitrification which allowed modeling areal denitrification rates down to depths of 500 m for the entire investigated region. The primary dependency of denitrification on grain size distribution shows that porewater transport is of increased importance for benthic denitrification in sands compared to other proxies such as benthic organic carbon content and bottom water nitrate, both of which are the commonly employed input parameters to model denitrification in marine sediments (Middelburg et al. 1996).

Denitrification in subtidal and naturally eutrophied sandy sediments has been rarely investigated. Does a similar dependency of denitrification rates on grain size distribution exist in other coastal area? A very productive region is the Arctic and permeable sediments on the shelf could be potentially important for the global N-loss, given the large area of this region. Denitrification in the permeable sediments on the Arctic shelf could be investigated with ^{15}N stable isotope techniques and to simulate *in situ* conditions, flow through cores should be used to quantify actual N-loss in the sediment and estimate the contribution to the global N-loss. These actual rates might be combined with molecular methods, as mentioned in the previous section to link activity to specific communities or even single cells.

Biologically mediated P-uptake in the sub-euphotic water column

Uptake of P in the sub-euphotic water column and in the benthic boundary layer (BBL) was measured in ^{33}P incubation experiments in combination with a sequential extraction of ^{33}P and nanoscale analysis of particles (chapter VI). The results of the ^{33}P incubation experiments on the shelf off Mauritania and Namibia suggest that P-uptake in the sub-euphotic zone is predominately biologically mediated. The current view on P-cycling is that P is assimilated in the surface and sinks down to greater depths as organic particle where it is remineralized and released into the water column. This study shows that significant parts of remineralized P is taken up and turned over within the water column, which has not been considered in marine P-cycling so far. Even though the P-uptake is very little compared to P-uptake in the surface, P-release due to respiration and P-uptake are in the same order of magnitude and seem to be in a steady state.

Labeling experiments using ^{33}P have great potential to gain insight into specific P transformation processes that otherwise would remain unnoticed in bulk P concentration measurements. For instance, the more detailed view from ^{33}P incubations provided insight into the kinetics of particulate P-formation in the sub-euphotic water column and BBL. The exact causes of this lag are still not clear (chapter VI), especially the lag phase at the beginning of the incubation experiments. This lag phase observed in many, but not all experiments, may result from exchange processes of the radiolabel on particle or cell surfaces. To investigate potential exchange and steady-state processes, ^{33}P uptake experiments in combination with nanoSIMS analysis with slow growing bacteria would help to shed light on the question, if a steady-state distribution of ^{31}P and ^{33}P is established in the cell itself or on the cell-surfaces during the lag phase. Moreover, results from the anoxic water column off Namibia suggest that ^{31}P and ^{33}P rapidly exchange on surfaces of e. g. iron oxides (chapter III,

SI). The formation of particulate P and Fe in hypoxic regions have been poorly investigated and should be further examined with methods such as energy dispersive X-ray spectroscopy (EDX) and Raman spectroscopy to understand the nature of the particles and the processes involved in their formation.

How N-removal and P-uptake influence N:P ratios

This study focuses on some of the most productive upwelling regions. The high productivity is coupled to a high O_2 consumption, which has led to decreased oxygen concentrations in most of the investigated areas. While the Arabian Sea has a permanent anoxic zone, the OMZ off Namibia is fluctuating and the OMZ off Mauritania is still developing. Under the aspect that upwelling might increase off NW-Africa and OMZs are thought to expand globally (McGregor et al. 2007; Stramma et al. 2008), these areas are very important regions for future ocean scenarios. For primary production, N:P ratios have severe effects because it determines the community structure of primary producers (Karl et al. 2002) and high P and ammonium concentrations are believed to cause harmful algae blooms (Ma et al. 2006). In this dissertation, influence of organisms on the N:P ratio was investigated from two different directions: N removal and P-uptake. Benthic N-loss removes N from the ocean so that the N:P ratio decreases. In contrast, P-uptake processes decrease the dissolved P concentration in the water column, hence result in a increase of the N:P ratio. Interestingly, comparing the effects of both mechanisms (N-removal and P-uptake) in the BBL and sediments off Mauritania, neither of these processes has an imprint on the N:P ratio in the water column. However, in other regions, such as off Namibia, very low N:P ratios (<2) were observed (Kuypers et al. 2005), which potentially affect the growth of organisms. This dissertation has provided mechanistic insight into the importance of biological activity in the sub-euphotic water column and surface sediments on processes affecting the N:P ratio. These processes have an impact on the overall steady-state N:P ratio in the global ocean, and, as such, deserve continuing attention.

References

Emery, K. O. (1968). "Relict sediments on continental shelves of world." AAPG Bulletin 52(3): 445-464.

Holz, C., J. B. W. Stuut and R. Henrich (2004). "Terrigenous sedimentation processes along the continental margin off NW Africa: implications from grain-size analysis of seabed sediments." Sedimentology 51(5): 1145-1154.

Jensen, M. M., P. Lam, N. P. Revsbech, B. Nagel, B. Gaye, M. S. M. Jetten and M. M. M. Kuypers (2011). "Intensive nitrogen loss over the Omani Shelf due to anammox coupled with dissimilatory nitrite reduction to ammonium." Isme Journal 5(10): 1660-1670.

Karl, D., A. Michaels, B. Bergman, D. Capone, E. Carpenter, R. Letelier, F. Lipschultz, H. Paerl, D. Sigman and L. Stal (2002). "Dinitrogen fixation in the world's oceans." Biogeochemistry 57(1): 47-98.

Kuypers, M. M. M., G. Lavik, D. Woebken, M. Schmid, B. M. Fuchs, R. Amann, B. B. JØrgensen and M. S. M. Jetten (2005). "Massive nitrogen loss from the Benguela upwelling system through anaerobic ammonium oxidation." Proceedings of the National Academy of Sciences of the United States of America 102(18): 6478-6483.

Lam, P., M. M. Jensen, A. Kock, K. A. Lettmann, Y. Plancherel, G. Lavik, H. W. Bange and M. M. M. Kuypers (2011). "Origin and fate of the secondary nitrite maximum in the Arabian Sea." Biogeosciences 8(6): 1565-1577.

Ma, S., E. B. Whereat and G. W. Luther, III (2006). "Shift of algal community structure in dead end lagoons of the Delaware Inland Bays during seasonal anoxia." Aquatic Microbial Ecology 44(3): 279-290.

McGregor, H. V., M. Dima, H. W. Fischer and S. Mulitza (2007). "Rapid 20th-century increase in coastal upwelling off northwest Africa." Science 315(5812): 637-639.

Middelburg, J. J., K. Soetaert, P. M. J. Herman and C. H. R. Heip (1996). "Denitrification in marine sediments: A model study." Global Biogeochemical Cycles 10(4): 661-673.

Raven, J. A. and P. G. Falkowski (1999). "Oceanic sinks for atmospheric CO2." Plant, Cell & Environment 22(6): 741-755.

Stramma, L., G. C. Johnson, J. Sprintall and V. Mohrholz (2008). "Expanding oxygen-minimum zones in the tropical oceans." Science 320(5876): 655-658.

Ward, B. B., A. H. Devol, J. J. Rich, B. X. Chang, S. E. Bulow, H. Naik, A. Pratihary and A. Jayakumar (2009). "Denitrification as the dominant nitrogen loss process in the Arabian Sea." Nature 461(7260): 78-81.

Acknowlegdements

Without the support and encouragement of many people, this dissertation would not have been possible, and for that, I am very thankful for their help, time and effort. Throughout my research, I received much support, for which I am extremely grateful, from the Max Planck Institute (MPI), which provided an excellent environment and number of resources to assist me in my research. I am also very thankful for the funding and support from the Center for Marine Environmental Sciences (MARUM).

For reviewing my thesis I am very thankful to Marcel Kuypers and Matthias Zabel.

I am especially grateful to Marcel Kuypers for the opportunity to pursue my doctoral research in the Biogeochemistry group, for supervising my thesis and providing helpful comments on the manuscripts. Your enthusiasm for science and new scientific techniques is very impressive, and our discussions were always interesting as well as valuable.

I am deeply thankful to Moritz Holtappels for his supervision during the past years, from whom I learned so much. Your encouragement and guidance were essential for me to develop a solid foundation in methods of data collection. Thank you for always being open to listen to my questions and problems.

To Tim Ferdelman I am very thankful for sharing his knowledge in radioactive tracer techniques as well as his help with calculations and his input on my dissertation.

For help and advice in terms of molecular methods and data collection, I would also like to thank Phyllis Lam. Your comments on my paper were especially helpful, and I am also very lucky to have shared an office with you during the last few years at the MPI.

I am vey thankful to Gaute Lavik, whose skills in core slicing and teaching on stable isotope techniques were vitally instructive for the development of this dissertation.

From MARUM, I am very grateful to Tobias Goldhammer for sharing his knowledge of the SEDEX extraction, for measuring many samples at the ICP and for his input on earlier manuscript versions.

I am also extremely thankful to Matthias Zabel for organizing the GB2 project as well as the cruise to Namibia. Moreover, I am thankful to the cruise leaders Karin Zonneveld, Olaf Pfannkuche, Matthias Zabel and Frank Malien for their collaboration, for providing many opportunities to take samples and for sharing data. Along these lines, I am also thankful for the excellent cooperation from the captain and crew of *RV* Meteor, *RV* Poseidon, *RV* Maria S. Merian, Littorina and Polarfuchs.

I am thankful to a number of colleagues from the MPI, to Sten Littmann and Daniela Franzke for the hours of nanoSIMS analysis and help during image analysis and to Lubos Polercky for his help and effort on look at nanoSIMS. I am also thankful to Gabi Klockgether for her help and for teaching me different chemical analysis techniques. For supervision in the radioactive lab, I am thankful to Gabi Schüssler, Kirsten Imhoff and Swantje Lilienthal. I also want to thank Jessika Füssel, Tim Kalvelage and Hannah Marchant for sharing their knowledge in measuring different N-cycling processes and data as well as for their discussion and advice. Thanks to the HiWis Karl Thieme, Inka Boosmann and Madalina Toader for their good work in measuring N_2, NO_X and extracting DNA. Lastly, I am thankful for the work of Joe Marshall and Clara Martinez Perez, which helped to clear some doubts about the SEDEX method.

For valuable discussions, help and advice as well as for the teakitchen small talk I am thankful to all biogeo and former nutrient group members.

Finally, I would like to thank my friends and wonderful family for their support and encouragement throughout this process.